Effects of sea surface warming, irradiance, and grazer abundance on organic matter cycling in a plankton community

Dissertation

In fulfilment of the requirements for the degree “Dr. rer. nat.”
of the Faculty of Mathematics and Natural Sciences at
Christian-Albrechts-University Kiel

submitted by
Antje Biermann

Rostock, 2014

First referee: Prof. Dr. Ulf Riebesell

Second referee: Prof. Dr. Anja Engel

Date of the oral examination: 16.01.2014

Approved for publication: 16.01.2014

Signed: Prof. Dr. Wolfgang J. Duschl, Dean

Table of Contents

Summary

Ocean warming affects all components of the food-web. Autotrophic processes, however, are less temperature sensitive than those conducted by heterotrophs, and changes in their balance can thus be expected, likely changing biogeochemical cycling in the oceans. The combined response of all food-web processes to temperature and other factors will thus determine the future direction of the biological carbon pump, which transports photosynthetically fixed CO_2 to deeper parts of the ocean via sinking biogenic particles or dissolved organic matter.

The aim of this study was to investigate the temperature-dependent partitioning of organic matter between dissolved and particulate matter pools and the changes in their stoichiometry, with emphasis on the impact of changes in irradiance or zooplankton abundance. To elucidate these questions, indoor-mesocosm studies were conducted with natural winter plankton communities from Kiel Bight (Baltic Sea) containing all trophic levels from bacteria to mesozooplankton.

Chapter 1 addresses the effects of temperature in combination with different irradiance levels. Rising temperature accelerated the production rate of particulate and dissolved organic matter (POM and DOM), while light intensity played a comparatively minor role for the bloom development. Maximum accumulation of POM was significantly reduced at elevated compared to ambient temperature. Although, heterotrophic loss processes were enhanced by temperature, also an increased formation of transparent exopolymer particles (TEP) was observed. This suggests that in a warmer ocean the accumulation of POM is controlled by two counteracting mechanisms: 1) enhanced heterotrophic remineralization processes, leading to a weakening of the biological pump; and 2) enhanced particle aggregation due to TEP and strengthened transport of POM to deeper parts of the ocean.

Chapter 2 describes the effects of temperature in combination with three different overwintering zooplankton grazer (copepod) densities. Increasing copepod abundance decreased the ratio of particulate organic carbon to nitrogen and phosphorus. DOC was positively affected by temperature, but when normalized to Chlorophyll *a* concentration, showed a tendency to decrease with increasing copepod abundance. This study indicates that the enhanced inorganic carbon consumption relative to N and P by phytoplankton under nutrient stress, which was suggested for a warmer sea surface ocean, could be counteracted by the effect of consumer-driven nutrient recycling.

Chapter 3 is a comparative data analysis that aims to identify recurrent patterns of biogeochemical parameters in response to an increase in water temperature. Warming stimulated heterotrophic bacterial processes in particular and had an accelerating effect on the temporal development of phytoplankton blooms. Warming increased the rate of POM

and DOC accumulation, whereas the magnitude of POM decreased with rising temperature.

Chapter 4 presents results on the effects of high and low light conditions during the months January and February. It was shown that it was possible to induce a diatom phytoplankton bloom in January, comparable to one in February. POM accumulation increased with increasing light levels, whereas DOM, TEP and "Coomassie stainable particles (CSP) remained unaffected by the different irradiance levels. However, CSP were found to occur at the same magnitude and size as TEP and might hence be as important for the partitioning of N as TEP are for the partitioning of C, and should receive more attention in future studies on organic matter cycling.

The results presented here show that temperature induced changes in biogeochemical cycling can have strong implications for the biological pump, which plays a vital role in Earth's climate. Additionally, they demonstrate the strong potential for interactive effects by the interplay of temperature with changes in irradiance and grazer abundance.

Zusammenfassung

Die Ozeanerwärmung betrifft alle Komponenten des Nahrungsnetzes. Jedoch sind autotrophe Prozesse weniger stark temperaturabhängig als heterotrophe, weswegen eine Verschiebung in deren Balance erwartet wird, mit Auswirkung auf die biogeochemischen Abläufe im Meer. Nur die Gesamtantwort aller Nahrungsnetzprozesse auf die Erwärmung im Zusammenspiel mit anderen Faktoren bestimmt die zukünftige Entwicklung der biologischen Pumpe, die das durch Photosynthese fixierte CO_2 in Form von sinkenden biogenen Partikeln und gelöstem organisches Material in die Tiefe transportiert.

Ziel dieser Studie ist die Untersuchung der temperaturabhängigen Verteilung von organischem Material zwischen gelösten und partikulären Phasen und Änderungen in dessen Stöchiometrie, in Kombination mit den Faktoren Licht und Zooplanktonabundanz. Dafür kamen Mesokosmen in Klimakammern mit natürlichen Winter-Planktongemeinschaften der Kieler Bucht (Ostsee) zum Einsatz, die alle trophischen Stufen von Bakterien bis zum Mesozooplankton beinhalteten.

Kapitel 1 beleuchtet die Effekte einer Temperaturerhöhung in Kombination mit verschiedenen Lichtintensitäten. Eine Temperaturerhöhung beschleunigte die Produktionsraten von partikulärem und gelöstem organischem Material (POM und DOM), während die Lichtintensität eine vergleichsweise geringere Rolle für die Blütenentwicklung spielte. Der maximale Aufbau von POM fiel bei erhöhter Wassertemperatur signifikant geringer aus. Obwohl es eine temperaturbedingte Verstärkung der heterotrophen Verlustprozesse gab, konnte auch eine verstärkte Bildung von transparenten exopolymeren Partikeln (TEP) beobachtet werden. Dieses Ergebnis lässt vermuten, dass in einem zukünftigen wärmeren Ozean zwei gegensätzliche Prozesse die Akkumulation vom POM steuern werden. Zum einen schwächt erhöhte Remineralisierung die biologische Pumpe, zum anderen wird die Aggregatbildung durch TEP und der Transport von POM in tiefere Schichten des Meeres verstärkt.

Kapitel 2 beschreibt Temperatureffekte in Kombination mit verschiedenen Dichten von überwinterndem Zooplankton (Copepoden). Steigende Copepodenzahlen senkten das Verhältnis von partikulärem organischem Kohlenstoff zu Stickstoff (N) und Phosphor (P). Gelöster organischer Kohlenstoff (DOC) stieg bei höherer Wassertemperatur, sank aber tendenziell pro Chlorophyll *a* mit steigender Copepodendichte. Der durch die Erwärmung vermutete erhöhte Verbrauch anorganischen Kohlenstoffes, im Vergleich zu N und P bei Nährstoffmangel, könnte somit durch konsumentengetriebene Nährstoffregenerierung verringert werden.

Kapitel 3 ist eine vergleichende Datenanalyse mit dem Ziel, wiederkehrende Muster biogeochemischer Parameter in Hinblick auf eine Wassertemperaturerhöhung zu ermitteln. Die Erwärmung stimulierte insbesondere heterotrophe bakterielle Prozesse und

hatte einen beschleunigenden Effekt auf die temporale Entwicklung der Phytoplanktonblüte. Die Erwärmung beschleunigte ebenso die Raten der POM und DOC Akkumulation, während die Gesamtakkumulation von POM verringert war.

In Kapitel 4 werden die Ergebnisse der Auswirkung hoher und geringer Lichtintensitäten während der Monate Januar und Februar auf die Planktongemeinschaft dargestellt. Es wird gezeigt, dass bereits im Januar eine Blüte vergleichbar mit einer im Februar möglich ist. Die POM-Akkumulation stieg mit der Lichtintensität, während DOM unbeeinträchtigt blieb, ebenso wie TEP und „Coomassie stainable particles“ (CSP). Jedoch war die Anzahl und Größe der CSP vergleichbar mit TEP, weswegen CSP für die Verteilung von N ähnlich bedeutsam sein könnten wie TEP für die von C und in zukünftigen Studien mehr Beachtung finden sollten.

Zusammenfassend zeigt sich, dass sich durch die temperaturbedingten Veränderungen in der Biogeochemie starke Auswirkungen auf die biologische Kohlenstoffpumpe ableiten lassen, die entscheidend das Klima der Erde mit beeinflusst. Es zeigt sich aber auch das große Potential für die interaktiven Effekte, die aus dem Zusammenspiel einer Temperaturerhöhung mit veränderten Lichtbedingungen und der Abundanz von Grazern entstehen können.

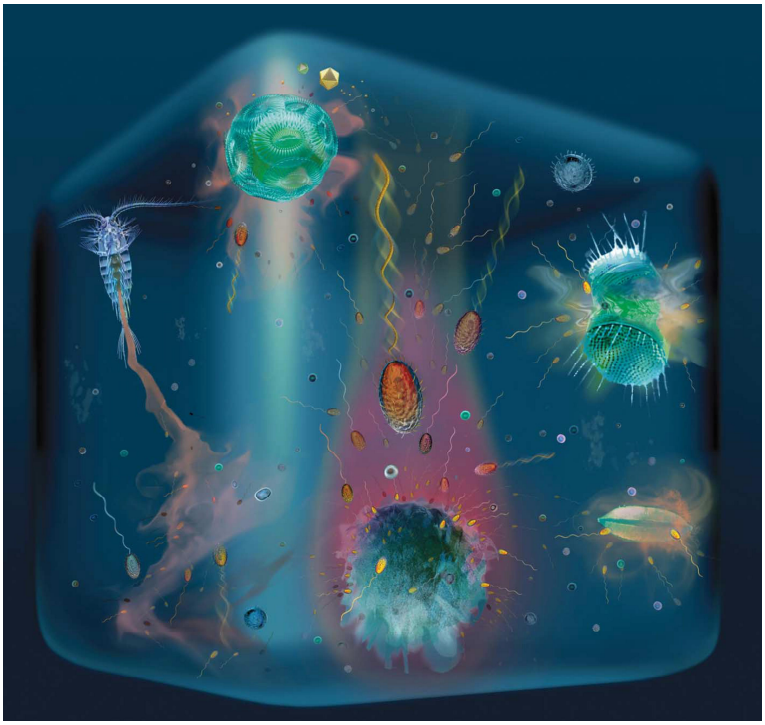

Fig. 1. Marine microbial microenvironments. DOM exudation by phytoplankton (top),cell lysis events (top right), stationary or sinking detritus and marine snow particles (bottom center), and copepod excretions (left). Source: Stocker (2012)

General Introduction

Climate change

Global atmospheric CO_2 emissions and temperature rise

The Earth's climate is changing. Global warming accounted for an increase of 0.85 °C between the years 1880-2012, whereby in the Northern Hemisphere the period of 1983-2012 was the warmest of the last 1400 years (Fig. 1-1) (IPCC 2013). The increase in global average temperature is attributable to the increase in greenhouse-gas emissions since 1750 as a result of human activities (IPCC 2013). Only the simulations using natural plus anthropogenic forcings match with the observed temperature incline. Four long-lived greenhouse-gases result from human activity: carbon dioxide (CO_2), methane (CH_4), nitrous oxide (N_2O) and halocarbons (group of gases containing fluorine, chlorine or bromine). Present day atmospheric CO_2, CH_4 and N_2O concentrations are at the highest level of the last 800,000 years (IPCC 2013). The CO_2 concentrations have increased from pre-industrial values of ~280 ppm and in May 2013 exceeded the threshold of ~400 ppm (http://www.esrl.noaa.gov/gmd/ccgg/trends/weekly.html).

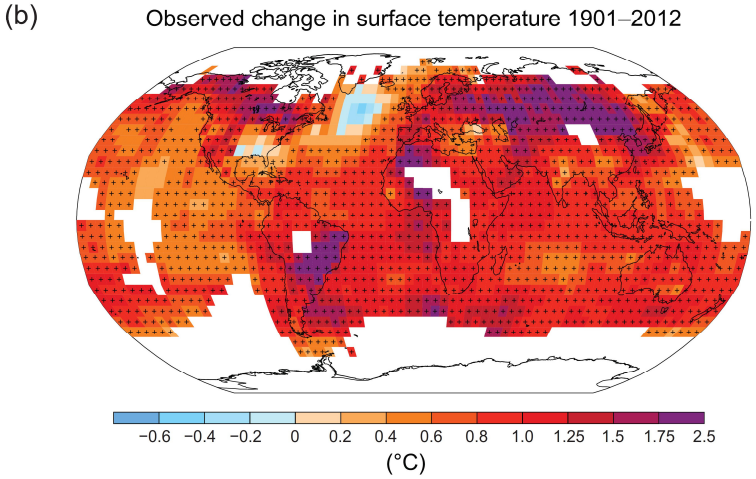

Figure 1-1: Map of the observed surface temperature change from 1901 to 2012 derived from temperature trends determined by linear regression from one dataset. Trends have been calculated where data availability permits a robust estimate (i.e., only for grid boxes with greater than 70% complete records and more than 20% data availability in the first and last 10% of the time period). Other areas are white. Grid boxes where the trend is significant at the 10% level are indicated by a + sign. Source: IPCC (2013).

CO_2 is the most important anthropogenic greenhouse-gas. From 1750 to 2011 cumulative anthropogenic emissions from fossil fuel combustion, cement production, deforestation, and land use change accounted for 555 Gigatons carbon (GtC). From these, 240 GtC have been accumulated in the atmosphere, 150 in the terrestrial ecosystem, and 155 have been

taken up by the ocean (IPCC 2013). With continuing emission of greenhouse-gases at or above current rate, IPCC scenarios, taking into account different pathways of demographic, economic and technical development, project an increase in Earth mean surface temperature in the range of 0.3 °C to 4.8 °C until the end of this century, relative to 1986-2005 (Fig. 1-2) (IPCC 2013). This projected temperature increase is accompanied by an increase in sea ice loss and sea level rise in the range 0.3 – 0.8 m for the same time period (IPCC 2013).

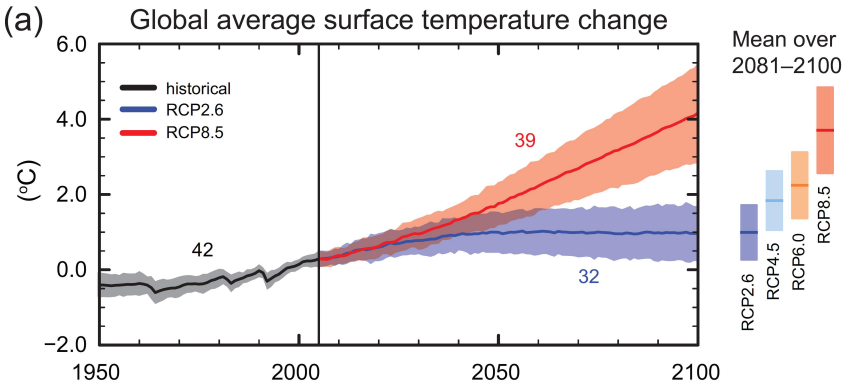

Figure 1-2: CMIP5 multi-model simulated time series from 1950 to 2100 for (a) change in global annual mean surface temperature relative to 1986–2005. Time series of projections and a measure of uncertainty (shading) are shown for scenarios RCP2.6 (blue) and RCP8.5 (red). Black (grey shading) is the modelled historical evolution using historical reconstructed forcings. The mean and associated uncertainties averaged over 2081−2100 are given for all RCP scenarios as colored vertical bars. The numbers of CMIP5 models used to calculate the multi-model mean is indicated. Source: IPCC (2013).

The oceans play a mitigating role in the global warming trend due to their ability to store high amounts of heat. Between 1955 and 2010, the oceans absorbed 93 % of the heat that has been added to the Earth system, resulting in an 0.18 °C increase in water temperature from the surface to 700 m depth (Levitus et al. 2012). However, with increasing water temperature, the oceans ability to take up atmospheric CO_2 decreases. This so-called positive carbon cycle feedback increases atmospheric CO_2 concentrations, thereby increasing the global average warming.

The concentration of CO_2 in seawater would be relatively low if it only depended on its solubility, that is if it only depended on the partial pressure of the atmosphere, the temperature and the salinity of the seawater. CO_2, however, has the property of reacting with water to form carbonic acid (H_2CO_3), that immediately disintegrates to bicarbonate (HCO_3^-) and hydrogen ions (H^+), that in turn disintegrates to carbonate (CO_3^{2-}) and hydrogen ions. This is called the buffering capacity of seawater. The pool of dissolved inorganic carbon (DIC) in the ocean accounts for ~38,000 Pg C (or Gt) and, on average, 90 % of it is in the form of HCO_3^- (Sarmiento and Gruber 2006). However, new estimates

suggest that the oceans storage capacity might not keep pace with the increasing growth rates of CO_2 emissions, which account today for ~41 % of total fossil fuel emissions since the preindustrial (Canadell et al. 2007; Gruber et al. 2009; Sabine and Tanhua 2010). On an annual basis, the oceans absorb one fourth to one third of the anthropogenic CO_2 emissions (Sabine et al. 2004; Canadell et al. 2007). CO_2 that reacts with seawater to form HCO_3^- shifts the partitioning of DIC towards increased CO_2, thereby increasing seawaters acidity (decreasing the pH). This process, called ocean acidification, has decreased the pH of the ocean surface water by 0.1 since the 18th century, corresponding to a increase in hydrogen ion concentrations of ~30 % (IPCC 2013).

Effects of climate warming on the underwater light environment

In the ocean, elevated sea surface temperature is accompanied by increasing water column stratification (Prentice et al. 2001). In the tropics and mid-latitude oceans, where phytoplankton are often nutrient-limited, a further increase in stratification would reduce water mass mixing and thus nutrient supply (Doney 2006). In high latitude oceans, where phytoplankton are typically light-limited, reduced mixing (caused by enhanced stratification due to warming) would keep the plankton at the surface were light levels are high (Doney 2006). Model simulations generally assume that enhanced vertical stratification favors autotroph growth in high and mid-latitude oceans, whereby in low-latitude oceans a reduction in upwelling would lower nutrient supply thereby dampening primary productivity (Bopp et al. 2001; Sarmiento et al. 2004).

Warming also increases the amount of water vapor in the atmosphere, leading to an expected increase in cloudiness as a co-occurring effect of global warming. Anthropogenic forcing has already contributed significantly to the observed increases in precipitation in the Northern-Hemisphere mid-latitudes and other latidunal zones (Zhang et al. 2007). However, projections for future changes in precipitation are not uniform and are shaped by the specific regional precipitation patterns (IPCC 2013).

The Baltic Sea in a changing climate

The Baltic Sea is one of the world's largest brackish water areas, spanning about 415,000 km² (including the Kattegat). It is generally shallow, but includes some deep basins, up to in 460 m depth. The inflow of oxygen-rich saline water from the North Sea is restricted by a small inlet, the narrow straits of Little and Great Belt in the area of Denmark. Freshwater enters the Baltic Sea by precipitation, land runoff and rivers, particularly by the large rivers that discharge into the northern and eastern parts. The high freshwater input into the Baltic Sea creates a salinity gradient from marine salinity in the Western part to almost freshwater quality (0 salinity) in the North-East. A permanently stratified water column exists in the central Baltic Proper with saline deep water overlaid by a

lower salinity water layer. Due to its geographical position, the climate of the Baltic Sea is characterized by seasonal contrasts. During winter time it is influenced by the North Atlantic Oscillation (NAO), affecting the atmospheric circulation and precipitation (Helcom 2007).

The warming trend for the Baltic Sea area resulted in a temperature increase of 0.85 °C during the last century (Meinke and Reckermann 2012). Regional modeling studies project a further warming in the range of 2 to 5 °C during the 21st century. This would increase sea surface temperature concomitant with a decrease in sea ice and an increase in precipitation in winter (Meinke and Reckermann 2012). Other regional simulations also project a decrease in salinity for the Baltic Sea (Helcom 2007). The projected surface water temperature increase may decrease the vertical convective mixing in spring and autumn with negative consequences for the circulation of nutrients from the deep to the upper layers. These climate induced hydrological changes will affect the ecosystem of the Baltic Sea, probably influencing bacterial production, phytoplankton and zooplankton development and distribution, and consequently also fish and other components of the Baltic Sea food-web.

The pelagic food web – organic matter production and removal processes

How carbon/CO_2 enters the ocean

The atmospheric CO_2 enters the ocean via two processes: 1) the so called "solubility pump", whereby CO_2 physically/chemically dissolves in seawater; 2) the "biological carbon pump", a suite of processes of inorganic carbon fixation by autototrophic organisms into organic matter (OM) in the euphotic zone, transformation of this OM by food web processes (Fig. 1-3) and its transport from the surface to the ocean's interior. In the classic pelagic food web, nutrients and CO_2 are used for photosynthesis by large chain forming diatoms that are then grazed on by zooplankton, most often copepods. In high- and mid-latitude oceans dense phytoplankton blooms develop when the well mixed surface ocean waters are provided with sufficient light in spring. Under these conditions, phytoplankton can grow exponentially. As a result, zooplankton are often not able to ingest the totality of the sudden food accumulation and intact phytoplankton cells sink in aggregates to deeper waters.

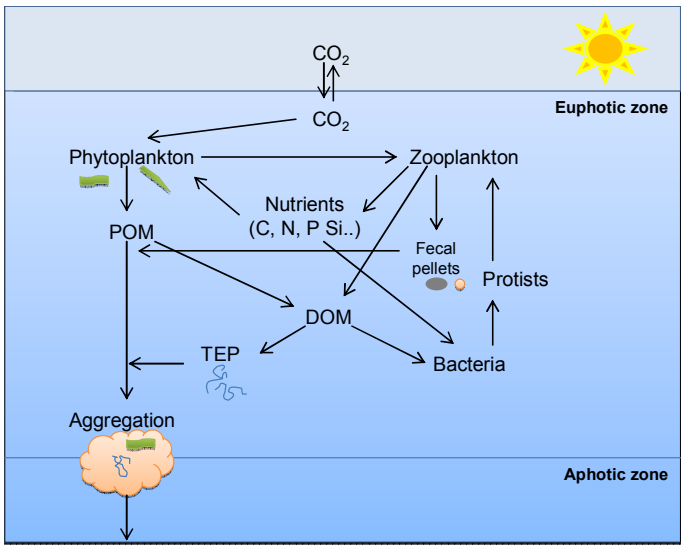

Figure 1-3:
Simplified scheme of the pelagic food-web and the here relevant organic matter production and removal processes.

Passive sinking of particulate carbon (including fecal pellets), vertical migration of zooplankton, and down-mixing of dissolved organic matter (DOM), are the main pathways how OM is transferred to the ocean's interior (Ducklow et al. 2001). The biological carbon pump can be separated into the organic carbon or soft-tissue pump and the calcium carbonate or hard-tissue pump, with the latter referring to the biologically mediated incorporation of carbon in calcium carbonate ($CaCO_3$) shells. Globally, photosynthetic carbon fixation by marine phytoplankton accounts for ~50 % and leads to formation of ~45 Gt of organic carbon per year (Field et al. 1998). An average of 16 Gt C yr^{-1} are exported to the deep (Falkowski et al. 1998). The $CaCO_3$ pump is estimated to account for about one tenth of the organic carbon pump (Sarmiento et al. 2002). Even small changes in the biological carbon pump, e. g. triggered by climatic changes, can have important feedbacks on the marine carbon cycle and atmospheric CO_2 concentration. The proportion of organic material that sinks below the thermocline is excluded from further decomposition and sequestered on time scales of hundreds or thousands of years (Falkowski et al. 1998). On geological time scales, the formation of calcium carbonate ($CaCO_3$) is the most important mechanism for the absorption of CO_2 as 50×10^{15} t CO_2 are bound in limestone and 12×10^{15} t in organic sediments (Lalli and Parons 1997).

The elements nitrogen and phosphorus

Not only carbon is important for the formation of particulate and dissolved material and its transport from the euphotic zone to the deep. Quantitatively important nutrients for phytoplankton growth are nitrogen, especially nitrate (NO_3^-), phosphate (PO_4^{3-}), and for some species, silicate ($Si(OH)_4$) (like e.g., diatoms or silicoflagellates that incorporate it into their frustules). The nitrogen cycle is complex as seawater contains four important forms of nitrogen for phytoplankton: gaseous molecular nitrogen (N_2), and dissolved

inorganic nitrogen (DIN) in the forms nitrate (NO_3^-), nitrite (NO_2^-), and ammonium (NH_4^+). N_2 is not readily available to most organisms, but can be fixed into organic matter by diazotrophic microorganisms such as cyanobacteria. This process plays a very important role in oceanic nitrogen cycling (Carpenter and Capone 2008).

Phosphorus (P) is an essential element contained in e. g. DNA, RNA, ATP and in cell membranes as phospholipids. Phosphorus is delivered to the ocean by continental weathering and discharge by rivers. Additionally, in some oceanic regions, atmospheric P deposition by volcano, mineral dust and aerosols can be important (Paytan and McLaughlin 2007). Dissolved inorganic carbon (DIP) in the sea is mainly present as orthophosphate (PO_4^{3-}), which plays a key role in photosynthesis. Although, one traditional concept in biogeochemistry is that new and regenerated production is strictly based on nitrate and ammonium availability (Dugdale and Goering 1967), in recent years it has been recognized that phosphorus can also be limiting in some oceanic regions (Cotner et al. 1997; Krom et al. 2004; Thingstad et al. 2005).

N and P are regenerated by bacteria or by the excretion of marine animals. The most important of these is the excretion of ammonium by zooplankton. Depending on the stoichiometric properties of the phytoplankton and the zooplankton species, the nutrient recycling due to grazing can differentially deliberate N or P (Elser and Urabe 1999; Sterner and Elser 2002) and provide feed back for autotroph growth (Ketchum 1962; Lehman 1980; Sterner 1986).

Dissolved organic matter

During algae growth particulate and dissolved organic matter (DOM) is produced. Most of the production of DOM occurs in the surface ocean and results from a temporal decoupling of production and consumption processes. DOM sources are extracellular release of healthy or senescent phytoplankton cells, bacterial release, release as a consequence of cell lysis due to grazing or viral infection, and solubilisation of particles (e. g. fecal pellets). Main sinks for DOM are bacterial consumption, photodegradation that occurs when seawater or freshwater DOM is exposed to natural sunlight (Mopper et al. 1991) and vertical and lateral transport by water masses.

The pool of dissolved organic carbon (DOC) accounts for ~700 Pg C (Williams and Druffel 1987; Hansell and Carlson 1998b), an about 200times larger carbon pool than the whole biomass in the sea (Hansell et al. 2009). Typical surface ocean (<1,000 m) DOC concentrations range from 50 to 70 µM (Sharp et al. 1995; Loh and Bauer 2000), and decrease with depth to deep ocean (>1,000 m) concentrations of 35 to 45 µM (Sharp et al. 1995; Hansell and Carlson 1998b; Loh and Bauer 2000). The Baltic Sea, due to its estuarine character, has much higher DOC concentrations than open ocean surface waters, typically ranging between 240 to 340 µmol C L^{-1} (Nausch et al. 2010).

Biological labile DOC is the smallest proportion of total DOC, contributing up to 6 % (Carlson and Ducklow 1995; Cherrier et al. 1996). It has fast turnover times and is composed of high and low molecular weight compounds (HMW defined as >1000 Da, LMW defined as < 1000 Da). Semi-labile DOC (LMW and HMW) is more resistant to biological decomposition, has turnover time scales of months to years and accounts for 15-20 % of net community production (Hansell and Carlson 1998a; Hansell et al. 2009). Semi-labile DOC is the fraction that is transported to deeper water bodies by convergence transport, down-welling or deep-water formation (Copin-Montégut and Avril 1993; Hansell and Carlson 2001; Hansell et al. 2009). Water that ventilates the deepest layers can provide effective sequestration of DOC for hundreds of years (Hansell et al. 2009). The largest part of DOC is biologically refractory and is dominated by LMW compounds. It is resistant to microbial degradation and has turnover times of centuries to millennia (Carlson 2002).

Polysaccharides are the main characterized part of DOM (Biddanda and Benner 1997; Biersmith and Benner 1998). They are generated in huge amounts by phytoplankton cells and are released to the surrounding water during mass development of phytoplankton (Ittekkot 1982; Myklestad 1995; Søndergaard et al. 2000). Extracellular release (ER) depends on multiple factors, such as temperature, light intensity, nutrient status and community structure, and is a normal process of autotrophic growth (Carlson 2002). The amount of ER by phytoplankton is highly variable and can yield up to 80 % of carbon fixed by primary production during the decline phase of a bloom (Nagata 2000 and references herein). Two mechanisms have been proposed to explain extracellular production by autotrophs, the “overflow” and the “passive diffusion” models (Fogg 1966). For both models support exists in the literature (see Carlson 2002 and references herein). According to the overflow model, photosynthates that are produced faster than can be incorporated by the cell may be actively released. The author argues that this may be due to the fact that photosynthesis is primarily controlled by light, whereas cellular growth is controlled by the availability of nutrients. Releasing the excess is hence energetically more favourable. In this case, DOM exudation should correlate with the photosynthetic rate. In the passive diffusion model, LMW DOM, such as neutral sugars, nitrogenous compounds and free amino acids, diffuse through the cell membrane (Fogg 1966) and the gradient is maintained by the uptake of LMW compounds by bacteria (Bjørnsen 1988). In this case ER should correlate with phytoplankton biomass (Bjørnsen 1988).

Dissolved organic nitrogen (DON) concentrations in ocean surface waters range between 2 to 8 µM (deep sea 2 to 3 µM) (Holm-Hansen et al. 1966; Loh and Bauer 2000). Baltic Sea DON concentrations are on average higher and can range between 13-18 µM (Nausch et al. 2010). Identified bioavailable LMW key substrates of DON are

urea, dissolved combined amino acids (DCAA), and dissolved free amino acids (DFAA). These can be taken up by bacteria and partially also by phytoplankton (Berman and Bronk 2003). Dissolved organic phosphate (DOP) surface concentrations range from 0.1 to 0.4 µM and decrease to deep ocean concentrations of 0.06 to 0.15 µM (Holm-Hansen et al. 1966; Loh and Bauer 2000). Bacteria and some phytoplankton have the ability to utilize DOP compounds (Karl and Björkman 2002).

Stoichiometry

The Redfield ratio, a tenet in biogeochemistry, describes an average molar ratio of carbon to nitrogen to phosphorus of phytoplankton in the ocean of 106:16:1 (CNP-ratio). Although generally this holds true, deviations from this concept are also often observed (Geider and La Roche 2002; Sterner and Elser 2002). Sterner and Elser (2002) suggested that for a nutrient *X*, the carbon (C) to *X* ratio of the autotroph (marine) biomass increases with limitation of *X* and with increasing light intensity. Certain phototrophic organisms have the ability to store C in the form of lipids or carbohydrates, or a P-sparing effect may be observed for some microorganisms, thereby producing biomass with C:P and N:P ratios that exceed Redfield-ratios. P can also be stored by the cell leading to decreased C:P and N:P ratios (Karl and Björkman 2002). Organic matter in the water column is first depleted in phosphorus and nitrogen by consumption and recycling, with the consequence that carbon accumulates and the C:N and C:P increases (Clark et al. 1998; Shaffer et al. 1999; Loh and Bauer 2000). Only particles with high sinking velocity have the chance to reach the seabed in Redfield proportions of C:N 6:1, where the material is further processed by benthos inhabitants and bacteria. C:N:P ratios of DOM ratios deviate substantially from Redfield ratio (DOM C:N:P 300:22:1, (Benner 2002), indicating a depletion of DOM in N and P compared with the bulk of phytoplankton.

The microbial loop

With the discovery of the importance of marine bacteria the ‘microbial loop’ came into recognition (Azam et al. 1983). Heterotrophic bacteria consume DOM and are then themselves grazed by protists, mainly heterotrophic nanoflagellates. These protists are in turn grazed upon by other protists and finally larger zooplankton, such as copepods, linking the microbial food web to the `classical´ food-web (Bernard and Rassoulzadegan 1990) (Fig. 1-3). In the microbial loop, DOM is hence transferred via bacteria back to the mesozooplankton. Up to 50 % of the DOC from primary production is channelled into bacterial secondary production (Williams 2000). In some oceanic regions bacterial respiration is the major component of total respiration. Thus, changes in bacterial respiration can constrain organic matter remineralisation and export of carbon. Bacterial growth efficiency, calculated from bacterial production (BP) and respiration (BR) (BGE

= BP/(BP+BR) was found to display a strong relationship with temperature and decrease from about 0.5 in polar to about 0.2 in tropical oceanic regions (Rivkin and Legendre 2001).

Microparticles TEP and CSP

Free DOM polymers that are not incorporated into the microbial food web can assemble to form gels (within minutes to hours) (Chin et al. 1998). An estimated ~10 % of DOM (~70 Pg C) is in the form of gels, representing a pathway for the transition from the DOM to the POM pool (Engel et al. 2004; Verdugo et al. 2004). Changes in the production and bacterial utilization of DOM may therefore also affect the POM pool. One ubiquitous class of gels are transparent exopolymer particles (TEP), discrete, transparent, gelatinous particles that form from polysaccharide precursors that can be visualized with the dye Alcian Blue (Alldredge et al. 1993). TEP are abundant in fresh and marine water and occur in the size class of > 5 µm in concentrations of up to 8,000 mL^{-1}, and > 2 µm up to 40,000 mL^{-1} (Passow 2002b). TEP play an important role in aggregation processes of phytoplankton (Passow et al. 1994; Engel and Schartau 1999; Passow 2002b), because of their high surface-active nature (stickiness) (Engel 2000; Kahl et al. 2008). The abiotic formation of TEP from dissolved organic precursors may therefore play an important role for the export of organic matter to the deep ocean.

Another important component of DOM are proteins, which can coagulate to form particles, the so-called coomassie stainable particles (CSP), since they stain with the protein dye Coomassie Brilliant Blue. CSP can be as abundant as TEP or occur in seawater at higher concentrations than TEP (Long and Azam 1996) or at lower abundances than TEP with high fluctuations during the year for both particle types (Berman and Viner-Mozzini 2001). Although CSP were found to play a minor role compared with TEP in aggregation dynamics (Prieto et al. 2002), they are often colonized by bacteria (Long & Azam 1996) and may therefore also play an important role as hot spots for nutrient recycling and as a food source for micrograzers (Berman & Viner-Mozzini 2001).

Biological responses to climate change and biogeochemical feedbacks

Temperature-dependency of biological processes

Temperature is the key factor for regulating metabolic processes as biochemical reactions are directly temperature-dependent, like the activity of enzymes. It was hence suggested that metabolic rate controls all levels of organization from individuals to the biosphere (Brown et al. 2004). In general, autotrophic processes, such as phytoplankton growth,

show a smaller sensitivity to temperature changes than heterotrophic processes, like bacterial growth. The Q_{10} describes the factorial increase of a process due to an increase in temperature of 10 °C. Pomeroy and Wiebe (2001) report that bacterial growth increased with a Q_{10} between 2-3, whereas phytoplankton growth increases with a Q_{10} between 1-2 (Eppley 1972). Likewise, metabolic rates (oxygen consumption, ammonium and phosphate excretion) of marine copepods increased with temperature in a Q_{10} range between 1.6 and 2.1 (Ikeda et al. 2001). Thus, an increase in temperature could lead to a more stringent top-down control of phytoplankton, or to enhanced heterotrophy and flux of carbon into the microbial loop. Hence, climate warming likely changes the balance between sources and sinks of organic matter in the surface ocean with consequences for the partitioning between particulate and dissolved pools of primary produced organic matter.

So far observed temperature effects on planktonic primary producers include an advancement in phytoplankton growth onset (Sommer & Lengfellner 2008, Sommer et al. 2012) and a general reduction of cell size with warming (Daufresne et al. 2009; Morán et al. 2010; Lewandowska and Sommer 2010). Additionally, a tighter bacteria-phytoplankton coupling was reported with warming (Hoppe et al. 2008), an increase in bacterial secondary production and community respiration (Wohlers et al. 2009), and a general shift in the balance from autotrophic to heterotrophic processes (Müren et al. 2005; O'Connor et al. 2009). Additionally, elemental stoichiometry of phytoplankton can change in response to temperature change (Berges et al. 2002). Some studies detected negative effects of rising temperature on phytoplankton biomass (Keller et al. 1999; O'Connor et al. 2009; Lassen et al. 2010) or, as a consequence of an enhancement in ocean stratification, on primary production (Behrenfeld et al. 2006). Some of those studies related the negative effect of warming on phytoplankton biomass to increased abundances of zooplankton (Keller et al. 1999; O'Connor et al. 2009). A recent mesocosm experiment found that respiration and ingestion rates of the copepod *Pseudocalanus sp.* increased by a factor of 3 for a 6 °C temperature increase (Isla et al. 2008).

Studies addressing changes in biogeochemical processes in the plankton community due to warming are still scarce or contradictory. While Wohlers et al. (2009) found a decrease in the biological drawdown of dissolved inorganic carbon with increasing temperature; Taucher et al. (2012) observed enhanced dissolved inorganic carbon consumption in response to warming, leading to increased accumulation of particulate and dissolved organic carbon. However, a uniform result was that the accumulation of organic matter in the dissolved phase increased due to experimental warming (Engel et al., 2011; Kim et al., 2011; Taucher et al., 2012; Wohlers et al., 2009).

A temperature dependent abiotic aggregation of dissolved and colloidal organic matter seems likely, as the underlying processes, e.g. Brownian motion and the conformation of macromolecules, are temperature sensitive. It was shown that TEP-mediated aggregation of the diatom *Skeletonema costatum* positively correlated with temperature (Thornton and Thake 1998). Aggregates grown at an elevated temperature in roller tank experiments also increased their aggregation potential compared to the ambient temperature treatment, probably due to the higher concentrations of TEP at elevated temperatures (Piontek et al. 2009).

Interactive responses to climate change

Climate change affects marine ecosystem function and biogeochemical cycling in the oceans in many ways (Riebesell et al. 2009). Several environmental factors have the potential to interact synergistically or antagonistically with major biogeochemical parameters. Aside from direct temperature effect, biological processes are controlled by a variety of other abiotic factors, including light and nutrient or substrate availability, and biotic interactions on the ecosystem level, such as grazer and bacteria abundance and activity. The response of the biological processes to these interacting factors will determine the future direction of the biological carbon pump.

After the recognition of the so called "other CO_2-problem" (Doney et al. 2009), that is the observed decrease in ocean surface pH, a lot of effort went into the investigation of biological responses to ocean acidification. While a stimulating effect of CO_2 was found for primary production, it was also shown that many organisms, especially those who incorporate $CaCO_3$ into their shells, are sensitive to changes in water pH (Riebesell and Tortell 2011 and references herein). As an example, the prominent coccolithophore *Emiliania huxleyi* decreased its particulate inorganic carbon (PIC or $CaCO_3$) to POC ratio with increasing CO_2 concentrations (Riebesell et al. 2000; Zondervan et al. 2002). $CaCO_3$ and opaline silicate (biogenic silicate in the frustules of diatoms) act as ballast for particle aggregates sinking through the water column (Armstrong et al. 2001; Klaas and Archer 2002). An experiment with *E. huxleyi* has shown that as a consequence of low PIC to POC at high CO_2 concentrations, aggregates decreased their porosity and their sinking velocity (Biermann and Engel 2010). To understand particle fluxes it is hence crucial to know how much of the dissolved inorganic carbon flows into particulate material and how much into dissolved organic material, which is usually quickly consumed. It should be noted however, that the response of coccolithophores to increasing CO_2 concentrations was also found to be species specific (Langer et al. 2006). Hence, the phytoplankton species composition has the potential to modulate positive or negative feedbacks in the community level response to rising CO_2 levels.

Changes in nutrient input may also have profound effects on the marine biota. Human activities have led to an increased nutrient input in coastal areas through river and groundwater discharge and atmospheric deposition, thereby changing N:P:Si ratios (Jickells 1998). Temperature and nutrient stoichiometry interactively modulated organic matter cycling in a batch culture experiment (Wohlers-Zöllner et al. 2011).

In (aquatic) photosynthetic organisms the abiotic factors temperature and light are tightly connected. The initial photochemical response of photosynthesis depends upon light availability and is in general independent of temperature, but photosynthetic carbon assimilation is enzymatically controlled and thereby temperature-dependent (Falkowski and Raven 2007). It has been suggested that only the light saturated rate of photosynthesis is affected by temperature (Falkowski and Raven 2007) and that the response of photosynthesis at light-limitation could thus be different (Davison 1991). For the ubiquitous marine diatom *Skeletonema costatum* and other algae it is well known that maximum photosynthetic rate at light saturation increases with temperature as an immediate or seasonal effect (Kirk 1983; Davison 1991). The relationship between primary production and ocean warming might, however, be more complicated on the community level, since different species have varying abilities to acclimate to environmental changes.

As heterotrophic processes are in general more sensitive to temperature, a strengthening in consumer control over primary consumers is expected with increasing sea surface warming (O'Connor et al. 2009). The analysis of a set of mesocosm experiments, (Gaedke et al. 2010) showed that biotic interactions, via grazing and the success of overwintering phyto- and zooplankton, may overrule direct climatic effects like temperature on spring phytoplankton bloom dynamics. An observed retardation in the phytoplankton spring bloom off Helgoland, North Sea, despite an increase in water temperature, led to the hypothesis that stronger grazing rates and an earlier increase in copepod populations could have caused the delay (Wiltshire and Manly 2004; Wiltshire et al. 2008).

Aim of the study

The aim of this study was to investigate the impact of temperature on biogeochemistry, specifically exploring the temperature-dependency of carbon partitioning between dissolved and particulate organic matter in a marine pelagic ecosystem, taking into consideration the effects of irradiance and grazer abundance. For this purpose, three experimental studies have been conducted at Geomar, Kiel, within the "Kiel mesocosm cluster" as part of the priority programme "AQUASHIFT" of the Deutsche Forschungsgemeinschaft (DFG). AQUASHIFT investigated the impact of climate warming on aquatic ecosystems. During the first funding period, the "Kiel mesocosm cluster" conducted 4 experiments with eight mesocosms containing the natural plankton community of Kiel Bight, exposed to 4 temperature settings (*in situ*, + 2 °C, + 4 °C, + 6 °C) with equal light regimes for each study. This thesis is based on three mesocosm experiments from the second funding period, but a deployed meta-analysis approach also considers results from the mesocosm experiments of the first funding period. One primary focus of the thesis was the influence of light intensity. Climate warming is likely changing the underwater light climate through the physical coupling of temperature and water column stratification as a consequence of winter warming; and through increasing cloudiness and precipitation. Primary production is a function of light and hence organic matter accumulation, composition and quality ultimately depend on the light regime. Additionally, the first set of mesocosm experiments revealed that temperature might affect grazing rates and the abundance of over-wintering populations of zooplankton, thus potentially leading to a strong climate related top-down effect on the spring bloom. Hence, a second focus of this thesis was on a potential top-down control on the spring bloom.

To address the potential importance of light climate and zooplankton grazers during winter/spring blooms, the "Kiel mesocosm cluster" conducted three independent mesocosm experiments with the natural winter plankton community from Kiel Bight, Baltic Sea. The first experiment in 2008 focused on the combined effects of temperature and light. The second experiment in 2009 addressed the effects of grazer abundance at two different temperature levels. Finally, the third experiment in 2010 investigated the effect of high and low light conditions.

In Chapter 1 and **2** I will present results from two mesocosm studies which compared the natural plankton community when exposed to the present-day, seasonal, *in situ* temperature of the study site, and to an elevated temperature of *in situ* + 6 °C, according to the most drastic scenarios projected by the Intergovernmental Panel on Climate Change (IPCC) (Meehl et al. 2007). Experiments were conducted with twelve mesocosms deployed in climate chambers, each individually controlled by a light system.

In Chapter 1 I address the effects of temperature in combination with three irradiance levels of 49 %, 57 %, 62 %, corresponding to a light reduction due to cloud cover or higher attenuation of sea surface irradiance. I analyzed changes in the dissolved inorganic nutrient pools and the dissolved and particulate organic matter pools of carbon, nitrogen, phosphorus and silica. In addition, I analyzed specific parts of the dissolved organic matter pool (carbohydrates); and I observed particle dynamics by means of transparent exopolymer particles.

Chapter 2 considers the effects of temperature in combination with three different grazer (copepod) densities (1.5, 4, 10 individuals L^{-1}) on the partitioning between dissolved and particulate organic matter pools. I present results for dissolved and particulate C, N, P (and Si) and study the stoichiometry of these elements in response to temperature and grazing. Additionally, I analyze carbohydrates and transparent exopolymer particles.

Chapter 3 is a comparative data analysis on selected "cardinal points" with data of two studies conducted in the first funding period and data from chapters 1 and 2 of this thesis (second funding period). This study aims to identify recurrent patterns of organic matter production, stoichiometry and degradation in response to an increase in water temperature.

In **Chapter 4** I present results from a mesocosm study on the effects of cloudy and sunny weather conditions on the plankton community exposed to *in situ* temperature + 2 °C. In addition to a close look on the partitioning between dissolved and particulate matter pools, I analyse abundance and size of transparent exopolymer particles. These are known to have high carbon:nutrient ratios in comparison to coomassie stainable particles that are of proteinaceous nature. Thus I attempt to elucidate the importance of the latter during our winter/spring blooms and to investigate the flow of carbon and nutrients in these particulate matter pools.

The indoor mesocosm system at Geomar, Kiel

Chapter 1

Changes in organic matter cycling in a plankton community exposed to warming under different light intensities

Abstract

To investigate the combined effect of temperature and light availability on organic matter production and degradation during a winter/spring phytoplankton bloom in Kiel Bight, we conducted a mesocosm study applying two temperature regimes, ambient (T+0) and plus 6 °C (T+6) and three irradiance levels. Rising temperature accelerated the onset of the phytoplankton bloom, while light intensity played only a minor role for the timing and bloom development. Maximum build-up of chlorophyll *a* and particulate organic carbon were ~20 % lower at T+6 compared to T+0, probably caused by a combination of elevated heterotrophic processes and enhanced sedimentation during the bloom. The latter is supported by increased TEP concentrations at T+6 (TEP/POC 0.18 mol C/mol C) compared to T+0 (0.11 mol C/mol C) during bloom conditions, which may have promoted cell aggregation and sinking. Dissolved organic carbon concentrations increased more rapidly at elevated temperature. For a warmer future ocean, we can hence expect two counteracting mechanisms controlling organic matter flow during phytoplankton blooms: 1) enhanced processing of organic matter via the microbial loop resulting in a faster recycling, and 2) depending on the dominating phytoplankton species, enhanced TEP formation resulting in increased particle aggregation and thus export of carbon and nutrients.

Introduction

Ocean warming affects all levels of biological organization, from individuals to the ecosystem, as temperature is a key factor for regulating metabolic processes. Due to different temperature sensitivities of autotrophic and heterotrophic organisms shifts in the balance between primary production and organic matter remineralization can be expected, likely changing biogeochemical cycling in the oceans. In general, autotrophic processes like phytoplankton growth show a lower sensitivity to temperature changes (Eppley 1972) than heterotrophic processes, like bacterial growth (Pomeroy and Wiebe 2001) and metabolic rates of herbivorous grazers like marine copepods (Ivleva 1980; Ikeda et al. 2001; Isla et al. 2008).

In the ocean, elevated temperature will be accompanied by increased water column stratification (Prentice et al. 2001). In the tropics and mid-latitude oceans, phytoplankton is often nutrient-limited and a further increase in stratification will reduce the mixing and the supply of nutrients (Doney 2006). In high latitude oceans phytoplankton are typically light-limited and a reduced mixing would keep the plankton at the surface were light levels are high (Doney 2006). An intensified stratification of low-latitude oceans due to climate warming is believed to be the major cause for the decrease in net primary production observed with satellite measurements of ocean colour between the years 1999-2006 (Behrenfeld et al. 2006).

In (aquatic) photosynthetic organisms the abiotic factors temperature and light are tightly connected, since the initial photochemical response of photosynthesis depends upon light availability and is in general independent of temperature, while photosynthetic carbon assimilation is enzymatically controlled and therewith temperature-dependent (Falkowski and Raven, 2007). It was suggested that only the light-saturated rate of photosynthesis is affected by temperature (Falkowski and Raven, 2007) and the response of photosynthesis at light-limitation can thus be different from that at light-saturated levels (Davison 1991). For the ubiquitous marine diatom *Skeletonema costatum* and other algae it is well known that maximum photosynthetic rate at light saturation increases with temperature as immediate or seasonal effect (Kirk 1983; Davison 1991). The relationship between primary production and ocean warming might, however, be more complicated on the community level, since species have different abilities to acclimate to environmental changes. A changing light environment may also affect the stoichiometry of phytoplankton, as principally the carbon to nutrient ratio increases with light intensity under limitation of the investigated nutrient (Sterner and Elser 2002). When nutrients are exhausted and photosynthesis continues, accumulating photosynthetic products can no longer be used for cell growth and are released through the outer cell membrane, a process that has been termed as ‘overflow’ or ‘passive diffusion’ production (Fogg 1966; Bjørnsen 1988).

Extracellular release (ER) depends on multiple factors like temperature, light intensity, nutrient status and community structure (Carlson 2002). ER can account for up to 80 % of carbon fixed by primary production during the decline phase of a bloom (Nagata 2000). Dissolved organic carbon (DOC) excretion by phytoplankton was found to increase with increasing light levels (Verity 1981a; Zlotnik and Dubinsky 1989) and increasing temperature (Morán et al. 2006). While bacterial consumption often causes fast depletion of fresh and labile DOC (Kirchman et al. 1991), an estimated 17 % of global new DOC production accumulates as semi-labile DOC in the surface waters (Hansell and Carlson 1998a). This fraction is available for export to the deep ocean. During phytoplankton blooms, the major fraction of DOM consists of polysaccharides (Ittekkot et al. 1981; Søndergaard et al. 2000). These polysaccharides can aggregate into transparent exopolymeric particles (TEP), thereby causing the transition from the DOM to the POM pool (Engel et al. 2004; Verdugo et al. 2004). Temperature or light dependent changes in the production and bacterial utilization of DOM may therefore also affect the POM pool. A linear relationship was observed between photosynthesis and TEP production for three diatom species (Claquin et al. 2008). Additionally, TEP play an important role in aggregation processes of phytoplankton (Passow and Alldredge 1995a; Engel and Schartau 1999; Passow 2002b). It was shown that TEP-mediated aggregation of the diatom *Skeletonema costatum* positively correlated with temperature (Thornton and Thake 1998). Hence, enhanced sedimentation due to elevated TEP concentrations could counteract intensified heterotrophic removal processes in a warmer surface ocean.

Mesocosm studies with Baltic Sea plankton communities revealed that peak biomass was negatively affected by increasing temperature, concomitant with a decrease in the contribution of larger diatoms to the phytoplankton community (Sommer and Lengfellner 2008). In line with those results, other mesocosm studies report of temperature effects on species abundance and a reduction in phytoplankton biomass at elevated temperatures (Müren et al. 2005; Lassen et al. 2010). Studies addressing biogeochemical changes due to warming in a plankton community are still scarce or contradictory. While Wohlers et al. (2009) found a decrease in the biological drawdown of dissolved inorganic carbon to increasing temperature, Taucher et al. (2012) observed enhanced dissolved inorganic carbon consumption in response to warming leading to increased accumulation of particulate and dissolved organic carbon. The accumulation of organic matter in the dissolved phase increased due to experimental warming (Wohlers et al. 2009; Engel et al. 2010; Kim et al. 2011; Taucher et al. 2012). The role of light intensity was not explicitly investigated in those former studies addressing biogeochemical responses to warming. Therefore, the aim of this mesocosm study was to disentangle the effects of light and temperature on the partitioning and stoichiometry of organic matter during a phytoplankton bloom in a two factorial experiment with two

temperature settings (ΔT+6 °C and ΔT+0 °C) and three light settings (high, intermediate, low).

Material and Methods

Experimental setup

The indoor-mesocosm experiment started on 4 February, 2008 and lasted until 19 March, 2008. Twelve 1400-L mesocosms were set up in climate chambers and filled with seawater with a salinity of 17.6 from Kiel Bight (Western Baltic Sea), containing the natural winter/spring plankton community (phytoplankton, bacteria, and protozoa) with an initial water temperature of 4.1°C. For more details on the mesocosm set-up see Sommer et al. (2007) and Lewandowska and Sommer (2010). Mesozooplankton, dominated by the copepod *Oithona* sp., was added from net catches yielding a density of 8 individuals L^{-1}. The T+0 temperature of ΔT = 0 °C was derived from the decadal (1993 – 2002) mean sea surface temperatures in Kiel Bight and applied to six mesocosms. Over the whole experimental period, the T+0 treatment yielded an average temperature of 2.7 ± 0.3 °C. For the other 6 mesocosms a temperature elevation of ΔT = 6 °C (T+6) was chosen according to the A1F1 scenario of the Intergovernmental Panel on Climate Change for the end of the 21st century (Meehl et al. 2007). The T+6 treatment yielded a temperature of on average 8.3 ± 0.3 °C.

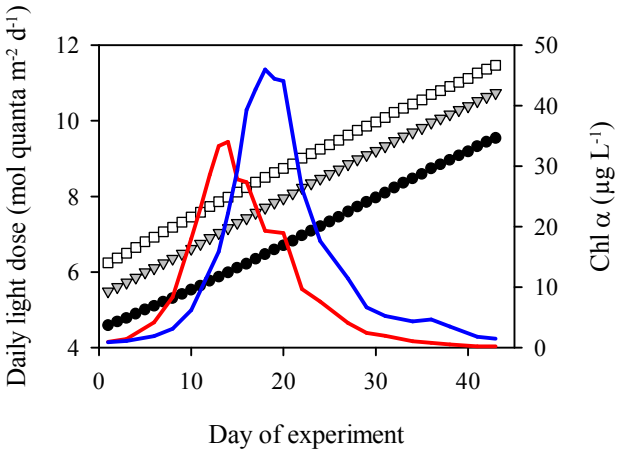

Figure 1-1: Daily light dose over the course of the experiment. Black dots = LL, grey triangles = IL, white squares = HL. Solid red line shows the average concentration of chlorophyll *a* (Chl *a*) for T+6, solid blue line the average Chl *a* concentration for T+0.

The light system simulated daily irradiance curves and a seasonal light pattern calculated from astronomic equations according to Brock (1981), controlled by a computer programme (GHL, Prometeus). For duplicate mesocosms the daily light dose was adjusted to a high light regime (HL ~ 8.9 mol quanta $m^{-2}d^{-1}$), an intermediate light regime (IL ~ 8.2 mol quanta $m^{-2}d^{-1}$) and a low light regime (LL ~ 7.0 mol quanta $m^{-2}d^{-1}$), corresponding to 104, 95, and 81 µmol photons m^{-2} s^{-1}, representing 62 %, 57 %, and 49 % of surface irradiance. HL represented a mixed water column mean daily light dose

at a cloudless day of 10 m water depth and a vertical attenuation coefficient of 0.18 m^{-1}. The two illuminating devices on top of each mesocosm were equipped with 12 full spectrum light tubes (10 solar tropic T5 Ultra, 4,000 K, 2 solar nature T5 Ultra, 9,000 K, JBL). The virtual start point for the light programme was set to be 15 February. Then the daily light dose increased over the duration of the experiment (Fig. 1-1).

Initial nutrient concentrations were 10 µmol L^{-1} nitrate, 1.1 µmol L^{-1} nitrite, 1.3 µmol L^{-1} ammonium, 0.9 µmol L^{-1} phosphate, and 29.5 µmol L^{-1} silicate. In order to obtain a Redfield N/P ratio of 16, and to make the experiment more comparable to former mesocosm studies (Sommer and Lengfellner 2008; Wohlers et al. 2009), 5 µmol L^{-1} nitrate in form of $NaNO_3$ were added one day before the first sampling (day 0). During the whole experiment, water inside the mesocosms was gently mixed with a propeller in order to keep cells and smaller particles in suspension, whereas larger particles and aggregates settled out of the water column. Sampling took place at least three times a week. Additional sampling was conducted during bloom conditions (e. g. days 11 and 12, days 18 and 19). Samples were taken with a silicone hose from the middle of the mesocosm water body between 08:30 and 09:00 in the morning (1 - 2 hours after lights turned on).

Analytical Methods

Temperature, salinity, and pH were measured with a WTW conductivity/pH probe on each sampling day at 0.2 m depth. Inorganic nutrients (nitrate, nitrite, phosphate, silicate) were determined with an autoanalyzer (AAII) according to Hansen and Koroleff (2007), and ammonium according to the method of Holmes et al. (1999) immediately after sampling or after overnight storage of the 0.2 µm (Filtropur, Sarstedt) filtrate. During bloom conditions samples were filtered through 5.0 µm cellulose acetate filters prior to nutrient analysis. For biogenic silicate (BSi) determination, 50 to 250 mL of sample were filtered onto 0.65 µm cellulose acetate filters (Sartorius) and stored at -20 °C until photometrical analysis according to Hansen and Koroleff (2007). Before analysis, BSi was converted to dissolved silicate by leaching with 0.1 M NaOH at 85 °C. For the determination of chlorophyll a (Chl *a*), between 100 and 500 mL were filtered onto glass fibre filters (GF/F, Whatman) and stored overnight at -20 °C. Pigment concentration was measured with a 10-AU Turner fluorometer after 90 % acetone (v/v) extraction (Welschmeyer 1994).

For particulate organic carbon (POC), particulate organic nitrogen (PN), and particulate organic phosphorus (POP) 100-500 mL of sample were filtered onto precombusted (500 °C, 8h) GF/F filters (Whatman) and stored at -20 °C. For the determination of POC and PN, filters were dried at 60 °C for 6 hours prior to analysis, and C and N concentrations measured with an elemental analyzer (EuroEA-3000,

Eurovector) according to Sharp (1974). POP was determined photometrically after the treatment with one dispensing spoon of Oxisolv® (Merck) (Hansen and Koroleff 2007).

Transparent exopolymer particles (TEP) concentration was determined colorimetrically (Passow and Alldredge 1995b). Samples were prepared in duplicate by gentle filtration (~ 150 mbar) of 5 to 50 mL sample onto 0.4 µm polycarbonate filters (Whatman) and staining with Alcian Blue. The dye was calibrated (f=175) with the standard polysaccharide Gum Xanthan before and after the experiment. The filters were stored at -20 °C until processing. The analysis was carried out by adding 80 % H_2SO_4 to the filters and measurement of supernatants absorption at 787 nm after 3 hours with a spectrophotometer (Hitachi U-2000). For the conversion from Gum Xanthan equivalents to carbon a factor of 0.63 (w/w) was applied according to Engel (2004). Samples for dissolved organic carbon (DOC) were filtered through precombusted (8 h, 500 °C) glass fibre filters (GF/F, Whatman) and collected in 20 mL precombusted glass ampoules. Then, 200 µL 85% H_3PO_4 was added, and the ampoules stored at 6 °C in the dark. DOC was analysed on a Shimadzu TOC_{VSH} using the HTCO method (Sharp et al. 1995). For dissolved carbohydrates (monosaccharides = M-CHO and polysaccharides = P-CHO) 15 mL of filtered sample was transferred into combusted glass vials and stored at -20 °C. For determination the 2,4,6-tripyridyl-s-triazine (TPTZ) spectrophotometric method was applied (Myklestad et al. 1997).

Calculations and statistics

Incline of particulate organic matter (POM): The slopes for the increase in Chl *a* and POM concentrations were fitted by best exponential fits ($y = e^{ax}$) for the growth phase (SigmaPlot 10.0). Rates for the increase of DOC, M-CHO and P-CHO were calculated by means of linear regression after phosphate was exhausted (DIP ≤ 0.1 µmol L^{-1}) until the end of the period of DOM increase (T+6) or until the end of the experiment (T+0) for each mesocosm. We applied an operational threshold of >3 µg Chl *a* L^{-1} (~ tenfold increase from the start of the experiment) for the definition of bloom conditions.

Statistics: Effects of temperature or light intensity were tested with general regression models (best subsets and R^2) with Statistica 8.0 (StatSoft), whereby temperature was defined as categorical and light as continuous factor.

Results

Bloom development and nutrient drawdown

A diatom-dominated phytoplankton bloom developed in each of the mesocosms. *Skeletonema costatum* contributed 55 % at T+6 and 19 % at T+0 to maximal total biomass. *Thalassiosira rotula* was more abundant at T+0 with 39 % of maximal total

biomass vs. 3 % of total biomass at T+6. The third most abundant species was *Rhizosolenia setigera* with 21 % at T+0 and 20 % of maximal total biomass at T+6. For a more detailed description of phytoplankton and zooplankton community see Lewandowska and Sommer (2010). The onset of the blooms was indicated by the decline of inorganic nutrients (Fig. 1-2), and by the rise of Chl *a* concentration (Fig. 1-3). Inorganic nutrients were depleted first at T+6 (Fig. 1-2). At T+6, nutrient drawdown occurred consecutively in HL, IL, and LL. However, a light effect on nutrient drawdown was not significant (p=0.39 for DIP). Dissolved inorganic phosphorus (DIP) was the first nutrient to become depleted, on day 12 ± 1 for T+6, and on day 15 ± 0 in all T+0 mesocosms. Then, dissolved inorganic nitrogen (DIN) followed by silicate (depleted on day 14 ± 1 in T+6, day 17 ± 0 in T+0) were diminished and remained below the detection limit for the rest of the experiment.

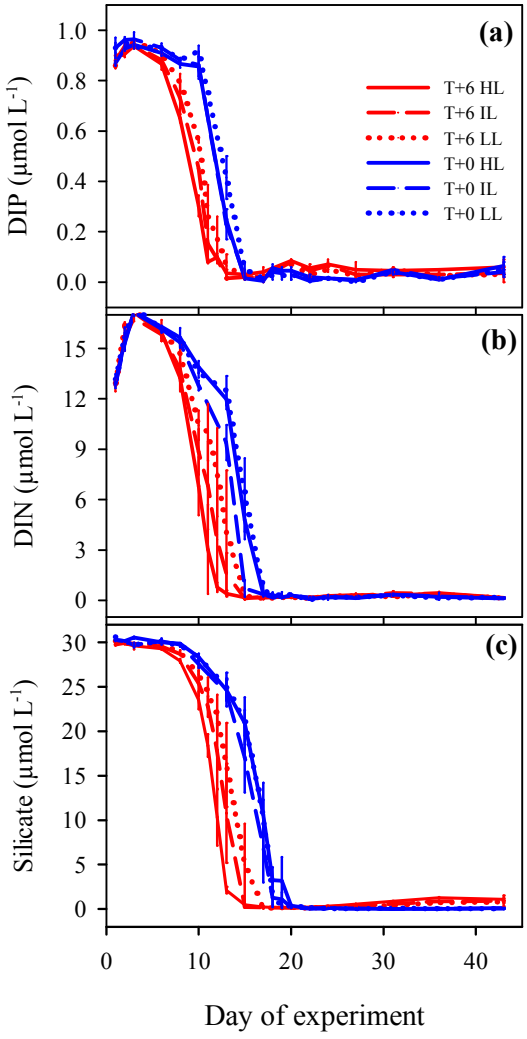

Figure 1-2: Nutrient drawdown ((a) DIP, (b) DIN, (c) silicate) in the treatments. Depicted are the mid points with range of the six temperature/light treatments during the course of the experiment. T+0 treatments are represented by the blue, T+6 treatments by the red colour, HL = solid, IL = dashed, and LL = dotted lines.

Consistent with the more rapid nutrient uptake, Chl *a* concentrations at T+6 peaked on average 4 days before T+0 (Fig. 1-3). The slopes of the exponential increase of Chl *a* and biogenic silica (BSi) differed significantly between T+0 and T+6 ($p < 0.001$, $p < 0.01$,

respectively) (Table 1). In line with a faster nutrient drawdown at higher light intensity in T+6, steeper slopes were observed for Chl *a* in the HL T+6, whereas a light effect was not detectable for the HL T+0. Chl *a* maximum concentration at T+6 was on average ~ 20 % less ($p < 0.001$) compared with T+0, while maximum BSi values were similar for all treatments (~ 26 µmol L^{-1}) (Fig. 1-3).

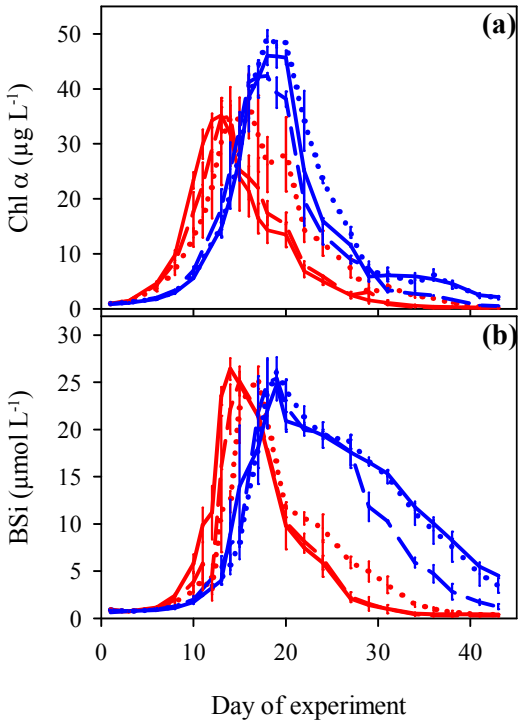

Figure 1-3: (a) Chlorophyll *a* (Chl *a*) and (b) biogenic silica (BSi) concentrations. (For more explanation see figure 1-2.)

Particulate organic carbon (POC), nitrogen (PN) and phosphorus (POP)

POC maximum concentrations were 220 ± 21.1 µmol L^{-1} at T+6 (Fig. 1-4) and therewith ~ 20 % less compared with maximum POC concentrations (284 ± 13.3 µmol L^{-1}) at T+0 ($p < 0.001$). Light significantly affected both POC peak timing ($p < 0.01$) and rise during exponential growth ($p < 0.05$) (Fig. 1-4, Table 1-1). POC concentration stayed above 50 µmol L^{-1} for about 27 days at T+0, 6 days longer than at T+6 ($p < 0.01$) (Fig. 4). Particulate nitrogen and particulate organic phosphorus (PN and POP) concentrations followed in general the development of POC (Fig. 1-4). Maximum peak concentration of PN and POP were negatively affected by temperature ($p < 0.001$, $p > 0.05$, respectively). In accordance with the slowest nutrient drawdown of all T+6 treatments, the bloom in the LL T+6 mesocosms took in an intermediate position with respect to timing and organic matter accumulation for POC, PN and POP and also for Chl *a* between T+6 and T+0 treatments (Figs. 1-4, 1-3).

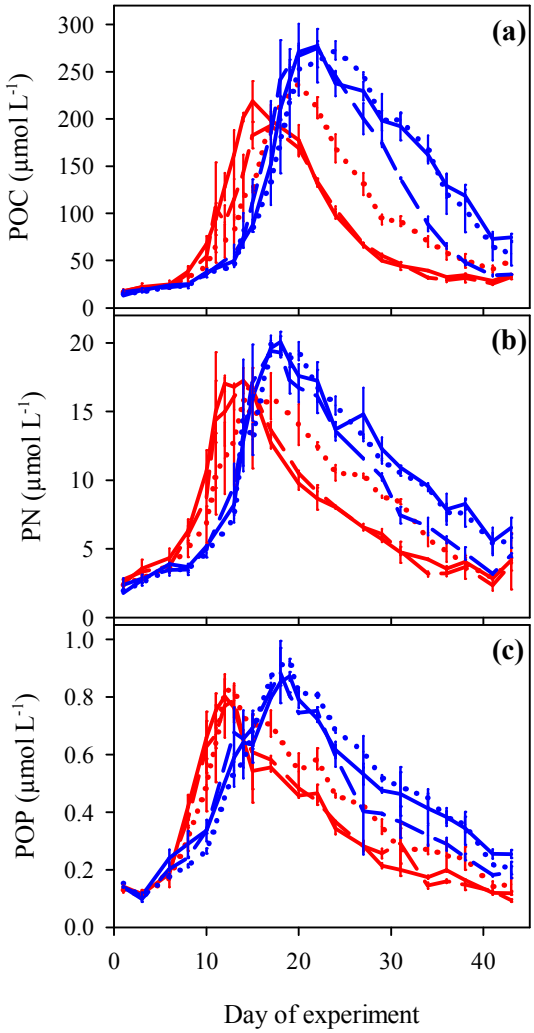

Figure 1-4: Concentrations of (a) particulate organic carbon (POC), (b) particulate nitrogen (PN) and (c) particulate organic phosphorus (POP). (For more explanation see figure 1-2.)

TEP formation pattern

Transparent exopolymer particles (TEP) increased at T+6 simultaneously with the phytoplankton bloom (Fig. 1-5). At T+6, the highest TEP concentration occurred significantly earlier (~ 10 days) than at T+0 ($p < 0.001$) (Fig. 1-5). In 5 out of 6 T+6 mesocosms, a decrease in TEP concentrations coincided with a sharp decrease in BSi, suggesting that some TEP was removed by aggregation and subsequent settling with diatom cells (Figs. 1-3, 1-5). Thereafter, TEP concentrations at T+6 stayed on a high level for the rest of the bloom-phase and for the degradation phase, beginning ~day 20. Along with a decline in Chl *a*, a drop in TEP occurred around day 20 at T+0 as well. But in contrast to T+6, TEP concentrations in all T+0 mesocosms slowly decreased after TEP maxima around day 24 (Fig. 1-5). Light effects were not detectable for T+0 treatments. For T+6 treatments a pronounced increase in LL T+6 during the degradation phase was observed in one mesocosm (no. 3).

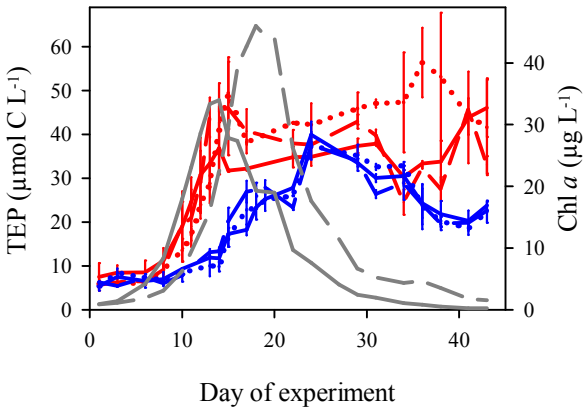

Figure 1-5: Tranparent exopolymer particle (TEP) concentrations. For more explanation see figure 1-2. Solid grey line shows the average concentration of chlorophyll *a* (Chl *a*) for the T+6 treatments, the dashed grey line the average Chl *a* concentration for the T+0 treatments.

Table 1-1: Regression analysis for the exponential curve fit $y = e^{ax}$, with x = day of the exponential incline of various variables determined for the time of exponential increase of the bloom. Significance level $p<0.0001$ (*p=0.0003).

y	Treatment		a	SE	r²
Chla [µg L^{-1}]	T+0	HL	0.227 / 0.216	0.0037 / 0.0038	0.95 / 0.95
		IL	0.237 / 0.224	0.0023 / 0.0036	0.98 / 0.95
		LL	0.232 / 0.212	0.0034 / 0.0032	0.96 / 0.96
	T+6	HL	0.299 / 0.317	0.0029 / 0.0035	0.99 / 0.99
		IL	0.263 / 0.286	0.0020 / 0.0040	0.99 / 0.96
		LL	0.241 / 0.278	0.0013 / 0.0017	0.99 / 0.99
POC [µmol L^{-1}]	T+0	HL	0.297 / 0.289	0.0019 / 0.0026	0.98 / 0.95
		IL	0.316 / 0.292	0.0019 / 0.0019	0.98 / 0.98
		LL	0.295 / 0.273	0.0025 / 0.0017	0.96 / 0.96
	T+6	HL	0.381 / 0.410	0.0035 / 0.0054	0.96 / 0.91
		IL	0.345 / 0.361	0.0033 / 0.0060	0.95 / 0.83
		LL	0.313 / 0.324	0.0035 / 0.0070	0.93 / 0.66
BSi [µmol L^{-1}]	T+0	HL	0.181 / 0.156	0.0136 / 0.0054	0.66 / 0.85
		IL	0.201 / 0.163	0.0170 / 0.0070	0.58* / 0.81
		LL	0.166 / 0.153	0.0099 / 0.0083	0.73 / 0.75
	T+6	HL	0.222 / 0.223	0.0116 / 0.0134	0.78 / 0.71
		IL	0.198 / 0.204	0.0116 / 0.0174	0.69 / 0.60
		LL	0.168 / 0.200	0.0130 / 0.0102	0.62 / 0.73
TEP [µmol C L^{-1}]	T+0	HL	0.159 / 0.156	0.0032 / 0.0038	0.80 / 0.68
		IL	0.201 / 0.182	0.0028 / 0.0018	0.95 / 0.96
		LL	0.191 / 0.174	0.0038 / 0.0022	0.90 / 0.95
	T+6	HL	0.257 / 0.311	0.0028 / 0.0056	0.97 / 0.90
		IL	0.271 / 0.300	0.0028 / 0.0025	0.97 / 0.98
		LL	0.247 / 0.274	0.0011 / 0.0021	0.99 / 0.98

Stoichiometry of particulate organic matter

The Redfield C/N of 6.6 was observed for POM in all treatments until the beginning of the bloom. Then, POC/PN increased to maximum values of 19.1 ± 0.6 around day 29 for T+0, and to 17.5 ± 1.3 around day 20 in T+6 (Fig. 1-6). These POC/PN maxima at T+0 and T+6 differed significantly (p<0.05). The decline was more pronounced at T+6, yielding ratios of 9.1 around day 29. In contrast, POC/PN ratios stayed between 16 - 19 at T+0 and did not decline until the end of the experiment (~ day 40). Interestingly, an increase in POC/PN was observed for the LL T+6 treatment after day 30 (Fig. 1-6) coinciding with an enhanced TEP formation in this treatment (Fig. 1-5). POC/POP ratios also increased with the onset of the bloom in all mesocosms (Fig. 1-6), reaching maximum values of 444 ± 16 at T+0 and 403 ± 62 at T+6. Maximum POC/POP ratios at T+0 and T+6 differed not significantly (p=0.17).

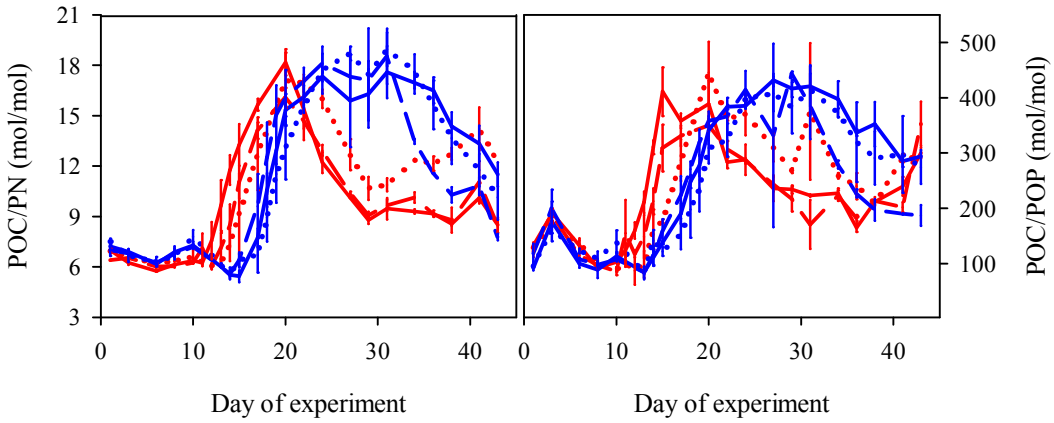

Figure 1-6: Particulate organic carbon to particulate nitrogen ratio (POC/PN, left) and POC to particulate organic phosphorus (POP) ratio (right). (For more explanation see figure 1-2.)

BSi/POC ratios during the bloom phase were similar for all treatments, yielding 0.16 ± 0.04 between the days 13 and 18 (Fig. 1-7). After the bloom phase, the decline of BSi/POC was much sharper for the T+6 compared with T+0.

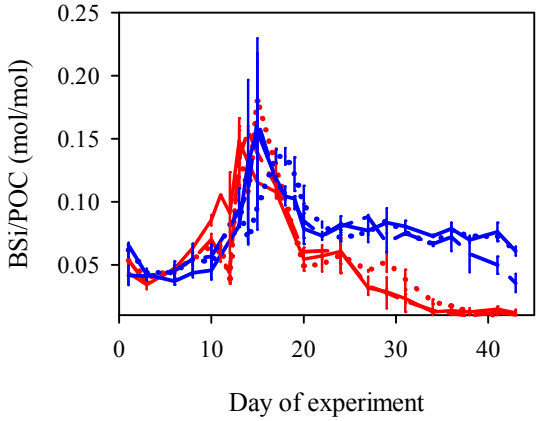

Figure 1-7: Biogenic silica (BSi) to particulate organic carbon (POC) ratio. (For more explanation see figure 1-2.)

The TEP to Chl *a* ratio at Chl *a* maximum was twice as high for T+6 compared to T+0 ($p < 0.001$) (Table 1-2). TEP/POC ratio and TEP/BSi ratio at POC and BSi maxima, respectively, yielded 60 % higher values at T+6 ($p < 0.001$) compared to T+0 ($p < 0.01$), suggesting an increased aggregation potential at biomass maxima due to elevated TEP concentrations at T+6.

Table 1-2: Ratios for TEP at the time point of maximum value of the denominator variable to illustrate the differences in TEP concentration on biomass during the bloom. Given are midpoint values of two replicates and the range.

Treatment		**Ratios**		
		TEP/Chl *a*	**TEP/POC**	**TEP/BSi**
		[µmol C/µg]	**[mol C/mol]**	**[mol C/mol]**
T+0	HL	0.53 ± 0.0	0.10 ± 0.0	1.02 ± 0.1
T+0	IL	0.64 ± 0.1	0.09 ± 0.0	1.11 ± 0.1
T+0	LL	0.47 ± 0.0	0.14 ± 0.0	0.95 ± 0.2
T+6	HL	0.95 ± 0.5	0.15 ± 0.0	1.41 ± 0.6
T+6	IL	1.29 ± 0.1	0.20 ± 0.0	1.82 ± 0.1
T+6	LL	1.10 ± 0.4	0.18 ± 0.0	1.79 ± 0.8
Average T+0		**0.55 ± 0.1**	**0.11 ± 0.0**	**1.03 ± 0.1**
Average T+6		**1.11 ± 0.2**	**0.18 ± 0.0**	**1.67 ± 0.4**

Dissolved organic matter

Dissolved organic carbon (DOC) concentrations declined at the beginning of the experiment in all mesocosms from an initial overall average of 311 ± 33 µmol L^{-1} to a minimum of 239 ± 5.2 µmol L^{-1} between days 8 and 10. DOC concentrations started to increase again after exhaustion of DIP and DIN, and hence earlier in T+6 treatments. However, the slope of DOC increase was twice as high ($p<0.001$) in all T+6 compared to T+0 mesocosms (Table 1-3, Fig. 1-8). Monosaccharide (M-CHO) and polysaccharide (P-CHO) concentrations followed a similar pattern as DOC. Both increased after nutrient exhaustion, and more pronounced at T+6 ($p < 0.01$) (Fig. 1-8). Accumulation of P-CHO was almost twice as high as M-CHO (Tab. 1-3).

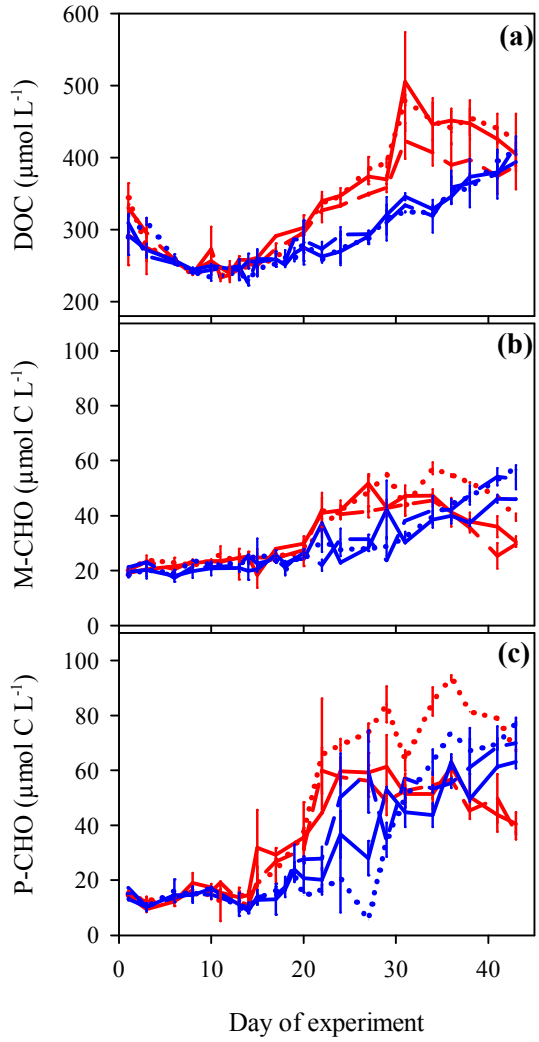

Figure 1-8: Concentrations of (a) dissolved organic carbon (DOC), (b) monosaccharides (M-CHO) and (c) polysaccharides (P-CHO). (For more explanation see figure 1-2.)

Discussion

Effects of temperature and light on the phytoplankton bloom timing

We observed an acceleration in bloom development and an earlier bloom peak due to elevated temperature that is in line with previous mesocosm studies (Sommer and Lengfellner 2008, Sommer et al. 2012) and batch culture experiments with diatoms (Wohlers-Zöllner et al. 2011), preponing phytoplankton peak timing by 1-1.8 days per degree Celsius. This shift in bloom timing is small compared to the large interannual variation in bloom onset and bloom peak observed in the natural environment. So far, a temperature dependency of diatom spring bloom timing was not confirmed by marine time series data (Edwards and Richardson 2004; Wiltshire et al. 2008).

Light intensity in this study played a minor role for the timing of the bloom compared to the effects of a six degree temperature elevation, probably because of the relatively modest differences in light levels between treatments.

Table 1-3: Regression analysis for the linear curve fit $y = ax+b$, with a = rate of increase, $b = y$-axis intercept, and x = day of increase, of DOM for the time after nutrient exhaustion until decrease (T+6) or end of the experiment (T+0). Significance level $p<0.0001$ (*p=0.0022).

y	Treatment		a	b	r²
DOC [µmol L^{-1}]	T+0	HL	5.04 / 5.55	176 / 147	0.95 / 0.92
		IL	5.71 / 4.65	169 / 167	0.92 / 0.88
		LL	5.67 / 5.56	159 / 145	0.88 / 0.91
	T+6	HL	8.57 / 12.0	144 / 85	0.96 / 0.78
		IL	7.53 / 9.26	151 / 117	0.98 / 0.90
		LL	12.3 / 10.6	57 / 106	0.94 / 0.92
M-CHO [µmol C L^{-1}]	T+0	HL	0.87 / 0.82	9.62 / 8.20	0.62 / 0.78
		IL	1.33 / 1.06	-0.04 / 1.96	0.96 / 0.87
		LL	1.16 / 1.19	1.80 / 1.05	0.81 / 0.88
	T+6	HL	1.53 / 2.18	2.89 / -7.07	0.86 / 0.80
		IL	1.35 / 2.11	4.62 / -6.46	0.89 / 0.58*
		LL	1.98 / 1.60	-9.15 / 4.04	0.85 / 0.84
P-CHO [µmol C L^{-1}]	T+0	HL	1.90 / 1.90	-18 / -13	0.82 / 0.86
		IL	2.14 / 1.83	-10 / -14	0.75 / 0.94
		LL	2.57 / 2.38	-28 / 31	0.96 / 0.77
	T+6	HL	2.08 / 3.35	-8.93 / -24	0.89 / 0.87
		IL	3.92 / 4.95	-41 / -55	0.96 / 0.86
		LL	3.81 / 3.43	-39 / -25	0.88 / 0.83

Nevertheless, higher light intensity slightly accelerated the bloom development at elevated temperature, as significant light effects were detected for the incline of POC concentration and the day of maximum POC accumulation with the same pattern as for the nutrient uptake, i.e. with HL before IL before LL. Contrary, light effects at T+0 were not detected. Onset of light saturation depends on multiple factors including light and temperature adaptation of the investigated species (Kirk 1983; Davison 1991), but in general, onset of light saturation increases with temperature (Kirk 1983). For *S. costatum* onset of light saturation was at 80 µmol m^{-2} s^{-1} when acclimated to 40 µmol m^{-2} s^{-1} and 18 °C, while onset of light saturation was at 50 µmol m^{-2} s^{-1} when cells were acclimated to the same light level at 3 °C (Mortain-Bertrand et al. 1988). Based on this, at T+0 the phytoplankton in our study was probably light saturated at all light levels and differences between light treatments were hence not detectable. During a similar mesocosm experiment, faster growth rates were determined for *S. costatum* compared to the other diatoms for the same range of daily light doses that were applied in this study (Sommer et al. 2012b). Thus, the enhanced incline for POC at higher light levels at T+6 may be attributable to faster growth rates of the dominant diatom *S. costatum* in that treatment.

Effect of temperature and light on particulate organic matter

As expected, POM maxima were lower at elevated temperature. Reasons for lower POM at T+6 include higher bacterial competition for inorganic nutrients, higher respiration rates, higher grazing losses, or enhanced sedimentation. Growth of algae on mesocosm walls represents another loss term for nutrients, that was, however, negligible during the bloom period, as the visible inspection of the mesocosm walls showed no significant growth until day 22 at T+6 and until the end of the experiment at T+0. In a similar mesocosm experiment it was concluded that it takes a few weeks until the development of wall growth plays a critical role (Sommer et al. 2007).

Competition for nutrients between phytoplankton and bacteria can affect phytoplankton biomass negatively. In a mesocosm study in Danish coastal waters, bacteria were able to out-compete phytoplankton for available inorganic nutrients in the presence of high concentrations of glucose (Joint et al. 2002). In this study, the first maximum of bacterial abundance at T+6 occurred concomitant with the phytoplankton peak (days 10 - 20), while bacterial abundance at T+0 started to increase after the phytoplankton bloom (von Scheibner et al. 2013). Bacterial peak biomass was 6 times higher at T+6 compared to T+0 during the phytoplankton bloom, yielding on average 3 µmol C L^{-1} at T+6 (von Scheibner et al. 2013). Hence, bacterial biomass accounted only for maximal ~4% of phytoplankton carbon biomass during bloom conditions, suggesting a minor importance of nutrient competition between phytoplankton and bacteria for this study. It is worth noting, however, that bacterial production and bacterial carbon demand were almost twice as high at T+6 compared to T+0 for the bloom period (von Scheibner et al. 2013). Community respiration amounted to on average 8.7 µmol C L^{-1} d^{-1} for T+6 and 6.8 µmol C L^{-1} d^{-1} for T+0 over the phytoplankton bloom period with a bacterial contribution of 46 % at T+6 and 35 % at T+0 (Breithaupt 2009; von Scheibner et al. 2013). Community respiration increased with temperature in the same range as in a previous mesocosm experiment, but without effect on maximal POC concentrations (Wohlers et al. 2009).

Grazing activity of copepods may have been increased at elevated temperature and have contributed to the difference in POM between T+0 and T+6 (Lewandowska and Sommer 2010). From a previous similar mesocosm experiment (4 temperature regimes, one light setting) it is reported that respiration and ingestion rates of the copepod *Pseudocalanus* sp. increased with a factor of 3 in the same temperature range (Isla et al. 2008). Unfortunately, grazing rates were not obtained for this study and therefore, we can't draw conclusions on the effect of temperature on the grazing activity. But we have data on the abundance of copepods for this study. Negative effects of warming on phytoplankton biomass were often related to increased abundances of zooplankton grazers at elevated temperature (Keller et al. 1999; O'Connor et al. 2009). In contrast to

those studies, the abundance of copepods was on average 8 ind. L^{-1} over the whole experiment for both temperature treatments in this study. However, the biomass of copepods increased at T+6, because the relatively small copepod species *Oithona sp.* was replaced by bigger copepod species *(Acartia, Centropages, Temora)* (Lewandowska and Sommer 2010).

In addition to the above-mentioned reasons for lower POM accumulation, another reason might be a more pronounced sedimentation of phytoplankton cells at T+6 already during the bloom. The fast decline of POM at T+6 compared with T+0 and the observation of high amounts of sedimented material at the bottom of the mesocoms indicate that a main loss term of organic carbon in this study can probably be attributed to enhanced sinking of suspended organic particles. Increasing temperature can directly enhance sinking velocity of cells by decreasing the density of the water (Bach et al. 2012). Unfortunately, it was not possible to quantify the amount of sedimented material directly after the bloom. But, it has been shown that the formation of rapidly sinking aggregates of mucous-producing diatoms is primarily controlled by TEP concentrations (Logan et al. 1995). TEP can promote the flocculation of phytoplankton cells due to the high sticking efficiency of these gel particles (Kiørboe and Hansen 1993; Engel 2000). (Kahl et al. 2008) concluded from a mesocosm experiment with the diatom *Thalassiosira pseudonana* that an increase in stickiness during phytoplankton blooms can result in enhanced particle export flux. It was shown that TEP-mediated aggregation of the diatom *Skeletonema costatum* positively correlated with temperature (Thornton and Thake 1998). Aggregates grown at +6 °C in roller tank experiments showed an increased aggregation potential compared to the ambient temperature treatment (Piontek et al. 2009). It might hence be possible that TEP acted as mediators for enhanced sedimentation especially at T+6.

TEP formation

Earlier increase in TEP concentrations and elevated maximum TEP concentrations at elevated temperature support the assumption that the release or the formation of extracellular substances is temperature sensitive. Increased temperature resulted in faster formation of TEP compared with ambient temperature despite lower maximum Chl *a* biomass. It can be speculated that the reason might be a temperature sensitive diversion of photosynthates from particulate to dissolved organic carbon at T+6 as was shown in response to an increase in CO_2 concentrations (Engel 2002). Extracellular release increased during a short-term incubation experiment with temperature (Morán et al. 2006) and an earlier and more pronounced accumulation in DOC, M-CHO and P-CHO at elevated temperature was also found in mesocosm studies (Wohlers et al. 2009; Engel et al. 2010) and in batch culture experiments (Wohlers-Zöllner et al. 2011). Kim et al.

(2011) observed lowered POC and increased DOC concentrations at warmer temperature and increased CO_2 concentrations (greenhouse scenario) whereby overall total organic carbon concentration did not change.

Since bacteria are able to also produce TEP (Stoderegger and Herndl 1999) they might have been partly responsible for the fast accumulation of TEP at T+6. Bacterial TEP production yielded a rate of 4 amol C $cell^{-1}$ h^{-1} (Stoderegger and Herndl 1999). At 2 million cells per mL the contribution of bacterial TEP would yield 0.19 µmol C L^{-1} d^{-1}. This would be a relatively small bacterial contribution compared with the total amount of TEP for this study.

In this context it is important to note that TEP production is highly species specific (Engel and Passow 2001; Passow 2002a; Claquin et al. 2008). In a previous study, TEP concentrations increased not until the phytoplankton bloom had long been over and only at +6 °C (Wohlers et al. 2009). The dominant species in that study were the chain-forming diatoms *Skeletonema costatum, Chaetoceros minimum, Chaetoceros curvisetus, and Thalassiosira nordenskioldii,* constituting 87 % to total phytoplankton abundance at Chl *a* maxima (Wohlers et al. 2009). Hence, the assemblage of the most important species was different compared to our study. For the diatom species *Rhizosolenia calcaravis,* a light cell-surface coating as well as free TEP were observed (Passow 2002a). Possibly, the related *Rhizosolenia setigera* occurring in this study was responsible for the higher TEP concentrations, since this diatom contributed ~ 20 % to total biomass in both, T+0 and T+6 treatments.

Stoichiometry of particulate organic matter

We observed a general tendency towards increased POC/PN and POC/POP far above Redfield ratio at both T+0 and T+6. This suggests “excess carbon fixation”, the process in which dissolved inorganic carbon is fixed by phytoplankton in excess of the Redfield C:N and C:P ratio (Sambrotto et al. 1993; Toggweiler 1993). Engel (2002) related the observed increase in POC/PN in their study to an enhanced uptake of dissolved inorganic carbon (DIC) after nitrate depletion with a large flow of carbon into TEP. Earlier increase in TEP formation at T+6 in this study may also indicate an enhanced channelling of photosynthates into TEP formation. A stimulating effect of temperature on “excess carbon fixation” as was suggested by Taucher et al. (2012) was not observed in this study, as we detected significantly lower POC/PN at T+6 compared to T+0 while TEP/POC was increased. However, different from this study, Taucher et al. (2012) investigated temperature effects on a summer bloom with temperatures between 10 °C and 18 °C.

Effects of temperature and light on dissolved organic matter

Concentrations of DOC, M-CHO and P-CHO started to rise in all mesocosms after nutrient depletion. It is often observed that extracellular release (ER) increases after nutrient depletion during phytoplankton blooms (Nagata 2000; Engel et al. 2002). DOM during phytoplankton blooms originates primarily from ER by autotrophic cells (Berman and Holm-Hansen 1974; Fogg 1983; Biersmith and Benner 1998). The slopes were markedly higher for T+6, indicating enhanced exudation or accumulation of fresh DOM at elevated temperature. During a short-term incubation experiment it was shown that ER can increase up to 54 % due to a 2 °C warming (Morán et al. 2006). An earlier and more pronounced increase in DOC, M-CHO and P-CHO at elevated temperature was also found in previous studies (Wohlers et al. 2009; Engel et al. 2010; Wohlers-Zöllner et al. 2011). While Wohlers et al. (2009) attribute the temperature-dependent increase in DOC and P-CHO accumulation to bacterial DOC release, Engel et al. (2010) concluded that phytoplankton exudation is temperature sensitive. Previous studies found that DOC and P-CHO accumulated not only faster but also increased to higher concentrations at elevated temperature (Wohlers et al. 2009; Engel et al. 2010; Wohlers-Zöllner et al. 2011). We observed that DOC increased as high at T+0 and P-CHO even increased to higher concentrations compared with T+6 at the end of the experiment. In contrast to the effect of temperature, DOC did not respond to the three different light levels. This is contradictory to several previous studies that found DOC excretion by phytoplankton to increase with increasing light levels (Verity 1981a; Zlotnik and Dubinsky 1989). But, differences in light levels in this study were probably too small for the detection of distinct differences in DOM accumulation.

Summary and potential consequences for DOM and POM pools in a future warmer ocean

As hypothesized, a reduction in organic matter accumulation under elevated temperature was found for the particulate pool. The release of DOC and carbohydrates by phytoplankton was advanced and enhanced at elevated temperature, but total accumulation was similar between temperature treatments. Although, enhancements in heterotrophic processes, such as respiration and bacterial production, were recorded, also an enhanced flow of dissolved organic matter into TEP production was observed at elevated temperature. Concerning the fate of DOC, in a future warmer ocean there may be two counteracting processes (indicated by 1. and 2. in Fig. 9), (1.) DOC is recycled more quickly in the microbial loop, leading to a faster release of carbon dioxide (CO_2). (2.) In the other process DOC is channelled into TEP formation, which favours aggregation and sinking of particulate organic matter. Thereby, the taxonomic

composition of the phytoplankton community seems to be crucial as TEP production is species specific. A positive effect of light on the maximum accumulation of POM could not be found in this study, probably because differences in light levels between treatments were too small. As onset of light saturation for phytoplankton generally increases with temperature, and stratification of the ocean is expected to increase due to warming, light intensity is an important yet often neglected cofactor in ocean warming experiments and should be considered in following studies on this subject.

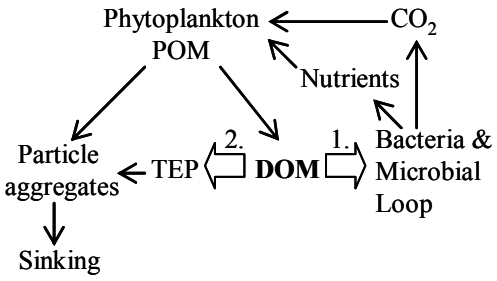

Figure 1-9: Simplified scheme for the sources and sinks of primary produced organic matter relevant for this study. Particulate and dissolved organic matter (POM and DOM) are mainly produced by autotrophs photosynthesis. One proportion of DOM is transferred to bacteria and the microbial loop (1.), the other proportion can abiotically aggregate to transparent exopolymer particles (TEP) (2.). TEP mediate aggregation processes with phytoplankton cells due to their high sticking efficiency. As both, bacterial carbon demand and TEP formation was found to be temperature sensitive, these two processes may counteract in a future warmer surface ocean.

Acknowledgements

We thank A. Ludwig, P. Fritsche, and T. Hansen for technical support and A. Ludwig and P. Fritsche for chlorophyll *a* and elemental analyses, and N. Händel for the analysis of dissolved organic carbon. This work was supported by the DFG (German Research Foundation) as part of the priority program 1162 AQUASHIFT.

Chapter 2

Organic matter partitioning and stoichiometry in response to rising water temperature and copepod grazing

Abstract

Rising ocean temperature is expected to change the balance between production and degradation of organic matter due to different temperature sensitivities of auto- and heterotrophic processes. Consequently, temperature may evoke shifts in the partitioning between particulate and dissolved pools of organic matter, e.g. during phytoplankton bloom events. Copepods are the most prominent zooplankton group and elevated temperatures raises their growth and grazing rates and may improve their overwintering success. So far it is unknown to what extent copepods affect the partitioning and stoichiometry of organic matter in a warmer surface ocean. We therefore conducted a mesocosm experiment with three copepod densities and two temperature scenarios to determine effects on the pools of dissolved and particulate organic matter and their carbon:nitrogen:phosphorus (C:N:P) ratios. Here we show that particulate organic C concentrations decreased with increasing copepod abundance. Thus, particulate organic matter decreased for C:N from 26 to 13 and for C:P from 567 to 257 from low to high copepod density at elevated temperature. Dissolved organic N and P accumulation were unaffected by temperature or copepod abundance, but dissolved organic C was positively affected by temperature resulting in high C:N and C:P ratios. Our study suggests that copepod grazing and egestion enhanced the recycling of N and P, thereby increasing the availability of these nutrients for autotrophs. The effect of this consumer-driven nutrient recycling could counteract the “excess carbon fixation” by phytoplankton under nutrient stress that was suggested for a warmer sea-surface ocean.

Introduction

The ongoing global warming is mitigated by the ocean's ability to absorb and store high amounts of heat. Between the years 1955 and 2010 the average surface ocean temperature in the upper 700 m has increased by 0.18 °C as the ocean has been taking up ~ 93% of the heat being added to the climate system (Levitus et al. 2012). This trend will continue, as an increase in Earth surface temperature between 1 °C to 6 °C, depending on the CO_2 emissions scenario, is projected until the end of this century (Meehl et al. 2007).

The warming trend is accompanied by increasing water column stratification (Prentice et al. 2001), decreasing the mixed layer depth, thereby changing nutrient supply and light availability for phytoplankton (Doney 2006). Apart from those indirect effects, temperature is the key factor for regulating metabolic processes. It was suggested that metabolic rate influences all levels of biological organization from individuals to the biosphere (Brown et al. 2004). In general, autotrophic processes, such as phytoplankton growth, show a lower sensitivity to temperature changes (Eppley 1972) than heterotrophic processes, like bacterial growth (Pomeroy and Wiebe 2001), or metabolic rates of grazers like marine copepods (Ivleva 1980; Ikeda et al. 2001; Isla et al. 2008).

In temperate and high latitude oceans, the phytoplankton spring bloom is an important pulse for the development of biomass at the basis of the food web. The observation of a retardation in the phytoplankton spring bloom off Helgoland, North Sea, between 1962 and 2002 despite an increase in water temperature since 1962, led (Wiltshire and Manly 2004) to hypothesize that the delay may be related to the occurrence and activity of zooplankton (Wiltshire et al. 2008). Analyzing a set of mesocosm experiments, Gaedke et al. (2010) pointed out that biotic interactions, via grazing and the success of overwintering phyto- and zooplankton, may overrule direct climatic effects like temperature on spring phytoplankton bloom dynamics. Grazing of copepods can enhance the proportion of dissolved organic matter (DOM) in the water column by sloppy feeding, excretion, egestion and release from fecal pellets (Nagata 2000; Kragh et al. 2006) with consequences for the production of substrate for bacterial growth (Strom et al. 1997; Møller and Nielsen 2001). Grazing has also been recognized to be an important source of nutrient regeneration that can feed back to autotrophs (Ketchum 1962; Lehman 1980; Sterner 1986). Owing to stoichiometric properties of the phytoplankton and the grazing species, this consumer-driven nutrient recycling can differentially deliberate N or P (Elser and Urabe 1999; Sterner and Elser 2002). Changes in the size of overwintering copepod populations or enhanced heterotrophic processes due to climate warming therefore likely change the balance between sources and sinks of organic matter in the surface ocean with consequences for the partitioning between particulate and dissolved pools of primary produced organic matter.

DOM in the ocean comprises ~700 Pg C and harbours therewith about 200 times more carbon than the marine biomass (Hansell et al. 2009; Sabine and Tanhua 2010). In the ocean, the largest characterized fractions of DOM are carbohydrates (CHO) (Biddanda and Benner 1997; Biersmith and Benner 1998). During phytoplankton blooms, CHO are released in high amounts by phytoplankton cells (Ittekkot et al. 1981; Myklestad 1995). Primary production of DOM was shown to increase with rising temperature (Morán et al. 2006). Recent mesocosm studies also found that rising temperature favours the partitioning between DOM and particulate organic matter (POM) towards DOM (Wohlers et al. 2009; Engel et al. 2010). A shift from the POM-pool towards the DOM-pool would not only favour substrate availability for bacteria but also the potential for the formation of transparent exopolymer particles (TEP) that form from polysaccharide precursors (Passow 2002b). TEP can abiotically spontaneously assemble from free DOM polymers (Chin et al. 1998) and are therefore a connection between the DOM and the POM pool (Engel et al. 2004; Verdugo et al. 2004). TEP can play a crucial role in aggregation processes during phytoplankton blooms (Logan et al. 1995). Moreover, Thornton and Thake (1998) observed a direct influence of temperature on the formation rate of particle aggregates, including phytoplankton cells, in the presence of acidic polysaccharides.

So far observed effects of warming on planktonic primary producers include an advancement in the onset of phytoplankton growth (Sommer and Lengfellner 2008; Sommer et al. 2012a), a general reduction of cell size (Daufresne et al. 2009; Morán et al. 2010; Lewandowska and Sommer 2010), a tighter bacteria-phytoplankton coupling (Hoppe et al. 2008; von Scheibner et al. 2013), and shifts in the community composition of phytoplankton (Lewandowska and Sommer 2010) and bacterioplankton (von Scheibner et al. 2013), and a shift in the balance from autotrophic to heterotrophic processes (Müren et al. 2005; O'Connor et al. 2009). Additionally, elemental stoichiometry of phytoplankton can change in response to a temperature change (Berges et al. 2002). Some studies detected negative effects of rising temperature on phytoplankton biomass (Keller et al. 1999; O'Connor et al. 2009; Lassen et al. 2010; Lewandowska and Sommer 2010) or, as a consequence of an enhancement in ocean stratification, on primary production (Behrenfeld et al. 2006). Some of those studies related the negative effect of warming on phytoplankton biomass to increased abundances of zooplankton (Keller et al. 1999; O'Connor et al. 2009) or enhanced grazing pressure (Lewandowska and Sommer 2010).

Several studies addressed the effects of rising temperature on biogeochemical dynamics at the ecosystem level (Wohlers et al. 2009; Kim et al. 2011; Taucher et al. 2012), however, without considering changes in grazer abundance. Therefore, the aims of this study were to assess the effect of a 6 °C temperature elevation in combination with

three different densities of overwintering copepods (1.5, 4, 10 Ind. L^{-1}) on biogeochemical cycling, partitioning between DOM and POM, and on organic matter stoichiometry during a winter-spring phytoplankton bloom.

Material and Methods

Experimental set-up

The experiment in principle followed the mesocosm set-up explained in detail in Sommer et al. (2007). The indoor-mesocosm experiment started on January 8, 2009 and lasted until February 16, 2009. Twelve 1400-L mesocosms of 1 m depth were set up in climate chambers and simultaneously filled with seawater with a salinity of 17.6 from the Kiel Fjord, containing the natural winter/spring plankton community (phytoplankton, bacteria and protozoa). The detailed mesocosm set-up with species composition and phytoplankton biomass is described in Sommer and Lewandowska (2011). Mesozooplankton was dominated by copepods (70% *Acartia* sp., 17 % *Oithona similis*, 7 % *Pseudocalanus* sp., 3 % *Temora longicornis*, 3 % *Centropages hamatus*), added from net catches. Target densities were 1.5 (low density, LD), 4 (intermediate density, ID) and 10 individuals L^{-1} (high density, HD). Abundances of copepods and copepodits did not change until the phytoplankton peak and mean realised densities during the pre-bloom period were almost identical to the initial target densities (Sommer and Lewandowska 2011). The temperature of $\Delta T = 0$ °C (T+0) was derived from the decadal (1993 – 2002) mean sea surface temperatures in Kiel Bight. The realised temperature over the whole experimental period was 2.5 ± 0.9 °C and applied to six mesocosms. For the other 6 mesocosms, an initial temperature elevation of $\Delta T = 6$ °C (T+6) above the baseline was chosen according to the A1F1 scenario of the Intergovernmental Panel on Climate Change (IPCC 2007). The realised temperature in the T+6 treatment was 8.2 ± 0.5 °C. According to the natural, seasonal water temperature increase during spring time a slow increase in temperature of ~1 °C over the whole experiment was programmed (Fig. 2-1). The realised temperatures in T+0 treatments showed a higher variability for the experimental period, as one climate chamber with three T+0 mesocosms (M10, 11, 12) was on average 1 °C cooler (Fig. 2-1).

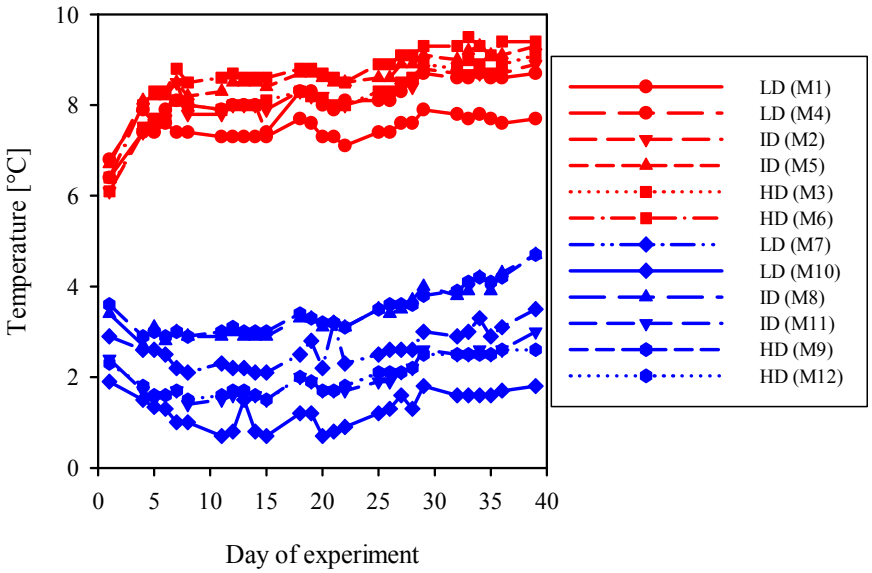

Figure 2-1: Realized temperatures for all 12 mesocosms over the course of the experiment.

The light system simulated daily irradiance curves and a seasonal light pattern calculated from astronomic equations according to Brock (1981), controlled by a computer programme (GHL, Prometeus). Two illuminating devices on top of each mesocosm were equipped with 12 full spectrum light tubes (10 solar tropic T5 Ultra, 4,000 K, 2 solar nature T5 Ultra, 9,000 K, JBL). The daily light dose was adjusted to an intermediate light of 57 % of the natural surface irradiance, whereby the light dose increased linearly over the whole experiment, yielding on average 7.9 mol quanta m^{-2} d^{-1}. The virtual start point for the light programme was set to be February 15. Initial nutrient concentrations (day 1) were 14.3 ± 0.22 µmol L^{-1} nitrate, 0.81 ± 0.01 µmol L^{-1} nitrite, 2.56 ± 0.12 µmol L^{-1} ammonium, 0.93 ± 0.04 µmol L^{-1} phosphate, and 30.3 ± 0.7 µmol L^{-1} silicate. During the whole experiment, water inside the mesocosms was gently mixed with a propeller in order to keep cells and smaller particles in suspension, whereas larger particles and aggregates were able to settle out of the water column. Sampling took place at least three times a week. Additional sampling was conducted during bloom conditions. Samples were taken with a silicone hose from the middle of the mesocosm water body between 08:30 and 09:00 in the morning (1 - 2 hours after lights on).

Analytical Methods

Temperature, salinity and pH (NBS scale) were measured with a WTW conductivity/pH probe on each sampling day at 0.2 m depth. Inorganic nutrients (nitrate, nitrite, phosphate, silicate) were determined with an autoanalyzer (AAII) according to Hansen and Koroleff (2007), and ammonium according to the method of Holmes et al. (1999)

immediately after sampling or stored after 0.2 µm prefiltering (Filtropur, Sarstedt) overnight at ~ 3 °C . During bloom conditions (see Tab. 1) samples were filtered through 5.0 µm cellulose acetat filters. For biogenic silicate (BSi) determination, 50 to 250 mL of sample were filtered onto 0.65 µm cellulose acetate filters (Sartorius) and stored at -20 °C until analysis according to Hansen and Koroleff (2007). For the determination of chlorophyll *a* (Chl *a*), between 100 and 500 mL were filtered onto glass fibre filters (GF/F, Whatman) and stored overnight at -20 °C. Pigment concentration was measured with a 10-AU Turner fluorometer after 90% acetone (v/v) extraction (Welschmeyer 1994). For particulate organic carbon (POC), particulate nitrogen (PN), and particulate organic phosphorous (POP) 100-500 mL of sample were filtered onto precombusted (500 °C, 8 h) GF/F filters (Whatman) and stored at -20 °C. For the determination of POC and PN, filters were dried at 60 °C for 6 hours prior to analysis, and C and N concentrations measured with an elemental analyzer (EuroEA-3000, Eurovector) according to (Sharp 1974). POP was determined photometrically after the treatment with one dispensing spoon of Oxisolv® (Merck) (Hansen and Koroleff 2007). TEP concentration was determined colorimetrically (Passow and Alldredge 1995b). Therefore, samples were prepared in duplicate by gentle filtration (~ 150 mbar) of 5 to 50 mL sample onto 0.4 µm polycarbonate filters (Whatman) and staining with Alcian Blue. The dye was calibrated (f = 40.65) with the standard polysaccharide Gum Xanthan before and after the experiment. The filters were stored at -20 °C until processing. The analysis was carried out by adding 80 % H_2SO_4 to the filters and measurement of supernatants absorption at 787 nm after 3 hours with a spectrophotometer (Hitachi U-2000). For the conversion from Gum Xanthan equivalents to carbon a factor of 0.63 (w/w) was applied according to Engel (2004). For dissolved organic carbon (DOC) and total dissolved nitrogen (TDN) determination, 15 mL of sample was filtered through pre-combusted glass fibre filters, collected in 20 mL pre-combusted glass ampoules, 200 µL 85 % phosphoric acid added, and stored at 6 °C in the dark. DOC and TDN were analysed on a Shimadzu TOC_{VSH} using the HTCO method (Sharp et al. 1995). DON was calculated by subtracting TDN with dissolved inorganic nitrogen (DIN) (DON = TDN - DIN, DIN = nitrate + nitrite + ammonium). For dissolved organic phosphorus (DOP), 40 mL of sample were filtered through pre-combusted glass fibre filters, collected in Nalgene bottles and immediately analyzed with Oxisolv® according to the method of Hansen and Koroleff (2007). For dissolved carbohydrates (TCHO) (monosaccharides = MCHO and polysaccharides = PCHO) 15 mL of filtered sample was transferred into combusted glass vials and stored at -20 °C. For determination the 2,4,6-tripyridyl-s-triazine (TPTZ) spectrophotometric method was applied (Myklestad et al. 1997).

Calculations and statistics

We applied an operational threshold of ≥ 3 µg Chl *a* L^{-1} (~ tenfold increase from the start of the experiment; corresponding to POC ~ > 40 µmol L^{-1}) for the definition of bloom conditions (Fig. 2-2). This yielded a bloom phase for T+0 from days ~ 8 to 29, and for T+6 treatments from days ~ 6 to 22 (Tab. 2-1).

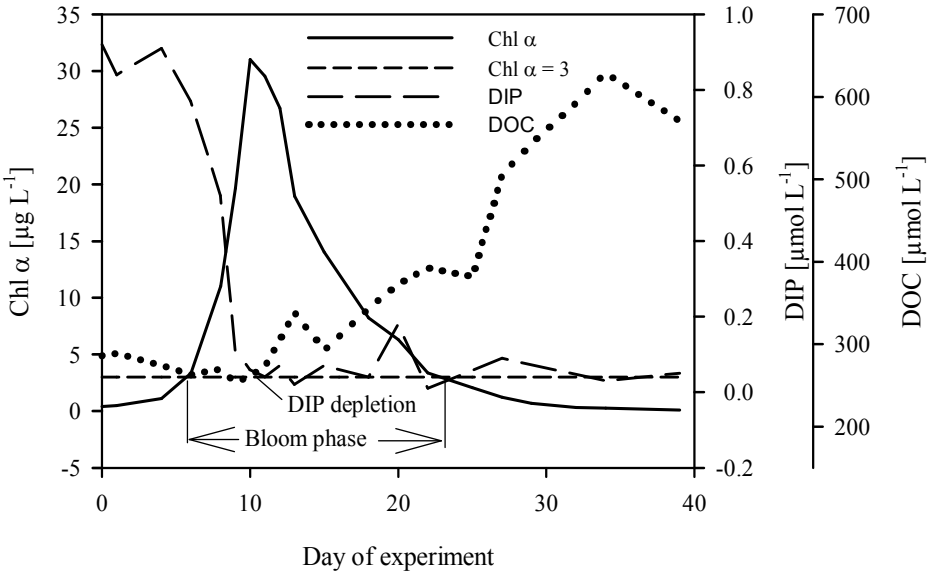

Figure 2-2: Exemplary representation for the drawdown of dissolved inorganic phosphorus (DIP, short dashed line), the development of chlorophyll *a* (Chl *a*) (solid line) and dissolved organic carbon (DOC) (dotted line) in mesocosm number 1. The medium dashed horizontal line indicates the threshold Chl *a* value (≥ 3 µg L^{-1}) for the definition of bloom conditions. The depletion of DIP (and also dissolved inorganic nitrogen (DIN), data not shown in this figure) mark the beginning of DOC and carbohydrate (TCHO, data not shown in this figure) accumulation.

Particulate organic matter (POM) maxima (POC_{max}, PN_{max}, POP_{max}, BSi_{max},) were derived on the day of maximum accumulation of the respective POM component. To investigate the quality of POM, ratios were calculated for each measurement day for POC:PN, POC:POP, and POC:BSi, and the ratio determined on the day of POC_{max}. PN:POP was determined on the day of its peak concentration (~day 16 for T+0 and ~day 9 for T+6). TEP was also derived on the day of POC_{max} (TEP at POC_{max}), and in addition, TEP maximum concentration on day 39 (mesocosms 4 and 12 on day 34) after DIP depletion were added to the analysis. The days of POC_{max} and the days for the onset of DIP depletion are given in table 1. The beginning of nutrient depletion in T+0 treatment was on average on day 14, and in T+6 on average on day 10, concomitant with the Chl *a* peak in this treatment (T+0 on average day 16) (Fig. 2-2).

Tab. 2-1: Bloom phase defined by chlorophyll *a* ≥ 3 µg L^{-1} for each mesocosm.

Mesocosm no.	Temperature	Copepod denstity	Bloom phase [days]	Onset of DIP depletion [day]	POCmax [day]
1	T+6	LD	6-22	11	15
2	T+6	ID	6-20	9	13
3	T+6	HD	6-18	10	13
4	T+6	LD	6-20	10	13
5	T+6	ID	6-18	9	11
6	T+6	HD	6-18	9	12
7	T+0	LD	10-27	14	20
8	T+0	ID	8-25	14	18
9	T+0	HD	8-22	13	16
10	T+0	LD	11-25	15	20
11	T+0	ID	10-25	14	18
12	T+0	HD	11-29	16	20

DOC and TCHO increased with the beginning of nutrient depletion. Therefore, fresh DOC and fresh TCHO were calculated by subtracting the highest concentration after DIP depletion (days 32-34) from concentration determined on the day after the onset of DIP depletion (day 15 for T+0 and day 11 for T+6). As DON concentrations showed a consistent increase over the whole experiment, fresh DON concentration was determined by subtracting the end concentrations on day 39 from initial concentrations on day 1.

For the proportion of fresh accumulated DOC of total organic carbon (TOC), we calculated the maximum new accumulated DOC and divided it through fresh accumulated POC plus DOC (POC+DOC=TOC) (Fig. 2-9). This was done for the bloom phase, indicated by Chl *a* ≥ 3 µg L^{-1} (Tab. 2-1), and for the post-bloom phase.

DOC:Chl*a* and DOC:TCHO were calculated by dividing DOC, respectively TCHO, with Chl *a* for each measurement day. Then, the maximum ratios after DIP depletion were statistically compared. The same was done for DOC:DON, DOC:DOP, and DON:DOP.

Effects of temperature or copepod abundance were tested with general regression models using Statistica 6.0 (StatSoft), whereby temperature was defined as categorical and copepod abundance as continuous factor. A significance level of $p<0.05$ was accepted.

Results

Bloom development

Phytoplankton blooms, dominated by the diatom *Skeletonema costatum* (Sommer and Lewandowska 2011), developed in each mesocosm and were indicated by the onset of inorganic nutrient drawdown and the concomitant exponential increase in Chl *a* concentrations (Figs. 2-3, 2-4).

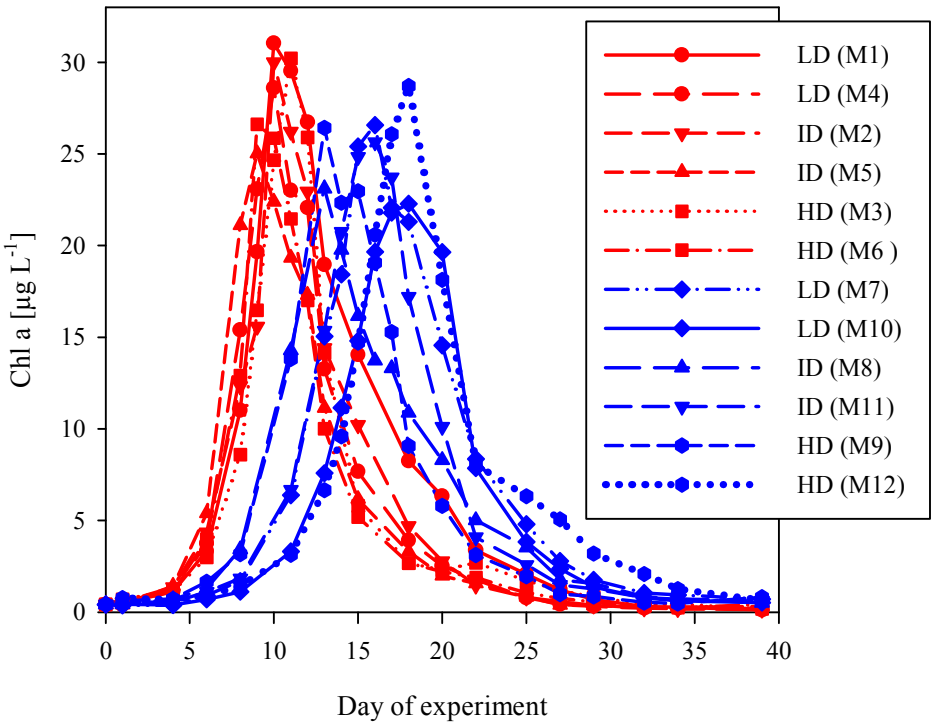

Figure 2-3: Chlorophyll *a* (Chl *a*) for all 12 mesocosms over the course of the experiment.

Rising temperature accelerated the onset of the phytoplankton bloom, leading to ~ 1 day per °C temperature elevation earlier maximum Chl *a* concentrations (p=0.0003), while copepod abundance had no effect on bloom timing (p=0.74). Bloom maxima were reached for T+6 treatments on day 10 ± 0 and for T+0 treatments on day 16 ± 1. Chl *a* maximum concentrations and bloom duration were not significantly affected by temperature or copepod abundance (Fig. 2-3). Higher variability in bloom peak timing at T+0 (Fig. 2-3) can probably be explained by a greater variability in temperature (Fig. 2-1).

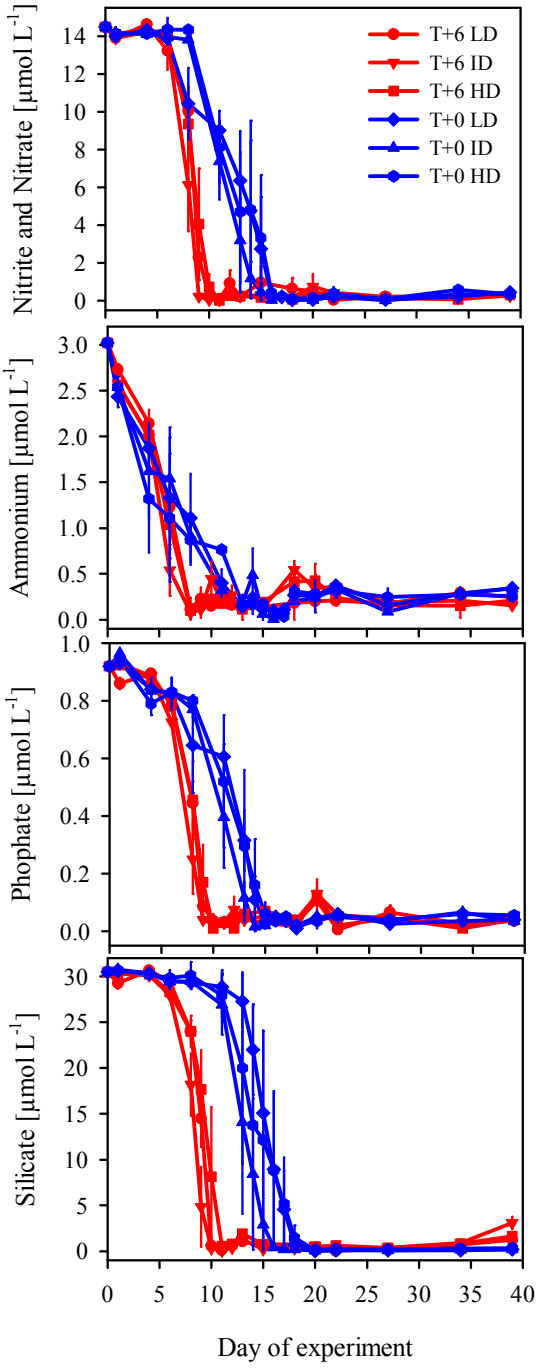

Figure 2-4: Inorganic nutrient drawdown (nitrate+nitrite, ammonium, phosphate, silicate) averaged for the two replicates with the vertical bars indicating the range between the replicates.

Effects of temperature and copepod abundance on particulate organic matter build-up and stoichiometry

In line with an earlier development of Chl *a*, also the time point for the maximum accumulation of particulate organic carbon (POC) was earlier at T+6 (~5 days) compared to T+0, and not affected by copepod abundance (Tab. 2-1, Fig. 2-5).

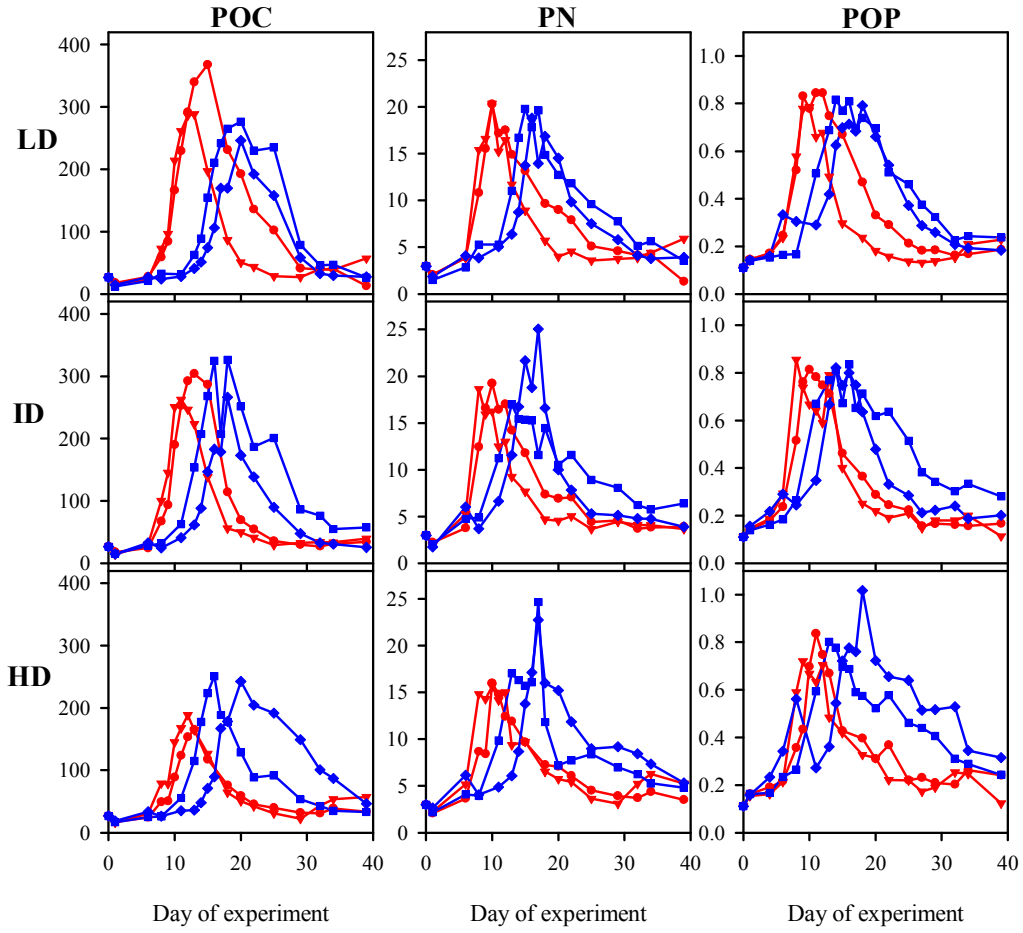

Figure 2-5: Particulate organic carbon (POC), particulate nitrogen (PN), and particulate organic phosphorus (POP) (in µmol L^{-1}) at low (LD), intermediate (ID), and high (HD) copepod density for each mesocosm. T+0 treatments are indicated by blue, T+6 by red lines and symbols.

Maximum POC (POC_{max}) concentrations decreased with increasing copepod abundance (p=0.02) (Tab. 2-2, Fig. 2-5). Thereby, the difference between HD and LD seemed more pronounced for T+6 (Δ152 µmol L^{-1} POC at T+6 vs. Δ15 µmol L^{-1} POC at T+0). However, this effect of temperature was insignificant (p=0.83). Contrary to POC, maximum particulate nitrogen (PN_{max}) and particulate organic phosphorus (POP_{max}) accumulation were neither affected by temperature nor by copepod abundance (Tab. 2-2, Fig. 2-5). Hence, the POC:PN and POC:POP ratios (at the time point of POC_{max}) decreased with increasing copepod abundance (p=0.003; p=0.006) (Tab. 2-2, Fig. 2-6). POC:PN decreased from HD to LD from ~19 to 16 at T+0 and from ~26 to 13 at T+6.

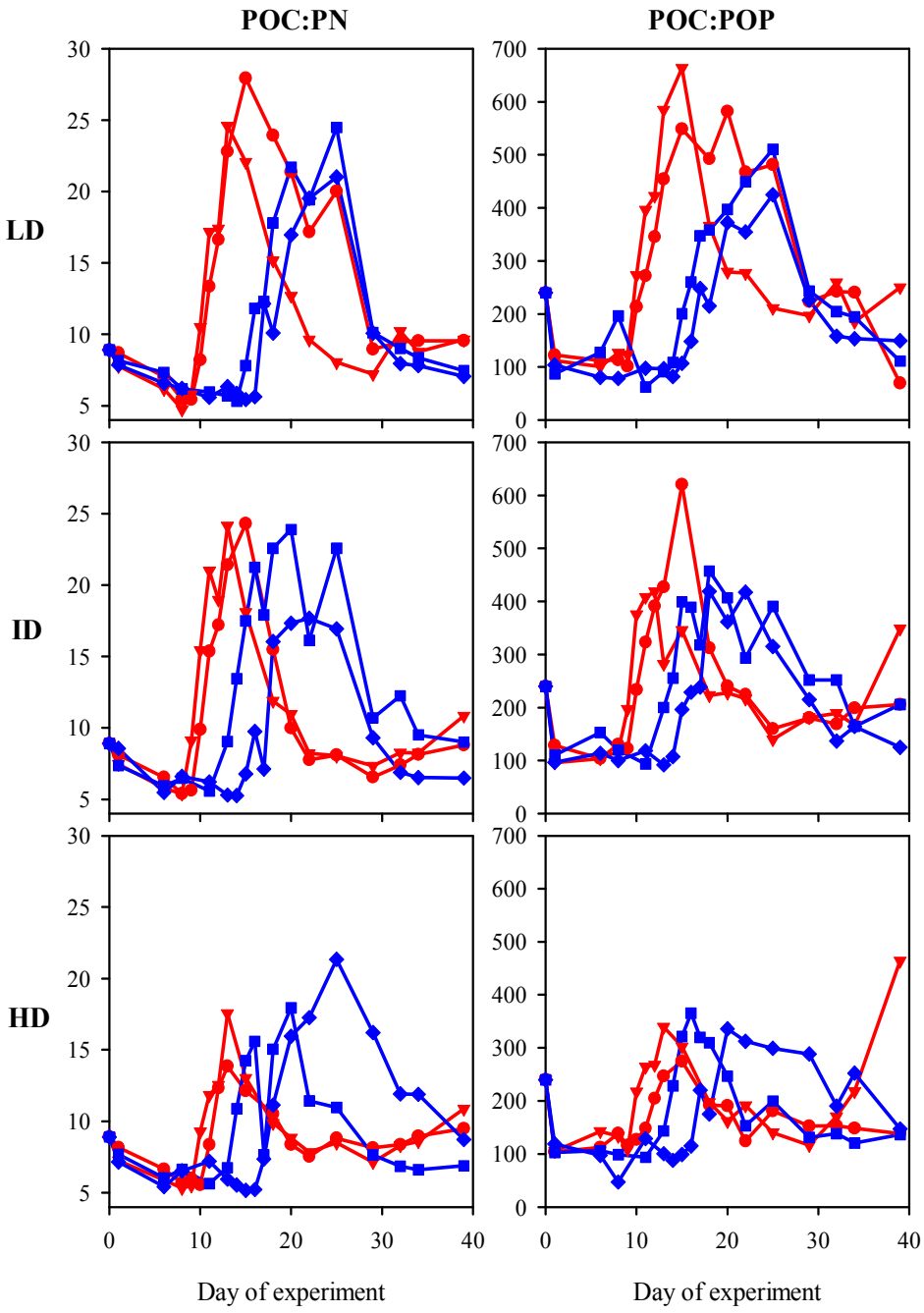

Figure 2-6: Particulate organic carbon to particulate nitrogen (POC/PN) and to particulate organic phosphorus (POC/POP) at low (LD), intermediate (ID), and high (HD) copepod density for each mesocosm. T+0 treatments are indicated by blue, T+6 by red lines and symbols.

Maximum accumulation of biogenic silica (BSi_{max}) was slightly negatively affected by copepod abundance (p=0.05, Tab. 2-2), as a consequence, POC:BSi ratios at POC_{max} were not significantly affected (p=0.48), although, POC:BSi at T+6 showed the tendency to decrease with increasing copepod abundance (Tab. 2-2).

Table 2-2: Maximum or mean concentrations (in µmol L^{-1}) and stoichiometry of particulate and dissolved organic matter (mean points and range of two replicates).

	T+0			T+6		
	LD	ID	HD	LD	ID	HD
Carbon:						
POC_{max}	261 ± 15	296 ± 30	247 ± 4	328 ± 40	283 ± 21	177 ± 12
$_{fresh}$ DOC	171 ± 44	221 ± 74	190 ± 10	287 ± 69	266 ± 19	113 ± 44
$_{fresh}$TCHO	132 ± 56	181 ± 72	138 ± 11	196 ± 49	165 ± 7	69 ± 5
Nitrogen:						
PN_{max}	19.3 ± 0.5	21.0 ± 4.0	19.9 ± 2.9	20.3 ± 0.0	18.9 ± 0.3	15.8 ± 0.2
$_{fresh}$DON	5.76 ± 1.34	5.60 ± 0.81	5.08 ± 0.60	1.56 ± 1.56	4.48 ± 0.11	3.40 ± 0.59
Phosphorus:						
POP_{max}	0.80 ± 0.01	0.83 ± 0.01	0.91 ± 0.11	0.81 ± 0.03	0.84 ± 0.02	0.78 ± 0.06
DOP_{mean}	0.25 ± 0.00	0.24 ± 0.00	0.24 ± 0.02	0.25 ± 0.00	0.24 ± 0.02	0.24 ± 0.01
Silica:						
Bsi_{max}	30.3 ± 5.2	33.1 ± 5.7	24.5 ± 1.5	27.2 ± 0.4	27.2 ± 0.3	22.2 ± 0.0
Stoichiometry:						
POC:PN at POC_{max}	19.3 ± 2.4	19.3 ± 3.3	15.8 ± 0.2	26.3 ± 1.7	21.2 ± 0.2	13.2 ± 0.7
$DOC:DON_{max}$	33.4 ± 3.5	35.3 ± 6.3	35.1 ± 0.9	40.8 ± 3.5	36.4 ± 0.4	26.6 ± 1.2
POC:POP at POC_{max}	385 ± 12	438 ± 19	351 ± 15	567 ± 18	418 ± 9	257 ± 11
$DOC:DOP_{max}$	1967 ± 115	2341 ± 222	3192 ± 1132	2590 ± 720	3227 ± 795	1960 ± 80
$PN:POP_{max}$	26.0 ± 0.3	28.2 ± 5.3	26.3 ± 3.7	26.4 ± 0.3	24.2 ± 0.1	24.7 ± 0.4
$DON:DOP_{max}$	73.1 ± 2.4	74.6 ± 5.8	66.2 ± 10.8	75.0 ± 9.9	97.3 ± 21.8	75.3 ± 5.1
POC:Bsi at POC_{max}	13.3 ± 1.7	10.7 ± 0.7	13.4 ± 2.0	15.4 ± 1.9	12.1 ± 3.3	11.2 ± 0.9

TEP concentration did not differ between treatments at POC_{max}, yielding 7 ± 1 µmol C L^{-1}. In contrast, TEP maximal accumulation after nutrient depletion responded positively to the warming (p=0.001), with almost 6times higher concentrations at T+6 with 35 ± 13 µmol C L^{-1} compared to 6 ± 3 µmol C L^{-1} at T+0 (Fig. 2-7).

Response of dissolved organic matter to increasing temperature and copepod abundance

DOC started to increase with the onset of nutrient depletion ~ on day 10 for T+6 and ~ on day 14 for T+0 (Figs. 2-1, 2-7). By normalizing DOC to Chl *a*, a clear positive temperature effect (p=0.03) was detectable for the maximum ratio after nutrient depletion (Fig. 2-8). The negative effect of increasing copepod abundance on DOC:Chl *a* was more pronounced at T+6, but statistically insignificant (p=0.21).

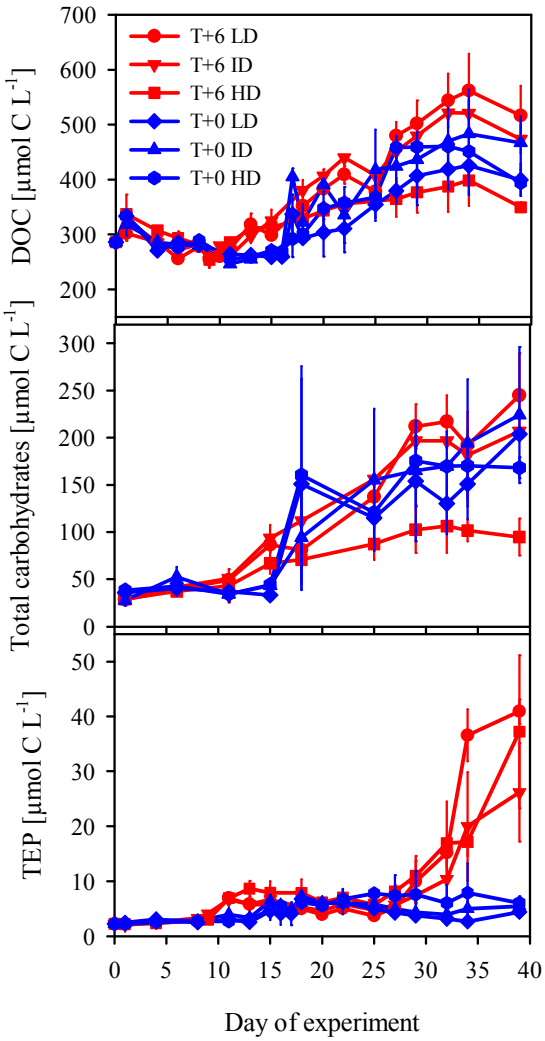

Figure 2-7: Dissolved organic carbon (DOC), total carbohydrates, and transparent exopolymer particles (TEP) averaged for the two replicates with the vertical bars indicating the range between the replicates.

The newly accumulated TOC comprised of ~ 35 % fresh DOC at T+0, and of 29 % at T+6 during the bloom phase, while the average post-bloom contribution was ~ 40 % at T+0 and ~ 69 % at T+6, showing a temperature effect (p=0.02) on the partitioning of DOC (Fig. 2-9). Similar to DOC, carbohydrates (TCHO) started to rise with the onset of nutrient depletion (Fig. 2-7). The newly accumulated DOC comprised between 61 and 94 % of TCHO, without significant differences in response to temperature or copepod abundance. TCHO normalized to Chl *a* was positively affected by temperature (p=0.03), but not by copepod abundance (p=0.13) (Fig. 2-8).

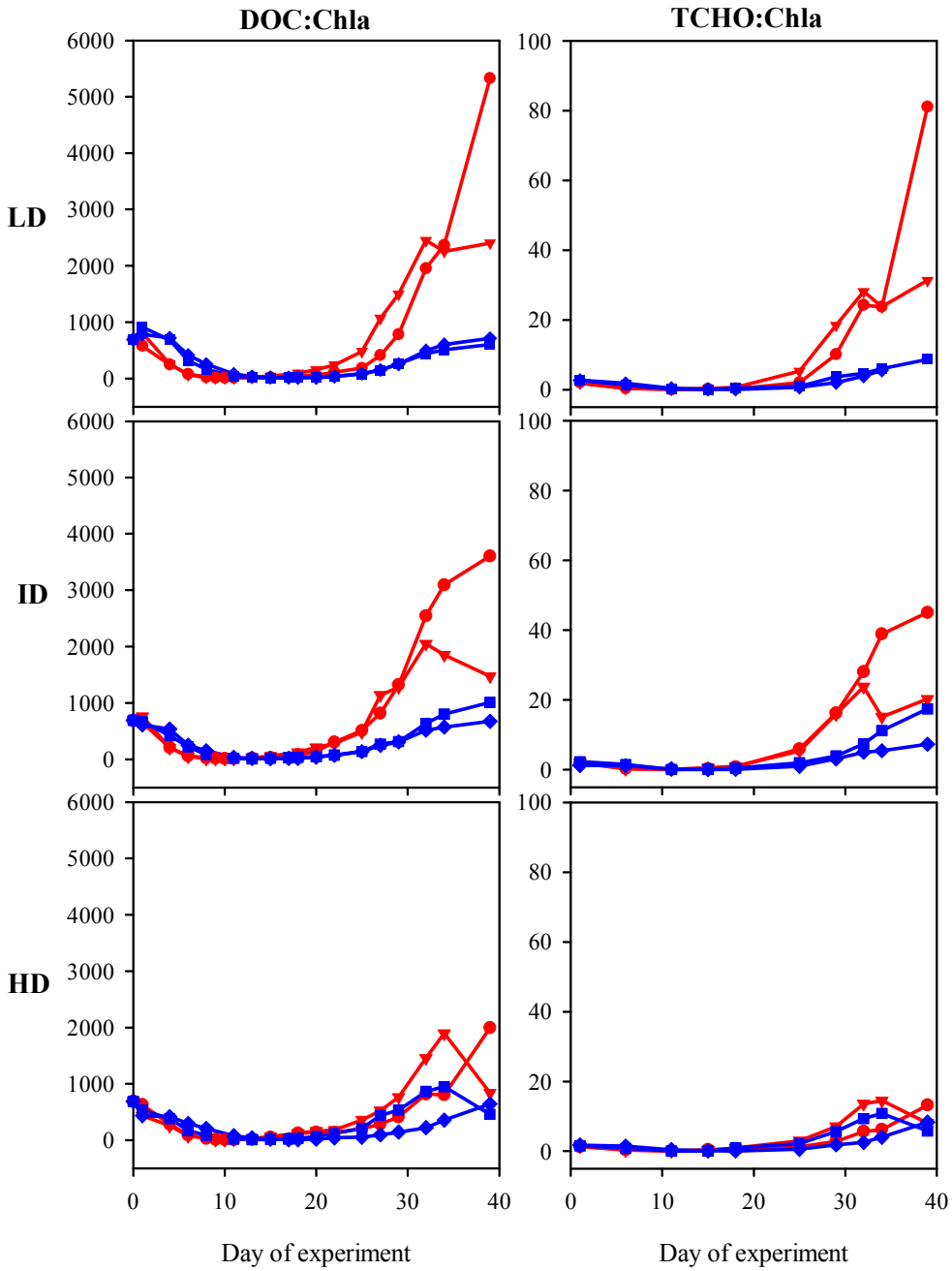

Figure 2-8: Dissolved organic carbon to chlorophyll *a* (DOC/Chl*a*) and total carbohydrates (TCHO) to chlorophyll *a* (TCHO/Chl*a*) at low (LD), intermediate (ID), and high (HD) copepod density for each mesocosm. T+0 treatments are indicated by blue, T+6 by red lines and symbols.

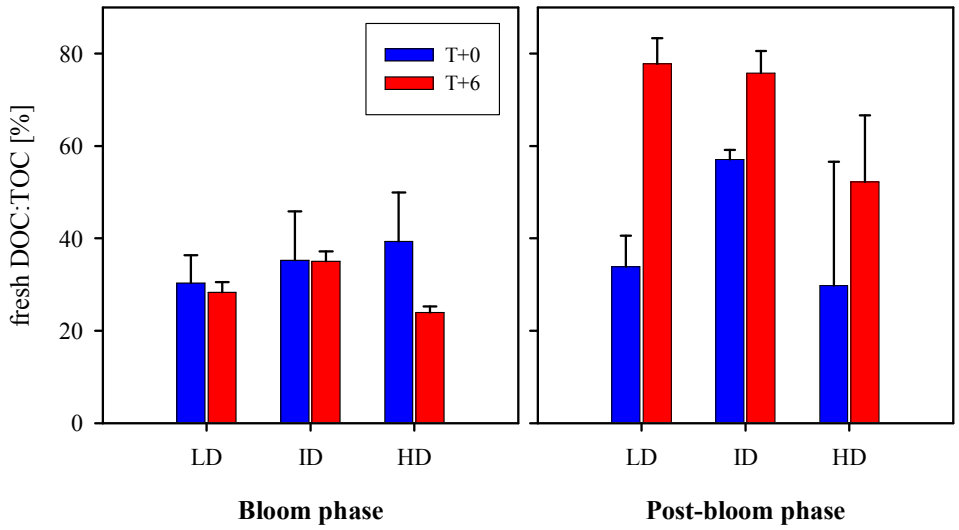

Figure 2-9: Proportion of fresh dissolved organic carbon (DOC) on total organic carbon (TOC) during the bloom phase and during the post-bloom phase.

DON and DOP dynamics were completely different from those of DOC and carbohydrates (Fig. 2-10). DON increased throughout the experiment from initially 10.4 ± 2.1 to 14.8 ± 0.7 µmol L^{-1} at the end of the experiment. In contrast, DOP concentrations stayed at the same level of on average 0.25 ± 0.02 µmol L^{-1} for the whole time. Relatively low DON and DOP and high DOC concentrations led to extreme deviations from Redfield ratio, yielding for total DOC:DON before nutrient depletion higher values for T+0 with 21 ± 1 (day 13) compared to 19 ± 1 (day 9) for T+6 (p=0.03). After nutrient depletion maximum DOC:DON ratios were 35 ± 5 for all treatments, showing a negative trend with increasing copepod abundance for T+6 (Tab. 2-2). DOC:DOP ratios showed no response to changes in temperature or copepod abundance, yielding for all treatments 986 ± 147 before DIP depletion (days 13, day 9, respectively) and increasing to maximum concentrations of 2546 ± 864 after nutrient depletion (day 15, day 11, respectively). DON:DOP ratios also showed no response to changes in temperature or copepod abundance, yielding for all treatments 50 ± 6 before DIP depletion (days 13, day 9, respectively) and increasing to maximum concentrations of 77 ± 15 after nutrient depletion (day 15, day 11, respectively) (Tab. 2-2).

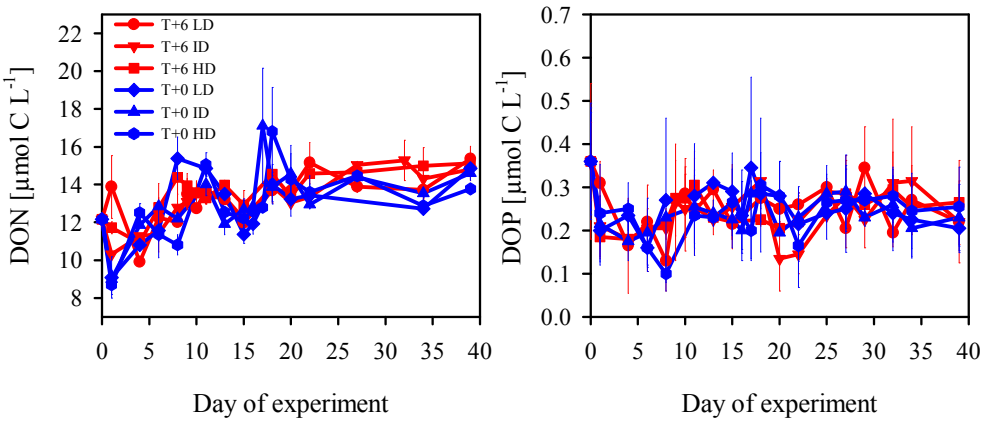

Figure 2-10: Dissolved organic nitrogen (DON) and phosphorus (DOP) averaged for the two replicates with the vertical bars indicating the range between the replicates.

Discussion

Bloom timing

The bloom peak timing was accelerated by ~1 day per degree Celsius temperature elevation. In general, spring bloom timing in the ocean can vary by several weeks. While the available marine time series data so far did not provide evidence for an advancement in diatom spring bloom timing in response to ocean warming (Edwards and Richardson 2004; Wiltshire et al. 2008), an acceleration in the range obtained in this study was previously observed during other mesocosm studies (Sommer and Lengfellner 2008; Wohlers et al. 2009; Winder et al. 2012). In this study, copepod abundance had no effect on the phytoplankton bloom timing, although, one would expect an enhanced top-down control on phytoplankton due to accelerated copepod metabolic rates at warmer temperature (Wiltshire et al. 2008; Gaedke et al. 2010).

Particulate organic matter accumulation

As expected, POC_{max} decreased in response to increasing copepod density. In contrast, a significant negative effect of temperature on POC accumulation was not determined. This result contradicts findings of Sommer and Lewandowska (2011), who found for the same study phytoplankton biomass to decrease with warming. Different from our measurement of POC, Sommer and Lewandowska (2011) estimated phytoplankton biomass as biovolume and subsequent conversion to carbon equivalents. Other mesocosm experiments also reported of negative effects of elevated temperature on phytoplankton biomass (Keller et al. 1999; O'Connor et al. 2009; Lassen et al. 2010; Lewandowska and Sommer 2010). While the study of Lassen et al. (2010) did not investigate grazer effects, the other three studies related the negative effect of warming on phytoplankton biomass

to increased abundances of zooplankton. After all, the difference between HD and LD for POC_{max} was more pronounced at T+6, hinting to a negative effect of temperature on POC accumulation due to enhanced heterotrophy. Indeed, bacterial secondary production (BSP) was about two times higher at T+6 during the bloom period in this study (Wohlers-Zöllner et al. 2012). Higher BSP at similar temperature elevation was observed before, but without significant effect on maximum POM accumulation (Wohlers et al. 2009). Warming in particular stimulated heterotrophic bacterial processes during a series of mesocosm experiments (Wohlers-Zöllner et al. 2012). The bacterial to primary production ratio doubled with an increase in temperature of 6 °C during phytoplankton bloom conditions (von Scheibner et al. 2013). Müren et al. (2005) calculated a five times higher heterotrophic to autotrophic biomass ratio when increasing the temperature from 5 to 10 °C and observed a 45 % reduction in sedimentation at warmer temperatures and attributed this to enhanced respiration and bacterial degradation. Warming also enhanced the degradation of aggregates (Piontek et al. 2009).

Stoichiometry of particulate organic matter

Increased particulate C to N and P during the bloom

Highest particulate C:N and C:P ratios were observed shortly after nutrient (N, P, Si) exhaustion. That carbon and nitrogen dynamics can decouple after nitrate depletion during phytoplankton blooms was observed before and attributed to excess carbon fixation (Engel et al. 2002; Wetz and Wheeler 2003). Excess carbon fixation or carbon overconsumption describes the process, in which dissolved inorganic carbon relative to inorganic nitrogen (or phosphorus) is taken up by phytoplankton in excess of the Redfield-ratio (Sambrotto et al. 1993; Toggweiler 1993). Engel et al. (2002) traced increased POC:PN back to an enhanced channelling of carbon into the formation of TEP from the DOC pool. In our study, higher POC:PN ratios were observed during the bloom and were thus not directly related to TEP formation.

The effect of grazer abundance

The stoichiometry of POM changed due to grazer abundance, namely POC:PN and POC:POP decreased with increasing copepod abundance. This trend was also observed for POC:BSi at T+6. In this study, the phytoplankton assemblage did not change between treatments (Sommer and Lewandowska 2011) and hence can not explain the observed differences in POM stoichiometry. Differences in stoichiometry, however, may have occurred due to physiological responses. That grazing by copepods reduced the proportion of C-rich but nutrient-poor detritus in POM seems unlikely, as the calanoid copepods present in this study are able to catch selectively for their prey and prefer living algae to dead cells (Sommer 1994). It is known that consumers, via egestion and

excretion, can be important drivers for nutrient regeneration and recycling. This can feed back to autotrophs by increasing the availability of nutrients (Ketchum 1962; Lehman 1980; Sterner 1986; Elser and Urabe 1999). For example, in a pond, C:P and N:P ratios of sestonic particles were high at low zooplankton biomass and low at high zooplankton biomass (Urabe 1995). The effects of altered nutrient uptake and recycling were the most probable underlying mechanisms for lowered C:N and C:P ratios of periphyton in response to grazing according to a meta-analysis (Hillebrand et al. 2008). Consumer-driven nutrient recycling probably also increased the nutrient availability for autotrophs in our study resulting in reduced C:N and C:P ratios of POM.

The effect of temperature

In a recent mesocosm study, POC accumulation increased with increasing temperature, probably caused by the effect of carbon overconsumption, whereby more POC than PN accumulated resulting in elevated POC:PN ratios (Taucher et al. 2012). A similar process may have occurred in our study, since POC:PN ratios were higher at T+6 than at T+0, albeit not statistically significant. Contradictory results, however, come from previous mesocosm experiments in which maximum POC:PN (Biermann, unpublished results) and mean POC:POP declined with increasing temperature (Wohlers-Zöllner et al. 2012). PN:POP was not significantly affected by temperature, but at T+6 a declining trend with increasing copepod abundance was observed, hinting at a preferential remineralisation of P. In general, P is remineralized faster than N and C (Shaffer et al. 1999; Loh and Bauer 2000). Higher abundance of bacteria may enhance remineralisation. Indeed, total bacteria numbers (TBN) were positively affected by temperature, as their peak was earlier at T+6 compared to T+0 and almost concomitant with the phytoplankton peak. A tighter temporarily coupling between phytoplankton and bacterial maximal abundance was previously reported (Hoppe et al. 2008; von Scheibner et al. 2013). Although this result may imply higher nutrient remineralisation at T+6 compared with T+0, were TBN were low during the phytoplankton bloom, also a competition of nutrients between phytoplankton and bacteria could be possible, leading to earlier nutrient deficiency for phytoplankton. Bacteria biomass was, however, only 1 % of phytoplankton biomass at T+6 and less than that at T+0 at the time of the phytoplankton biomass peak, indicating a minor importance of nutrient competition between bacteria and phytoplankton.

Dissolved organic matter

Dissolved organic matter accumulation

DOC increased only after the depletion of inorganic nutrients. It is often observed that extracellular release increases at the end of phytoplankton blooms in response to nutrient depletion (Nagata 2000; Engel et al. 2002). Extracellular release by phytoplankton can

comprise up to 80-90 % polysaccharides (Myklestad 1995). As TCHO simultaneously increased with DOC, and DOC consisted on average of 70 % TCHO, an algal origin of this DOC is very likely.

Contrary to DOC, DON showed an increasing trend that continued over the whole experimental period. This effect was observed before in mesocosm studies (Engel et al. 2010; Taucher et al. 2012). For DOP no trend was observed at all. Neither DON nor DOP showed a response to increased temperature or copepod abundance. This can probably be attributed to the fact that N and P can be severely limiting nutrients, while C can generally be only rate limiting. DOP is the fraction of DOM that is preferentially mineralized (Clark et al. 1998) and organic phosphorus is easily hydrolysed back to DIP at the alkaline pH of seawater (Lalli and Parons 1997). Small molecules (amino acids, urea) of DON and DOP can be utilized by phytoplankton and bacteria (Bronk 2002; Karl and Björkman 2002). Dissolved amino acids (DAA) are the main part of characterized DON. Engel et al. (2010) found a contribution of dissolved free amino acids (DFAA) of up to 20 % of DAA and pointed out that DFAA are small enough to be taken up by microbes with turnover times of a few hours. Hence, DON and DOP were probably quickly recycled and an accumulation was therefore at least for DOP not detectable. In contrast, DOC accumulated in the water column until day 34, indicating that bacteria were temporarily not able to balance the increase in DOC. This can be attributed to either nutrient limitation (Thingstad et al. 1997) or a refractory nature of the fresh DOC (Fry et al. 1996).

Stoichiometry of DOM

Owing to relatively high DOC concentrations right from the start of this study, ratios for DOC:DON and DOC:DOP were at the upper end or higher compared to literature values. A summary of surface and deep ocean DOM gives a range for DOC:DON of 9-18 and for DOC:DOP of 180-570 (Benner 2002). After nitrate depletion, DOM with a C:N $\geq$ 16 accumulated during a phytoplankton bloom, dominated by the diatom *Chaetoceros* sp. (Wetz and Wheeler 2003). Kähler and Koeve (2001) calculated a DOC:DON of 23.5 for surface water (5 m depth) along a transect in the North Atlantic - a similar high ratio as observed for DOC:DON ratios at least for bloom conditions in our study. After nutrient depletion, DOC increased and therewith DOC:DON and DOC:DOP, however, the increase was more pronounced for elevated temperature and lower copepod abundance (see below).

The effect of temperature on DOM

DOC:Chl *a* after nutrient depletion was positively affected by the temperature elevation. A more pronounced production of dissolved organic matter at higher temperatures was

found in short-time incubations (Morán et al. 2006) and mesocosm studies (Wohlers et al. 2009; Engel et al. 2010; Taucher et al. 2012), and was hence also confirmed by this study. Taucher et al. (2012) suggest that higher temperatures enhance excess dissolved inorganic carbon consumption leading to increased C:N of POM and DOM. As a possible explanation the authors assume an enhancement of the channelling of excess carbon into TEP. TEP formation began to increase at T+6 during the last days of the experiment (day 25 until end). DOC can abiotically form to polymer particles (Chin et al. 1998; Kerner et al. 2003). This mechanism was probably also valid during our study, but only at elevated temperature. This result is in line with the observed temperature effect on TEP formation in a previous mesocosm experiment (Wohlers et al. 2009) and confirms, that physical aggregation processes are enhanced at elevated temperature.

The effect of copepod abundance on DOM

DOM did not increase due to higher grazer abundance as shown by other studies (Nagata 2000; Kragh et al. 2006). Rather, DOC decreased with increasing copepod abundance. We detected a small increase in ammonium at T+6 in HD and ID but not LD treatments around days 18 to 20 (Fig. 2-4), supporting the hypothesis of enhanced nutrient recycling at higher copepod abundance. Hence, nutrient deficiency was likely higher at LD. This may have contributed to enhanced nutrient stress and subsequent DOC release by phytoplankton.

Consequences for a future ocean

Changes in the balance of POM and DOM can affect the efficiency of the biological carbon pump that transports CO_2 bound in organic carbon compounds to greater ocean depth where it is sequestered on time scales of hundreds of years. This and previous studies showed that a temperature increase shifts the partitioning between particulate and dissolved organic carbon towards the DOM pool (Engel et al. 2010; Wohlers-Zöllner et al. 2012; Taucher et al. 2012) and TEP formation (Wohlers-Zöllner et al. 2012). This study, combining projected climate warming and different copepod abundances, suggests that the "excess carbon consumption" by phytoplankton that is favoured by nutrient stress and suspected to increase due to sea-surface warming, could be moderated by the effect of copepod-driven nutrient recycling and counteract increases in C:N or C:P ratios of POM and DOM.

Acknowledgements

This work was funded by the German Research Foundation (DFG) as part of the priority program 1162 “AQUASHIFT”. P. Fritsche, N. Händel, T. Hansen, A. Ludwig, C. Meyer, and K. Nachtigall are gratefully acknowledged for technical support.

Chapter 3

Effects of rising temperature on pelagic biogeochemistry in mesocosm systems – a comparative analysis of the AQUASHIFT Kiel experiments

Abstract

A comparative analysis of data, obtained during four indoor-mesocosm experiments with natural spring plankton communities from the Baltic Sea, was conducted to investigate if biogeochemical cycling is affected by an increase in water temperature of up to 6 °C above present-day conditions. In all experiments, warming stimulated in particular heterotrophic bacterial processes and had an accelerating effect on the temporal development of phytoplankton blooms. This was also mirrored in the build-up and partitioning of organic matter between particulate and dissolved phases. Thus, warming increased both the magnitude and rate of dissolved organic carbon (DOC) build-up, whereas the accumulation of particulate organic carbon (POC) and phosphorus (POP) decreased with rising temperature. In concert, the observed temperature-mediated changes in biogeochemical components suggest strong shifts in the functioning of marine pelagic food webs and the ocean's biological carbon pump, hence providing potential feedback mechanisms to Earth's climate system.

Introduction

Earth's climate system is tightly linked with the ocean through the uptake and storage of heat (Barnett et al. 2005) and the exchange of climate-active gases, such as carbon dioxide (CO_2), at the air-sea boundary (Siegenthaler and Sarmiento 1993). While the ocean thus acts as a mitigating agent of anthropogenic climate change, it experiences major changes itself as a result of this. The absorption of heat, for instance, has led to an increase in global surface ocean water temperature (0-3000 m) of 0.037 °C in the period 1955-1998 (Levitus et al. 2005), with a further projected rise in global surface temperature of 1 to 6 °C until the end of the 21st century (Meehl et al. 2007).

Temperature is a major environmental factor that can both directly and indirectly affect biological processes in the ocean (Boyd and Doney 2002; Sarmiento et al. 2004). While in principle all biological processes are directly dependent on temperature, heterotrophic processes are generally expected to display a stronger sensitivity to changes in temperature than autotrophic processes (Tilzer and Dubinsky 1987; Müren et al. 2005; López-Urrutia et al. 2006). Concerning the latter, an additional pronounced dependence on light and nutrient availability is usually assumed, thus suggesting an indirect effect of warming on autotrophic processes through temperature-induced alterations in water column stratification (Sarmiento et al. 1998; Bopp et al. 2001). In concert, the projected increase in surface ocean temperature is expected to profoundly affect the dynamics and interplay of auto-and heterotrophic processes in the pelagic marine food web and the associated biogeochemical cycling of major elements, such as carbon (C), nitrogen (N), and phosphorus (P) (O'Connor et al. 2009; Finkel et al. 2009; Riebesell et al. 2009; Morán et al. 2010).

In the framework of the 6-year program AQUASHIFT, a series of indoor-mesocosm experiments was conducted to investigate the effects of sea surface warming on the food web dynamics of natural Baltic Sea spring plankton communities and the cycling of C, N, and P within. In a synthesis of the first three years of AQUASHIFT experiments, in which the plankton community was exposed to a range of four temperatures (ambient and three elevated temperatures) with differing daily light doses between the years, Sommer and Lengfellner (2008) observed recurrent temperature effects on the timing of the bloom as well as on key characteristics of the phytoplankton community. Thus, the bloom peak displayed a uniform acceleration of 1-1.4 days per °C increase above ambient temperature, the composition of the autotrophic community members shifted from a diatom- to a flagellate-dominated system, and phytoplankton biomass and cell size decreased with rising temperature. In the experiments in 2008 and 2009 a different approach was chosen, exposing the plankton community to a factorial combination of two temperatures (ambient and one elevated temperature) and either three levels of daily light dose (2008) or three levels of copepod abundance (2009). While in principle showing the same effects of warming on the timing of the bloom and characteristic features of the phytoplankton community, these experiments revealed that temperature was the main driving force behind the observed acceleration of bloom dynamics, whereas daily light dose and copepod density were equally important with temperature in regulating phytoplankton biomass, average cell size and community composition (Lewandowska and Sommer 2010; Sommer and Lewandowska 2011). Moreover, Lewandowska et al. (2011) showed, using a meta-analytical approach, a direct effect of experimental warming on biomass-normalized primary production (PP) across

all experiments, which was most pronounced at low grazing pressure and high daily light dose.

In the first of two experiments in 2006, Wohlers et al. (2009) showed, that also heterotrophic processes strongly responded to rising temperature, thereby affecting the build-up, stoichiometry, and the POM-DOM partitioning of organic matter. Thus, elevating the temperature by up to 6 °C above ambient conditions notably stimulated both bacterial secondary production (BSP) and community respiration already during the build-up phase of the bloom. This caused a significant reduction in the biological net drawdown of dissolved inorganic carbon, a reduced availability of particulate organic matter (POM) for sedimentation, and an enhanced accumulation of dissolved organic carbon compounds. Moreover, experimental warming led to a reduced net build-up of particulate organic phosphorus (POP) and an elevated as well as accelerated accumulation of dissolved combined carbohydrates (dcCHO), thereby also affecting the stoichiometry of particulate and dissolved organic matter (Wohlers et al. 2009; Engel et al. 2010).

Based on these findings, we reanalyzed the AQUASHIFT data to test the following hypotheses:

(1) Temporal dynamics of bloom development

$H1_0$: Warming has no effect on the temporal coupling of autotrophic production and heterotrophic degradation of biomass.

$H1_A$: Heterotrophic processes respond stronger to warming than autotrophic processes. Thus, increasing temperature will lead to an acceleration of heterotrophic compared to autotrophic processes, thereby altering the timing of cardinal bloom events.

(2) Organic matter net build-up and partitioning between particulate (i.e., POM) and dissolved phases (i.e., DOM):

$H2_0$: Warming has no effect on the balance between autotrophic production and heterotrophic degradation of biomass, with hence no changes occurring in organic matter net build-up and partitioning.

$H2_A$: Heterotrophic processes respond stronger to warming than autotrophic processes. Thus, increasing temperature will stimulate the heterotrophic degradation of POM more than its autotrophic production, thereby decreasing the overall net-build-up of POM. Moreover, warming will increase the partitioning of organic matter to the DOM pool through changes in algal exudation and the heterotrophic dissolution of POM.

(3) Organic matter elemental composition:

$H3_0$: Warming has no effect on the elemental stoichiometry of autotrophic production and heterotrophic degradation of biomass.

$H3_A$: Increasing temperature stimulates the preferential recycling of nitrogen (N) and phosphorus (P) compared to carbon (C), thereby causing an increase in the C:N:P ratio of POM and DOM. Moreover, warming increases the competition for nutrients

between algae and bacteria. This promotes an enhanced exudation of dissolved organic carbon-rich compounds by algae and further increases the C:N:P ratio of DOM.

To test these hypotheses and to check for recurrent patterns in the response obtained as part of the AQUASHIFT mesocosm project, we have carried out a comparative analysis of the AQUASHIFT experiments of the years 2006, 2008 and 2009. In particular, we will present results on the effects of experimental warming on the timing of cardinal bloom events, the build-up, partitioning and qualitative nature of particulate and dissolved organic matter, as well as on the dynamics of transparent exopolymeric particles (TEP).

Material and Methods

Experimental design and set-up

In the framework of the AQUASHIFT project yearly indoor mesocosm experiments were conducted during the spring season in the years 2005-2010. Our comparative analysis includes data of the experiments conducted in 2006 (AQ2, AQ3), 2008 (AQ5), and 2009 (AQ6). The experiments of the years 2005, 2007 and 2010 had to be excluded from this analysis due to low-light induced problems with biomass development on the mesocosm walls in the first two studies, as well as due to a differing conceptual design of the latter study.

For the experiments AQ2 and AQ3, eight mesocosms (1400L volume, 1m depth, high density-polypropylene) were distributed among four temperature-controlled climate chambers, thereby allowing for a simulation of four different temperature scenarios: *in situ* temperature (T+0) and temperatures elevated by 2 °C, 4 °C, and 6 °C above *in situ* temperature (T+2, T+4, and T+6; see also Sommer et al. 2007 for more details).

The experiments AQ5 and AQ6 focused on the combinations of the environmental factors temperature and light intensity (AQ5), as well as temperature and overwintering copepod density (AQ6) in a factorial design. For this purpose, a total of twelve mesocosms (1400L volume, 1m depth, HD-PP) were distributed among four climate chambers. Two chambers were run at *in situ* temperature T+0, whereas the temperature of the other two chambers was increased by 6 °C above T+0 (i.e., T+6). The two temperature regimes were then combined with either three different light intensities (high light (HL), intermediate light (IL), and low light (LL)) or three levels of initial copepod densities (high density (HD), intermediate density (ID), and low density (LD)), simulating changes in water column mixing depth and cloud cover, as well as in the overwintering copepod population, respectively (see Tab. 3-1 for details on daily light doses and copepod abundances). All treatments were duplicated.

The ambient temperature T+0 was derived from the decadal mean (1993-2002) spring water temperature of the investigation area Kiel Bight (Baltic Sea), yielding a value of approx. 2.5 °C. The elevated temperature scenarios T+2, T+4, and T+6 were chosen according to the projections of the IPCC report for the end of the 21st century (Meehl et al. 2007). In the experiments AQ3, AQ5, and AQ6 the temperature of the individual mesocosms was gradually increased in the course of the experimental period to mimic the natural late winter/early spring environmental conditions, thus causing a step-wise decrease in the temperature difference between treatments by 0.25 °C per month (Sommer et al. 2007). As the algal blooms in these studies always occurred within the first 4 weeks of the experimental period, the effective water temperatures remained close to initial values, thus maintaining also the reported temperature differences between treatments.

Prior to the experiments, the mesocosms were simultaneously filled with natural seawater from Kiel Fjord (Baltic Sea), containing a natural spring plankton community as present in the fjord at the time of filling. Due to their fragile nature, copepods were added from net catches in natural densities of 1.5-11 individuals L^{-1} (ind L^{-1}) as described in Tab. 3-1. The phytoplankton community was usually dominated by diatoms (>90% of total algal biomass), predominantly by *Skeletonema costatum*.

Table 3-1: Summary of the environmental core settings during the various AQUASHIFT experiments. ΔT describes the net temperature difference (in °C) between the in situ (T+0) and the elevated temperature treatments. The daily light dose value represents the average daily light dose during the bloom period (in mol quanta m^{-2} d^{-1}). $N:P_{inorg}$ describes the molar ratio of dissolved inorganic nitrogen to dissolved inorganic phosphorus. The initial copepod density at the start of the experiment is given in ind. L^{-1}. All combinations of temperature, light, and copepod density were carried out in duplicate.

	AQ 2	AQ 3	AQ 5			AQ 6		
			HL	IL	LL	HD	ID	LD
Year	2006	2006	2008			2009		
ΔT	+0, +2, +4, +6	+0, +2, +4, +6	+0, +6			+0, +6		
Daily light dose	1.9	4.3	7.7	7	6	6.8		
Copepod density	5	9	8			10	4	1.5
Replicate number	2	2	2	2	2	2	2	2
$N:P_{inorg}$	30:1	15:1	18:1			17:1		

Light was supplied by separate light benches above each of the mesocosms, containing 12 full-spectrum light tubes (10 solar tropic T5 Ultra (4000K), 2 solar nature T5 Ultra (9000 K); JBL, Germany). The light benches were controlled by a computer simulating daily irradiance curves. In addition, a seasonal light pattern based on astronomic equations (Brock 1981) was imposed on the light system in all but one experiment (i.e., AQ2), causing a gradual increase in daily light dose over the

experimental period. During AQ2 the daily light dose was kept constant over the whole experimental period. The daily light doses are given as mixed water layer values averaged over the bloom period using an attenuation coefficient of 0.25 m^{-1} (i.e., as typical for Baltic Sea winter water; (Sommer and Lengfellner 2008)). Due to technical changes in the light system between the first and second phase of AQUASHIFT, the daily light doses are generally higher in the second compared to the first phase with values ranging between 6.0-7.7 and 1.9-4.3 mol photons m^{-2} day^{-1}, respectively (Tab. 3-1).

In AQ2, AQ3, and AQ5 an initial copepod density of approx. 10 individuals L^{-1} (ind. L^{-1}) was aspired, but depended largely on the prevailing situation at the investigation site at the time of mesocosm filling (Tab. 3-1). In AQ6 an initial copepod density of 10 (AQ6-HD), 4 (AQ6-ID), and 1.5 (AQ6-LD) ind. L^{-1} was achieved.

Dissolved inorganic nutrient concentrations varied naturally between years. In AQ2 and AQ5 13 and 5 µmol L^{-1} nitrate (NO_3^-), respectively, were added to all mesocosms in order to obtain comparable ratios of dissolved inorganic nitrogen to phosphorus ($N:P_{inorg}$). Thus, $N:P_{inorg}$ was in all experiments above the canonical Redfield ratio of 16:1 (Tab. 3-1; Redfield and Ketchum 1963), implying phosphorus to be the limiting nutrient.

The water in the mesocosm was gently mixed by means of a motor-driven propeller attached to the side of the mesocosms. This kept living cells and smaller particles in suspension, whereas larger particles and aggregates were allowed to sink out of the water column.

Sampling was in general carried out at least three times a week, but up to daily during bloom phases. Samples were either taken at intermediate depth by means of a silicone hose or as depth-integrated samples with a plexiglas-tube that was lowered into the mesocosms and closed underneath the surface with silicon stoppers. The total sample volume taken in the course of the experiments depended on the overall duration, the frequency of sampling, and the parameters investigated, but was in general below 20% of the total mesocosm volume.

Parameters

For a comparative analysis of recurrent patterns a range of suitable parameters was chosen to describe the effect of experimental warming on food web dynamics and the associated cycling of the major elements C, N, and P.

The timing of the spring plankton bloom is represented by the bloom peak (i.e., the day of maximum biomass as characterized by particulate organic carbon (POC) concentration) and the onset of nutrient depletion (i.e., based on phosphate (PO_4^{3-}) concentration).

Temperature-related changes in the build-up and accumulation of particulate and dissolved organic matter are investigated through changes in the concentration of POC, POP, and dissolved organic carbon (DOC; data available only for AQ2, AQ5, AQ6). Moreover, we present data on the pool of dissolved combined carbohydrates (dcCHO), as well as on the dynamics of Transparent Exopolymer Particles (TEP; data available only for AQ2, AQ5, AQ6). The latter form from dissolved organic carbon compounds and can play a decisive role in the aggregation and sedimentation of particulate matter to greater depths at the end of bloom situations (Passow 2002b).

Warming-related shifts in the quality of the accumulating particulate and dissolved organic matter are investigated by analysing the ratio of POC to POP (POC:POP) as well as DOC to dissolved organic phosphorus (DOP), i.e., DOC:DOP (data available only for AQ2, AQ5, AQ6).

Included in the analysis are also the average rates of algal primary production (PP; i.e., particulate and dissolved) and bacterial secondary production (BSP) to elucidate temperature-related shifts in central autotrophic and heterotrophic processes that are key drivers of biogeochemical cycling within the planktonic food web.

Measurements

Dissolved inorganic nutrient concentrations were analyzed colorimetrically from filtered (cellulose acetate filters, 5 µm pore size) water samples following the protocol of (Hansen and Koroleff 1999). All nutrient analyses were carried out on the day of sampling, except for samples taken during AQ6, where samples were filtered through 5 µm celluloseacetate-filters (Whatman) and stored at -20 °C until analysis.

For the determination of POC and POP 100-200 mL of sample were filtered onto pre-combusted (450 °C, 5 h) GF/F-filters (Whatman) and stored at -20 °C until analysis. Prior to analysis on a Eurovector EuroEA-3000 elemental analyzer (Sharp 1974), POC samples were dried at 60 °C for 6 h. Particulate inorganic carbon (PIC) was not accounted for due to the absence of lithogenic carbonates and calcifying organisms. POP concentrations were determined colorimetrically after oxidation with peroxodisulphate or Oxisolv reagent (Merck) following the protocol of Hansen and Koroleff (1999).

Samples for the analysis of DOC and dissolved total carbohydrates (dtCHO) were filtered through pre-combusted (450 °C, 5 h) GF/F-filters (Whatman). The filtrate was subsequently collected in pre-combusted (450 °C, 12 h) 20 mL glass ampoules and frozen at -20 °C. DOC samples were analysed on a Shimadzu Total Organic Carbon analyser (TOC_{VCN}) using the High Temperature Combustion Oxidation method (Qian and Mopper 1996). The concentration of dCHO was measured spectrophotometrically using the 2,-4,-6-tripyridyl-s-triazine approach (Myklestad et al. 1997). Dissolved combined

carbohydrates (dcCHO) were obtained by subtracting the concentration of dissolved free monosaccharides from dtCHO after acid hydrolysis (1M HCl).

The concentration of TEP was determined colorimetrically (Passow and Alldredge 1995b). Samples were gently (< 150 mbar) filtered through 0.4 µm polycarbonate filters (Whatman), stained with 1 mL of an aqueous solution of Alcian Blue (0.02 %) and stored at -20 °C until analysis. The dye was redissolved in 80% H_2SO_4 for three hours and the supernatant analysed on a Hitachi U-2000 spectrophotometer. All filters were prepared in duplicate. The acidic polysaccharide Gum Xanthan was used as a standard. The carbon content of TEP (μmol C L^{-1}) was calculated using a conversion factor (*f'* = 0.63; (Engel 2004)).

Rates of autotrophic PP and heterotrophic BSP were determined three times a week. Primary production was determined through measurements of ^{14}C-bicarbonate ($H^{14}CO_3^-$) uptake (Steemann Nielsen; Gargas 1975). For this purpose, $H^{14}CO_3^-$ was added to 30 mL-samples at a final activity of 4 µCi per bottle. The samples were then incubated *in situ* for approx. 4 h at intermediate water depth inside the respective mesocosms. All incubations were carried out in duplicate with one dark bottle serving as a blank. After incubation, sample aliquots were filtered onto 0.2 μm cellulose acetate in order to determine particulate primary production rates (PP_{part}). The filters were then fumed with concentrated hydrochloric acid (HCl) for 10 min in order to remove excess $H^{14}CO_3^-$ and 4 mL of scintillation cocktail (Lumagel Plus) were added. For dissolved primary production (PP_{diss}), 20 mL of filtrate received 100 μL of 1 N HCl. The filtrate was then stored in a desiccator, containing 1N NaOH to ensure maximum outgassing of expelled CO_2, under vacuum for eight days. Following this, a volume of 10 mL of scintillation cocktail (Aquasol) was added to each PP_{diss} sample. Finally, all samples were radio-assayed on a Packard TriCarb scintillation counter. Daily PP (µmol C L^{-1} d^{-1}) was calculated by multiplying the obtained production rates with a light factor (total amount of light throughout the day divided by the amount of light received during the incubation).

Bacterial secondary production was assessed by measuring the incorporation of ^{3}H-leucine (^{3}H-leu; only AQ2, 5), ^{14}C-leucine (^{14}C-leu; only AQ6), or ^{3}H-methyl-thymidine (^{3}H-thy; only AQ3), following the protocols by (Fuhrman and Azam 1982; Simon and Azam 1989). ^{3}H-leu (specific activity: 160 μCi $nmol^{-1}$), ^{14}C-leu (specific activity: 306 mCi $mmol^{-1}$) and ^{3}H-thy (specific activity: 63 μCi $nmol^{-1}$) were added to the samples at final concentrations of 103 nmol L^{-1}, 97.8 nmol L^{-1}, and 8 nmol L^{-1}, respectively. The samples were dark-incubated at *in situ* temperature (i.e. in the respective climate chambers) for 1.5 – 3 h. Incubation was terminated by adding formaldehyde (1% v/v). A sample volume of 5-10 mL was then filtered onto 0.2 μm polycarbonate membrane filters (Poretics®). The filters were subsequently rinsed with ice cold 5% TCA solution before being radio-assayed in 4 mL of scintillation cocktail

(Lumagel Plus) on a Packard TriCarb scintillation counter. All incubations were carried out in triplicate. A formalin-killed sample was used to correct for background absorption of radioactivity. To convert the incorporation of ^{3}H-leu and ^{3}H-thy into carbon production (μg C L^{-1} h^{-1}), a theoretical conversion factor of 3.1 kg C mol^{-1} leucine (Simon and Azam 1989) and an empirically determined conversion factor of 30.87 kg C mol^{-1} thymidine (Breithaupt 2009), respectively, were used. The daily carbon production rates (μmol C L^{-1} d^{-1}) were then calculated, assuming that bacterial production rates were constant throughout the day.

Calculations

For direct comparison of the different experiments, we defined cardinal points of the temporal bloom development, such as the beginning and end of the bloom period, as well as the onset of nutrient depletion (Fig. 3-1). The bloom period to be included in the analysis was determined by calculating the natural logarithm of POC concentration (ln[POC]; Fig. 3-1). During exponential growth and decay, ln[POC] should scale linearly with time. We took advantage of this for defining the first day during the build-up phase as well as the last day during the degradation phase by applying general linear regression models to ln[POC] data (for the build-up phase from the approximate onset of increasing ln[POC] to maximum ln[POC], for the degradation phase from maximum ln[POC] to the approximate minimum ln[POC]; see also Fig. 3-1). The range of data yielding the best fit in terms of r^2 was chosen to be the best representative for defining the respective build-up and degradation phase. The day of bloom peak was defined as the day of maximum POC concentration. Another important time point during bloom development is the onset of nutrient depletion, which was defined as the first day where PO_4^{3-} concentration fell below the detection limit of 0.05 µmol L^{-1} (Fig. 3-1).

Following the above criteria, the average build-up of POC (POC_{mean}), POP (POP_{mean}), and DOC (DOC_{mean}) were determined by calculating their geometric mean over the defined bloom period. For comparison of organic matter quality between treatments, the geometric mean of the ratios of POC to POP ($POC:POP_{mean}$) and DOC to DOP ($DOC:DOP_{mean}$) was calculated for the period from nutrient depletion onward until the last day of the bloom period. With regard to the accumulation of dissolved organic components and the elemental composition of organic matter, the onset of nutrient depletion is generally a cardinal time point in bloom situations, as it may trigger the exudation and accumulation of dissolved carbon-rich material (Norrman et al. 1995; Thingstad et al. 1997; Van Den Meersche et al. 2004). This often leads to strong deviations in organic matter stoichiometry and may hence affect food web dynamics.

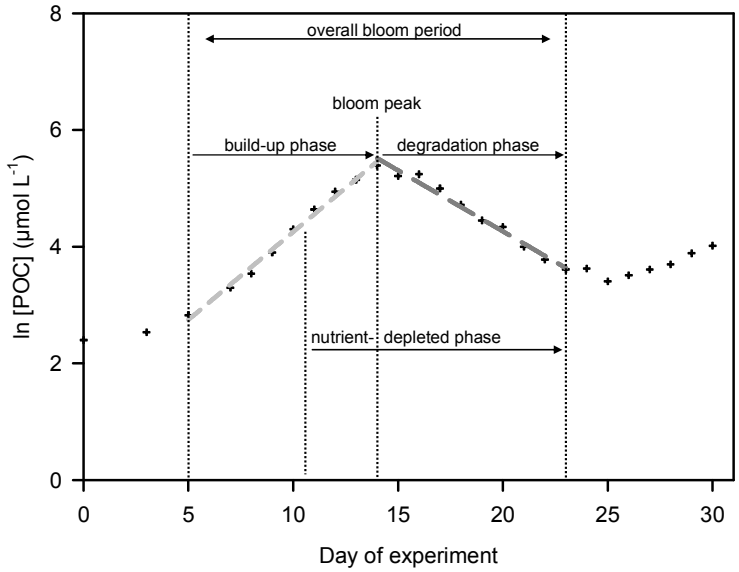

Figure 3-1: Schematic representation of a characteristic development of POC concentration in the course of an algal bloom, illustrating relevant definitions of cardinal bloom events. The *symbols* represent exemplary logarithmic POC concentration (ln[POC]; in µmol C L^{-1}; *cross symbol*) and the dissolved inorganic phosphate concentration(PO_4^{3-}; in µmol L^{-1}; *open circles*) from one of the AQUASHIFT studies (AQ2). The *dashed lines* represent the linear regression models that were fitted to the build-up phase *(light grey)* and the degradation phase *(dark grey)* of the bloom.

The rate of increase in [DOC] (DOC_{slope}) and [dCCHO] ($dCCHO_{slope}$) was determined by applying a general linear regression model for the time period from nutrient depletion until the end of the bloom period. For the analysis of TEP dynamics, both the geometric mean concentration during the full bloom period (TEP_{mean}) as well as the maximum TEP concentration (TEP_{max}), which was reached at approximately 11 days (AQ2) and 20 days (AQ5, AQ6) after the bloom peak, were determined.

For the average rates of algal primary production (PP_{part}, PP_{diss}) and heterotrophic bacterial production (BSP_{mean}) a geometric mean was calculated over the bloom period. Additionally, the average BSP at the time of maximum [POC] was calculated (BSP_{bloom_peak}).

Statistical analysis

The primary goal of our comparative analysis is to identify and describe recurrent trends in the response of important biogeochemical parameters to experimental warming across a series of mesocosm experiments with natural Baltic Sea plankton communities. In order to provide objective criteria to describe the direction and amplitude of these trends with increasing temperature, two statistical strategies were pursued, depending on the specific experimental set-up (i.e., with experimental warming as the sole environmental stressor or in factorial combination with daily light dose or copepod density). For AQ2 and AQ3,

where the plankton communities were exposed to a range of four temperatures, the parameter responses to rising temperature were investigated using linear regression models (STATISTICA, Statsoft). For AQ5 and AQ6, where a factorial combination of three light doses or three copepod densities with two temperature regimes was applied, the parameter responses were investigated through general linear models (GLM; STATISTICA, Statsoft) with temperature as a categorical factor and light dose or copepod density as a continuous factor. For cases of a significant single effect of light dose or copepod density on a specific parameter, a separate linear regression of this response parameter (y) versus light dose or copepod density (x) was calculated. For all analyses, a significance level of $P<0.05$ was applied.

In order to determine the overall effect of experimental warming on the various parameters across all experiments, the ln-transformed response ratio (*Ln*RR) was calculated for the relevant biogeochemical parameters for each experiment with

$$LnRR=\ln(M_E)-\ln(M_C),$$

where M_E and M_C are the mean values of observations in the elevated (T+6) and ambient temperature treatments (T+0), respectively. Following this, an overall mean effect size was calculated across all studies, including the 95% confidence interval (CI). A mean effect size of zero indicates that temperature had no or not a consistent effect on the investigated parameter, whereas positive and negative values indicate consistent temperature effects. Following the meta-analysis approach of (Kroeker et al. 2010), the effect size was considered to be significant ($\alpha=0.05$) when the CI did not overlap with zero.

Results

Timing of biomass maximum and nutrient exhaustion

The timing of the bloom peak ($bloom_{peak}$), as characterised by maximum POC accumulation, showed a significant ($P<0.01$) forward shift with increasing temperature in all experiments, ranging between 1.0 and 2.8 days $°C^{-1}$ (Tab. 3-2 to 3-5; Fig. 3-2). In AQ5 also increasing daily light dose significantly accelerated the timing of the bloom peak by 2.1 days $°C^{-1}$ ($P<0.01$; Tab. 3-4; Fig. 3-2), whereas changes in copepod density had no notable effect during AQ6 ($P=0.3$; Tab. 3-2).

Similarly, the onset of exhaustion of the limiting nutrient PO_4^{3-} ($PO_4^{3-}{}_{depl}$; Tab. 3-2 to 3-5; Fig. 3-2), occurred earlier by 0.3 to 2.3 days $°C^{-1}$ ($P<0.01$) across all studies. In comparison, increasing daily light dose or copepod density did not alter the timing of $PO_4^{3-}{}_{depl}$ ($P\geq0.6$; Tab. 3-4 to 3-5).

Algal primary production and bacterial secondary production

Both bloom-averaged particulate and dissolved primary production showed a mostly negative, but overall weak response to rising temperature throughout all experiments. Thus, particulate PP_{mean} displayed a significant negative trend with increasing temperature only in AQ6 (P<0.05; Tab. 3-5; Fig. 3-2), whereas AQ2 showed a significant negative effect of experimental warming on dissolved PP_{mean} (P<0.01; Tab. 3-2; Fig. 3-2). Copepod density affected particulate PP_{mean} significantly during the AQ6 study, causing a decrease with increasing grazer density (P<0.05; Tab. 3-5; Fig. 3-2).

In contrast, BSP rates showed a mostly positive response to increasing temperature, with a significant stimulation of BSP_{mean} by warming in three out of four studies (AQ3, AQ5, AQ6; P<0.01; Tab. 3-3 to 3-5; Fig. 3-2). Interestingly, this effect became already visible when looking at an earlier stage of the bloom period. Thus, BSP rates measured at the time of maximum POC accumulation ($BSP_{bloom\ peak}$) also displayed a significant positive trend with rising temperature in three out of four studies (AQ2, AQ5, AQ6; P<0.01; Tab. 3-2, 3-4, and 3-5; Fig. 3-2). In contrast, daily light dose and copepod density had no significant effect on both BSP_{mean} and $BSP_{bloom\ peak}$ across all studies (P≥0.09; Tab. 3-4 to 3-5; Fig. 3-2).

Table 3-2: Summary of results for AQ2. A linear regression model was applied to all data sets (n=8; df=1).

Dependent variable	Slope	*P* model	F	r^2
$Bloom_{peak}$ (day of experiment)	-1.4	0.0020	27.53	0.82
$PO_4^3{}_{depl.}$ (day of experiment)	-0.69	0.0009	14.71	0.71
part.PP_{mean} (µg C L^{-1} day^{-1})	-7.12	0.2640	1.51	0.20
diss.PP_{mean} (µg C L^{-1} day^{-1})	-0.71	0.0019	27.71	0.82
BSP_{mean} (µg C L^{-1} day^{-1})	0.53	0.5220	0.46	0.07
$BSP_{bloom\ peak}$ (µg C L^{-1} day^{-1})	4.63	0.0070	15.47	0.72
POC_{mean} (µmol C L^{-1})	-3.39	0.2400	1.72	0.22
POP_{mean} (µmol P L^{-1})	-0.012	0.0005	45.44	0.88
DOC_{mean} (µmol C L^{-1})	5.70	0.0219	9.42	0.61
$dcCHO_{mean}$ (µmol C L^{-1})	2.36	0.2500	1.63	0.21
DOC_{slope} (µmol C L^{-1} day^{-1})	0.73	0.0100	13.62	0.69
$dcCHO_{slope}$ (µmol C L^{-1} day^{-1})	0.68	0.0008	38.12	0.86
$POC:POP_{mean}$ (mol:mol)	-0.11	0.9900	0.00	0.00
$DOC:DOP_{mean}$ (mol:mol)	11.20	0.5400	0.42	0.07
TEP_{mean} (µmol C L^{-1})	-0.264	0.3340	1.10	0.16
TEP_{max} (µmol C L^{-1})	1.09	0.0474	6.18	0.51

Build-up of particulate and dissolved organic matter

The average build-up of POC during the bloom period showed a variable response to increasing temperature throughout all experiments. While no effect of warming could be observed in AQ2 and AQ6, POC_{mean} significantly decreased with rising temperature by 7.3 and 17.0 µmol C L^{-1} in AQ3 and AQ5 (P<0.01, Tab. 3-3 to 3-4, Fig. 3-2),

respectively. Changes in daily light dose and copepod density did not affect POC_{mean} ($P \geq 0.15$, Tab. 3-4 to 3-5; Fig. 3-2). Similarly, the average build-up of POP showed a significant negative trend with increasing temperature in AQ2 and AQ5 ($P<0.001$, Tab. 3-2, 4; Fig. 3-2). Warming also negatively influenced POP_{mean} in the AQ3 and AQ6 studies, but the effect was slightly insignificant ($P \leq 0.1$; Tab. 3-3, 3-5; Fig. 3-2). POP_{mean} remained unaffected by both daily light dose and copepod density ($P \geq 0.12$; Tab. 3-4 to 3-5; Fig. 3-2).

In contrast to the build-up of particulate organic matter, the average accumulation of DOC throughout the bloom period displayed a significant positive trend with rising temperature in two out of three studies (AQ2: $P<0.05$, AQ5: $P<0.01$; no data available for AQ3; Tab. 3-2, 3-4; Fig. 3-2).

Table 3-3: Summary of results for AQ3. A linear regression model was applied to all data sets (n=8; df=1).

Dependent variable	Slope	*P*	F	r^2
$Bloom_{peak}$ (day of experiment)	-0.98	0.0040	21.04	0.78
PO_4^3 $_{depl.}$ (day of experiment)	-0.34	0.0070	16.37	0.73
$part.PP_{mean}$ ($\mu g\ C\ L^{-1}\ day^{-1}$)	-2.79	0.1955	2.12	0.26
$diss.PP_{mean}$ ($\mu g\ C\ L^{-1}\ day^{-1}$)	-0.66	0.0507	5.94	0.50
BSP_{mean} ($\mu g\ C\ L^{-1}\ day^{-1}$)	1.52	0.0010	31.44	0.84
$BSP_{bloom\ peak}$ ($\mu g\ C\ L^{-1}\ day^{-1}$)	0.04	0.9640	0.00	0.00
POC_{mean} ($\mu mol\ C\ L^{-1}$)	-7.31	0.0047	19.18	0.76
POP_{mean} ($\mu mol\ P\ L^{-1}$)	-0.013	0.0940	3.95	0.40
$POC:POP_{mean}$ (mol:mol)	-14.227	0.0040	20.32	0.77

Table 3-4: Summary of results for AQ5. A general linear model was applied to all data sets with temperature as categorical factor and daily light dose as continuous factor (n=12; df=2).

Dependent variable	Temperature		Daily light dose		*P* model	F model	r^2
	b	*P*	b	*P*			
$Bloom_{peak}$ (day of experiment)	-2.25	0.0011	-2.08	0.0075	0.0009	17.12	0.79
PO_4^3 $_{depl.}$ (day of experiment)	-1.00	0.0008	-0.56	0.0566	0.0014	14.79	0.77
$part.PP_{mean}$ ($\mu g\ C\ L^{-1}\ day^{-1}$)	-3.97	0.1500	3.67	0.2800	0.1600	2.30	0.34
$diss.PP_{mean}$ ($\mu g\ C\ L^{-1}\ day^{-1}$)	-0.46	0.1379	0.20	0.5978	0.2791	1.48	0.25
BSP_{mean} ($\mu g\ C\ L^{-1}\ day^{-1}$)	3.75	0.0045	0.57	0.6600	0.0115	7.63	0.63
$BSP_{bloom\ peak}$ ($\mu g\ C\ L^{-1}\ day^{-1}$)	10.61	0.0001	-4.09	0.0900	0.0004	21.49	0.83
POC_{mean} ($\mu mol\ C\ L^{-1}$)	-16.98	0.0002	3.08	0.4200	0.0005	19.73	0.81
POP_{mean} ($\mu mol\ P\ L^{-1}$)	-0.04	0.0001	0.01	0.5800	0.0004	21.75	0.93
DOC_{mean} ($\mu mol\ C\ L^{-1}$)	17.48	0.0032	-8.98	0.1400	0.0090	8.33	0.65
$dcCHO_{mean}$ ($\mu mol\ C\ L^{-1}$)	4.37	0.0600	-4.44	0.1200	0.0700	3.67	0.45
DOC_{slope} ($\mu mol\ C\ L^{-1}\ day^{-1}$)	2.67	0.0005	-0.75	0.2800	0.0018	13.78	0.75
$dcCHO_{slope}$ ($\mu mol\ C\ L^{-1}\ day^{-1}$)	1.25	0.0014	-1.15	0.0099	0.0012	15.47	0.77
$POC:POP_{mean}$ (mol:mol)	-13.44	0.0900	3.25	0.7300	0.1800	2.05	0.31
$DOC:DOP_{mean}$ (mol:mol)	-15.29	0.6400	43.17	0.3100	0.4800	0.80	0.15
TEP_{mean} ($\mu mol\ C\ L^{-1}$)	4.05	0.0001	-0.93	0.2900	0.0005	20.38	0.82
TEP_{max} ($\mu mol\ C\ L^{-1}$)	6.85	0.0018	-2.72	0.2100	0.0054	9.83	0.69

No effect of daily light dose in the AQ5 study or of temperature and copepod density in AQ6 was observed ($P \geq 0.14$; Tab. 3-4 to 3-5; Fig. 3-2). In line with this, also the rate at which DOC accumulated (DOC_{slope}) showed a significant positive trend with increasing temperature in AQ2 ($P<0.05$; Tab. 3-2; Fig. 3-2) and AQ5 ($P<0.001$; Tab. 3-4; Fig. 3-2).

Looking at a specific compartment of DOC, i.e. the pool of dcCHO, revealed a more complex picture. Thus, the $dcCHO_{mean}$ displayed no significant response to any of the tested environmental stressors across all three studies (Fig. 3-2). In contrast, the rate of dcCHO accumulation ($dcCHO_{slope}$) responded positively to warming in two out of three studies (AQ2: $P<0.001$, AQ5: $P<0.01$; Tab. 3-2, 3-4; Fig. 3-2), whereas increasing light dose and copepod density had a significant negative effect on $dcCHO_{slope}$ in AQ5 ($P<0.01$; Tab. 3-4; Fig. 3-2) and AQ6 ($P<0.05$; Tab. 3-5 to 3-6; Fig. 3-2).

TEP dynamics

The dynamics of TEP concentration during and after the bloom period showed two divergent patterns in the different experiments. The first modus was characterized by low and temperature-independent TEP concentrations during the algal bloom phase, followed by a steep increase in TEP during the late post-bloom phase, which only occurred in the elevated temperature treatments. This pattern was observed in the studies AQ2 and AQ6. The second modus was characterized by a substantial increase in TEP already during the algal bloom phase. While the concentration of TEP thereafter decreased in the *in situ* temperature treatments, it stagnated or even increased at elevated temperature. Study AQ5 represents an example of this pattern.

In line with these observations, a significant positive trend of TEP_{mean} with rising temperature was observed only in AQ 5 ($P<0.001$; Tab. 3-4; Fig. 3-2), whereas TEP_{mean} did not respond significantly to warming in the AQ2 and AQ6 studies ($P \geq 0.22$; Tab. 3-2, 3-5; Fig. 3-2). In AQ6, TEP_{mean} decreased significantly with increasing grazer density ($P<0.05$; Tab. 3-5 to 3-6; Fig. 3-2).

TEP_{max}, on the other hand, displayed a significant positive trend with rising temperature in all studies (AQ2: $P<0.05$; AQ5: $P<0.01$; AQ6: $P<0.05$; Tab. 3-2, 3-4 to 3-5; Fig. 3-2), whereas changes in light dose and copepod density had no apparent effect on this parameter ($P \geq 0.21$; Tab. 3-4 to 3-5; Fig. 3-2).

Elemental stoichiometry of POM and DOM

The average ratio of POC to POP showed a significant negative trend with rising temperature only in one out of four studies (AQ3: $P<0.01$, Tab. 3-3; Fig. 3-2). A significant negative response of $POC:POP_{mean}$ was also observed with increasing copepod density in AQ6 ($P<0.05$; Tab. 3-5 to 3-6; Fig. 3-2). $DOC:DOP_{mean}$ did not show a

significant response to any of the environmental stressors temperature, light, or grazing pressure ($P \geq 0.3$; Tab. 3-2 to 3-5; Fig. 3-2).

Table 3-5: Summary of results for AQ6. A general linear model was applied to all data sets with temperature as categorical factor and copepod density as continuous factor (n=12; df=2).

Dependent variable	Temperature		Copepod density		*P* model	F model	r^2
	b	*P*	b	*P*			
$Bloom_{peak}$ (day of experiment)	-2.83	0.0001	-0.13	0.2993	0.0003	23.67	0.84
PO_4^{3} $_{depl.}$ (day of experiment)	-2.33	0.0000	-0.03	0.6869	0.0001	34.66	0.89
part.PP_{mean} (µg C L^{-1} day^{-1})	-15.79	0.0119	-3.56	0.0326	0.0097	8.10	0.64
diss.PP_{mean} (µg C L^{-1} day^{-1})	0.06	0.9841	0.51	0.5664	0.1773	0.84	0.04
BSP_{mean} (µg C L^{-1} day^{-1})	9.71	0.0045	-3.65	0.2800	0.0110	7.74	0.63
$BSP_{bloom\ peak}$ (µg C L^{-1} day^{-1})	18.29	0.0012	-9.66	0.0906	0.0024	13.03	0.74
POC_{mean} (µmol C L^{-1})	4.91	0.4300	-2.59	0.1500	0.2600	1.55	0.26
POP_{mean} (µmol P L^{-1})	-0.02	0.0500	0.01	0.1200	0.0600	3.97	0.47
DOC_{mean} (µmol C L^{-1})	-10.99	0.2400	-0.86	0.7300	0.4500	0.86	0.16
$dcCHO_{mean}$ (µmol C L^{-1})	-5.41	0.2700	-0.98	0.4700	0.4100	0.97	0.18
DOC_{slope} (µmol C L^{-1} day^{-1})	-0.28	0.4200	-0.21	0.5400	0.5900	0.56	0.11
$dcCHO_{slope}$ (µmol C L^{-1} day^{-1})	0.34	0.3600	-0.26	0.0260	0.0600	4.01	0.47
$POC:POP_{mean}$ (mol:mol)	31.73	0.0600	-12.09	0.0176	0.0180	6.49	0.59
$DOC:DOP_{mean}$ (mol:mol)	27.67	0.6600	-7.02	0.6900	0.8300	0.19	0.04
TEP_{mean} (µmol C L^{-1})	0.19	0.2200	0.14	0.0079	0.0170	6.64	0.60
TEP_{max} (µmol C L^{-1})	7.47	0.0144	-0.49	0.5000	0.0340	4.82	0.52

Meta-analysis

Mean effect sizes were calculated for all available parameters (Tab. 3-7; Fig. 3-3). The timing of the bloom peak, as well as the onset of PO_4^{3-} depletion were clearly accelerated by experimental warming, with low variance in mean effect size across all studies. The mean effect size of both particulate and dissolved PP_{mean} showed a tendency to reduced autotrophic production at elevated temperature, although the variance between studies was high for dissolved PP_{mean}. In contrast, bloom-averaged heterotrophic bacterial production was clearly stimulated by warming across all studies, with an even stronger response already at the time of the biomass peak (i.e., $BSP_{bloom\ peak}$).

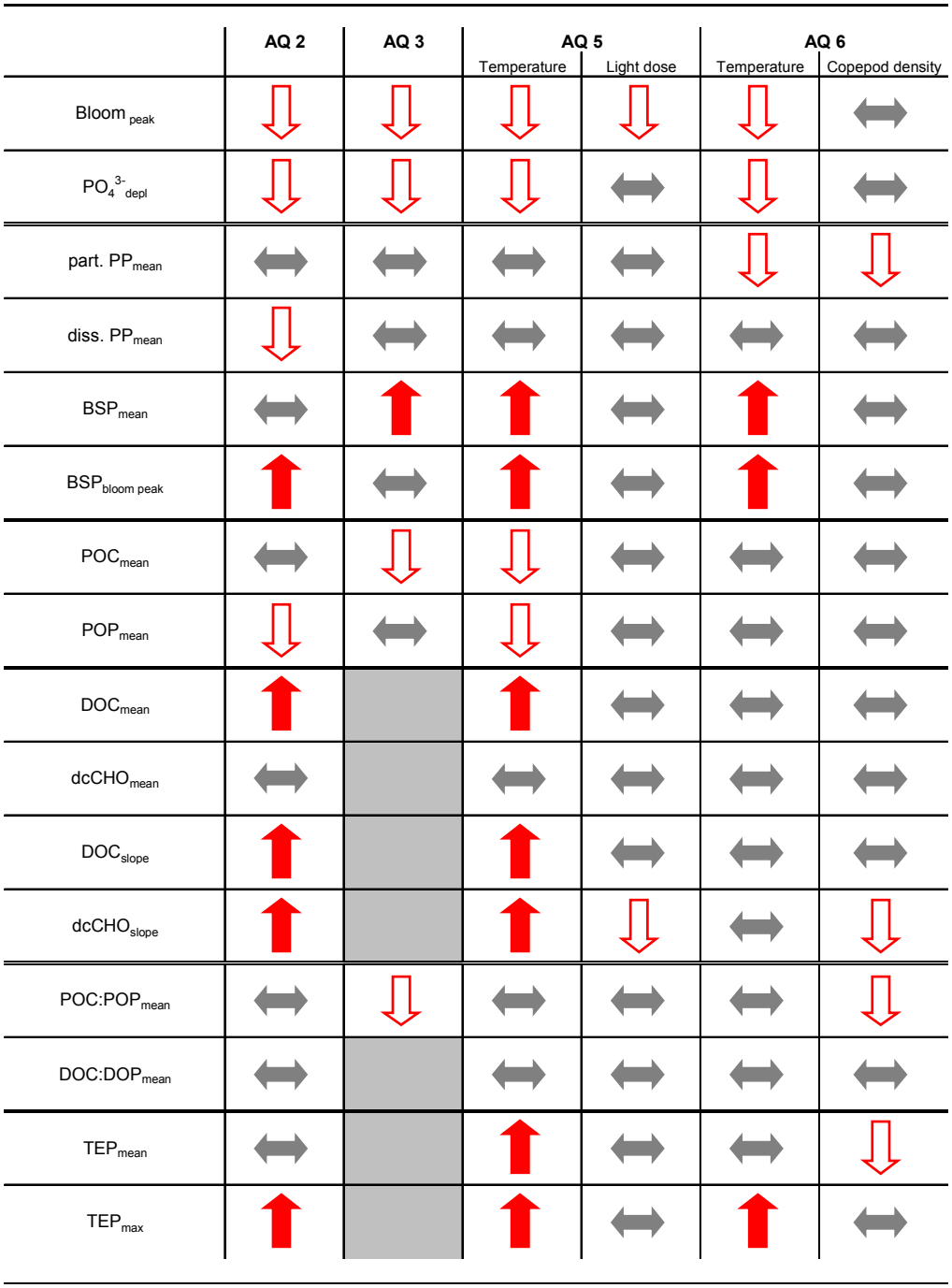

Figure 3-2: Synthesis of observed effects of experimental warming by up to 6 °C above ambient temperature, changes in daily light dose (only AQ5), and overwintering copepod density (AQ6) on selected biogeochemical parameters during the AQUASHIFT experiments. The *red upward/filled* and *downward/empty arrows* denote significant ($P < 0.05$) positive or negative effects of the investigated environmental stressors on individual parameters. *Grey horizontal arrows* denote insignificant results. *Grey filled areas* denote parameters where no data were available.

As a consequence of these changes in the balance between autotrophic and heterotrophic processes with an increase in temperature of 6 °C, marked alterations in the build-up and partitioning of organic matter were observed across studies. Both the

average accumulation of POC and POP throughout the bloom period showed a negative tendency with rising temperature, which, in the case of POP_{mean}, was clearly significant. In contrast, both the average build-up of DOC and of dcCHO did not respond notably to experimental warming, although the latter parameter showed a fairly high variability between studies. Looking at the rate of increase in DOC and dcCHO, however, showed a clear positive trend with increasing temperature. Due to a high variability of DOC_{slope}, this was, however, only significant in the case of $dcCHO_{slope}$.

The mean effect size of $POC:POP_{mean}$ showed a very weak tendency to decrease with rising temperature, but overall the elemental stoichiometry of POM and DOM did not show a pronounced response to warming across the AQUASHIFT studies. The mean effect sizes of both TEP_{mean} and TEP_{max} showed a tendency to increasing TEP accumulation with rising temperature across studies was significant only for TEP_{max}.

Discussion

Despite substantial differences in environmental conditions (e.g., daily light dose, grazer density and plankton community composition), our analysis showed several recurring trends of biogeochemically relevant parameters with a rise in temperature of up to 6 °C (Fig. 3-2, 3-3). These will be discussed in detail within the context of our working hypotheses.

Table 3-6: Linear regression analysis of selected variables versus copepod density (AQ6), separated for the two temperature regimes T+0 and T+6 (n=6, df=1).

Dependent variable	slope	*P*	F	r^2
At T+0 °C				
$POC:POP_{mean}$	-2.8	0.580	0.36	0.08
$dcCHO_{slope}$	-0.16	0.34	1.19	0.23
TEP_{mean}	0.13	0.15	3.28	0.45
At T+6 °C				
$POC:POP_{mean}$	-21.3	0.004	34.55	0.90
$dcCHO_{slope}$	-0.36	0.048	7.94	0.66
TEP_{mean}	0.142	0.033	10.42	0.72

Temporal dynamics of bloom development

Concerning the timing of cardinal plankton bloom events, such as the peak of the bloom and the onset of nutrient depletion, a consistent acceleration by on average 1.9 and 1.1 days $°C^{-1}$, respectively, was observed across all 4 AQUASHIFT studies. Similarly, also increasing light dose led to a significantly earlier bloom peak in the AQ5 study (Fig. 3-2; Tab. 3-5; Lewandowska & Sommer 2010). While this may indicate that the observed forward shift in the timing of cardinal bloom events may be partly due to an acceleration of autotrophic processes, the strong stimulation of BSP by warming already at the time of

the biomass peak in three out of four studies (Fig. 3-2) suggests a closer temporal coupling of autotrophic and heterotrophic processes with increasing temperature.

Table 3-7: Summary of the meta-analysis results on the effect of increasing temperature on selected biogeochemical parameters. Blank entries denote parameters where no data were available.

Experiment	$Bloom_{peak}$	$PO_4^3{}_{depl.}$	$part.PP_{mean}$	$diss.PP_{mean}$	BSP_{mean}	$BSP_{bloom\ peak}$	POC_{mean}	POP_{mean}
AQ2 - IL, ID	-0.39	-0.21	-0.20	-0.52	0.08	0.81	-0.25	-0.19
AQ3 - HL, HD	-0.62	-0.55	-0.28	-1.81	0.51	-0.04	-0.59	-0.24
AQ5 - HL, HD	-0.37	-0.21	-0.27	-0.50	0.33	0.60	-0.36	-0.23
AQ5 - IL, HD	-0.22	-0.13	0.02	0.13	0.23	0.69	-0.33	-0.13
AQ5 - LL, HD	-0.14	0.00	-0.42	-0.38	0.20	0.75	-0.34	-0.19
AQ6 - IL, HD	-0.36	-0.27	-0.29	-0.09	0.42	0.84	-0.11	-0.16
AQ6 - IL, ID	-0.41	-0.45	-0.33	0.22	0.25	0.55	0.02	-0.04
AQ6 - IL, LD	-0.33	-0.47	-0.38	-0.17	0.66	0.53	0.35	-0.10
Mean all	-0.35	-0.28	-0.27	-0.39	0.34	0.59	-0.20	-0.16
SD	0.14	0.19	0.14	0.63	0.19	0.28	0.29	0.07
Variance	0.02	0.04	0.02	0.40	0.03	0.08	0.08	0.00
+ 95 % CI	-0.24	-0.13	-0.15	0.14	0.49	0.82	0.04	-0.10
- 95 % CI	-0.47	-0.44	-0.38	-0.92	0.18	0.36	-0.44	-0.21
Experiment	DOC_{mean}	$dcCHO_{mean}$	DOC_{slope}	$dcCHO_{slope}$	$POC:POP_{mean}$	$DOC:DOP_{mean}$	TEP_{mean}	TEP_{max}
AQ2 - IL, ID	0.15	0.20	0.90	0.90	-0.02	0.11	-0.34	0.51
AQ3 - HL, HD					-0.39			
AQ5 - HL, HD	0.11	0.19	0.72	0.37	-0.12	-0.08	0.27	0.37
AQ5 - IL, HD	0.05	-0.02	0.50	0.85	-0.13	-0.03	0.32	0.34
AQ5 - LL, HD	0.16	0.51	0.81	0.94	-0.04	0.03	0.43	0.74
AQ6 - IL, HD	-0.15	-0.92	-1.02	-0.19	-0.03	-0.09	0.09	2.25
AQ6 - IL, ID	-0.09	-0.31	0.00	0.30	0.07	0.03	0.06	0.64
AQ6 - IL, LD	0.04	0.22	0.28	0.35	0.58	0.18	0.08	0.89
Mean all	0.04	-0.02	0.31	0.50	-0.01	0.02	0.13	0.82
SD	0.12	0.47	0.67	0.42	0.28	0.10	0.25	0.66
Variance	0.01	0.22	0.45	0.17	0.08	0.01	0.06	0.44
+ 95 % CI	0.15	0.42	0.93	0.89	0.22	0.11	0.36	1.43
- 95 % CI	-0.07	-0.45	-0.30	0.12	-0.24	-0.07	-0.10	0.21

Organic matter net build-up and its partitioning between particulate and dissolved phases

The data on POC and POP build-up showed significant trends towards a lower net accumulation of POM at elevated temperature in 2 of 4 studies for each parameter (Fig. 3-2). In the case of POP, the trend was comparable, but slightly insignificant also in a third study. Concerning the overall effect of rising temperature on these parameters, the mean effect size yielded a consistent negative trend for the net build-up of POP, whereas it remained inconclusive in the case of POC due to a high variance between studies.

In theory, the lower net build-up of POP may be caused both by a decline in the photosynthetic production of organic matter and/or an increase in its heterotrophic consumption. The here available data on algal primary production and BSP rates likely indicate a combination of both mechanisms. Thus, the mean effect size of particulate PP

showed an overall consistent negative trend with an increase in temperature of 6 °C (Fig. 3-3).

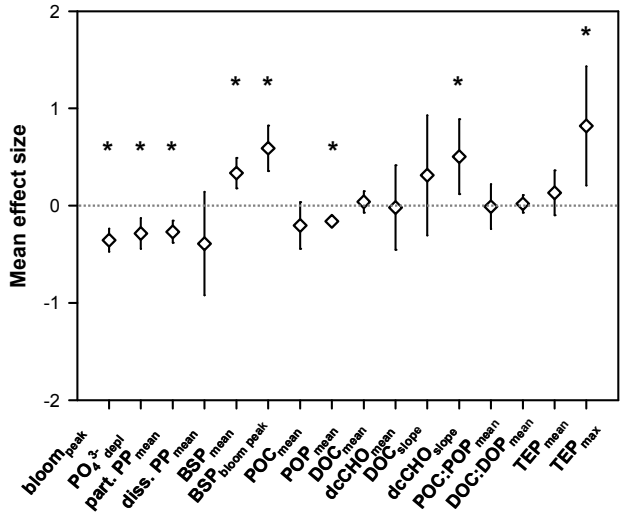

Figure 3-3: Variation in the overall response of various biogeochemical parameters to an increase in water temperature of 6 °C. *Symbols* represent the mean effect sizes. The *error bars* denote the individual ± 95% confidence intervals. The *zero line* indicates the absence of a temperature effect. *Asterisk* indicates accepted significance.

Looking at the individual studies, however, revealed a significant temperature effect in only one study (AQ6; Fig. 3-2). In line with this, (Lewandowska et al. 2012) reported in a recent analysis, dealing specifically with the effect of experimental warming on algal PP in the AQUASHIFT studies, an insignificant response of particulate PP to increasing temperature. These minor differences in the temperature response of algal PP between our analysis and that of Lewandowska and co-workers likely originate from differences in the experimental time periods that were included in the calculations. In contrast to the algal processes, both BSP_{mean} and $BSP_{bloom\ peak}$ were significantly stimulated by experimental warming in 3 of 4 studies (Fig. 3-2), thus yielding consistent and strong positive trends with increasing temperature (Fig. 3-3).

Considering the dynamics in the dissolved fraction of organic matter, a significantly faster and higher increase in the accumulation of DOC was observed at elevated compared to ambient temperature in 2 of 3 studies (AQ2; AQ5; Fig. 3-2). Likewise, also the rate of increase in dcCHO was significantly stimulated by warming in 2 of 3 studies. Due to contrary results for DOC_{mean} and DOC_{slope} in AQ6, however, only the mean effect size of $dcCHO_{slope}$ yielded a consistent positive trend with increasing temperature across studies (Fig. 3-3).

The accumulation of dissolved organic carbon species during bloom events has often been observed with the onset of nutrient depletion (Copin-Montégut and Avril 1993) and is generally attributed to the overflow of algal photosynthates (Engel et al. 2002; Schartau et al. 2007). In line with this, the analysis of the composition of the dcCHO pool for the AQ2 experiment showed a predominant accumulation of combined glucose (Engel et al. 2010), which is a main storage component of algal cells. While a stimulating effect of warming on primary production and the release of carbon-rich

compounds has also been reported from other studies (Verity 1981b; Davison 1991; Wolfstein et al. 2002; Morán et al. 2006; Claquin et al. 2008), the here determined rates of dissolved PP, however, either showed a negative (AQ2; Fig. 3-2) or no response to rising temperature (AQ5, AQ6; Fig. 3-2). Besides phytoplankton, also bacteria contribute to DOC accumulation, for instance by releasing cell-surrounding material during active growth or through modification of DOM compounds (Stoderegger and Herndl 1998; Azam 1998; Ogawa et al. 2001; Kawasaki and Benner 2006). As the heterotrophic bacterial production showed a consistent positive response to warming across the AQUASHIFT studies (Fig. 3-2, 3-3), we argue therefore that both algal exudation and bacterial decomposition processes contributed to DOM accumulation during the AQUASHIFT phytoplankton blooms. In concert, a higher partitioning of organic carbon from the pool of particulate to dissolved matter appears to be a probable consequence of ocean warming.

Interestingly, both increasing daily light dose (AQ5) and copepod density (AQ6) had a contrary effect on $dcCHO_{slope}$ compared to warming, leading to a slower accumulation of dcCHO (Fig. 3-2). The significantly lower temperature response of $dcCHO_{slope}$ with decreasing copepod density during AQ6, likely also masking a potential temperature response (Fig. 3-2), may indicate an indirect effect of copepod density on DOC dynamics, as it has been shown that changes in grazer abundance can have a notable effect on bacterial activities by triggering a trophic cascade via ciliates and heterotrophic nanoflagellates (HNF; Zöllner et al. 2009). Thus, a decrease in copepod density may likely have relieved bacteria from direct grazing pressure by HNF, thereby enabling a more pronounced accumulation of dissolved organic carbon species at elevated temperature. Regarding the negative effect of increasing daily light dose on $dcCHO_{slope}$, the underlying mechanisms remain elusive, but it may be speculated that any potential changes in algal exudation through increased light availability may have been compensated by the enhanced bacterial carbon consumption due to the likely labile nature of freshly produced algal solutes.

TEP dynamics

In most of the experiments, a slight decrease in DOC and dcCHO was observed towards the end of the experimental period in the elevated temperature treatments, which closely coincided with changes in the concentration of TEP. Carbohydrates are known to be the precursor material and basic component of TEP. In general, two ways of TEP production have so far been reported, i.e., the direct release of carbohydrate-rich cell surface material by phytoplankton cells and the abiotic aggregation of carbohydrate-containing components of the DOM pool (Chin et al. 1998; Engel et al. 2004). The TEP dynamics observed in the various AQUASHIFT experiments, in fact, indicate the presence of both

TEP production mechanisms. During AQ5 the TEP dynamics showed a considerable and temperature-dependent increase in TEP already during bloom development, likely indicating an algal origin (Fig. 3-2). Similarly, a stimulation of TEP production and aggregation by rising temperature has been previously reported for various monoalgal cultures (Thornton and Thake 1998; Claquin et al. 2008). In AQ5, this first peak was followed by a decline in TEP under *in situ* temperature conditions, whereas the concentration further increased in the post-bloom phase of the elevated temperature treatments, thus yielding an overall significant temperature response (Tab. 3-5; Fig. 3-2). In contrast to AQ5, low and temperature-independent average concentrations of TEP were observed during the bloom of the experiments AQ2 and AQ6, followed by a steep increase in TEP during the late post-bloom phase of the elevated temperature treatments, which suggests a strengthened influence of either heterotrophic or abiotic processes. Several mesocosm and field studies (e.g., Passow and Alldredge 1995a; Engel et al. 2004) have reported a strong potential of TEP to promote the aggregation and sinking of particulate matter to depth. This depends, however, critically on the timing and interplay of TEP production with other biological processes, such as microbial degradation and grazing. While a consistent positive trend of the post-bloom TEP dynamics in response to experimental warming was observed during the here presented AQUASHIFT studies (Fig. 3-3), its potential to influence the organic matter transport to depth via the biological pump remains uncertain due to the late timing of the event.

Organic matter elemental composition

Concerning the third hypothesis that warming would lead to a preferential remineralisation of phosphorus over carbon, thereby increasing their elemental ratios in POM and DOM, we cannot fully reject the null hypothesis. Only 1 of 4 studies showed an increase in particulate $C:P_{mean}$ with rising temperature (AQ 6). The effect was, however, slightly insignificant (Tab. 3-6, Fig. 3-2). In contrast, the other 3 studies displayed rather a decrease in $POC:POP_{mean}$, with a significant result in only 1 study (AQ3; Fig. 3-2). This decrease in the average ratio of POC to POP may, in fact, rather suggest a temperature-induced shift in the turnover dynamics of organic phosphorus compounds. Thus, results from an AQUASHIFT-related microcosm experiment have shown that experimental warming can substantially stimulate phosphorus cycling through the activity of the organic phosphorus-cleaving enzyme alkaline phosphatase (APA; (Wohlers-Zöllner et al. 2011)), hence enabling a faster replenishment of the POP pool at elevated temperature and reducing the C:P ratio of POM. The average ratio of DOC to DOP did not show a significant response to any of the investigated environmental stressors (Fig. 3-2). In summary, the strong divergence in temperature patterns between studies impedes

conclusions about the effects of ocean warming on POM and DOM elemental stoichiometry (Fig. 3-1).

Potential consequences for marine elemental cycling

One of the key drivers of biogeochemical cycling in the ocean is the biological carbon pump, which transports photosynthetically-bound carbon from the sunlit surface to deeper water layers. While most of the organic biomass is recycled back to carbon dioxide (CO_2) and other inorganic constituents on its way down, only the fraction that is transported below the winter-mixed layer actually contributes to the ocean's capacity to take up atmospheric CO_2. Ocean warming-mediated changes in the potential of the biological pump to transport carbon to depth, for instance through shifts in the partitioning of organic matter between its particulate and dissolved phases or in the elemental ratio of the produced biomass (Riebesell et al. 2007; Bellerby et al. 2008), may hence provide an important feedback mechanism to the climate system. In this context, a significant effect of experimental warming on the magnitude of POM and DOM build-up is also indicated by the results of the AQUASHIFT experiments (Fig. 3-2, 3-3). Concerning the latter, the enhanced and also accelerated accumulation of dissolved organic carbon compounds may shift pelagic ecosystems towards a microbial-dominated recycling system, thereby reducing the overall strength of the biological pump (Morán et al. 2006; Kim et al. 2011). To what extent the pronounced stimulation of heterotrophic microbial processes compared to autotrophic PP during AQUASHIFT (Fig. 3-2, 3-3) may lead to the build-up of a refractory DOC pool, hence contributing to the long-term storage of carbon in the marine biosphere (Jiao et al. 2010), is currently not predictable.

Conclusions

Despite the limited number of studies and treatment replicates, the AQUASHIFT experiments have provided important information on ocean warming effects on a range of biogeochemical parameters that directly or indirectly contribute to the ocean's mitigating role in Earth's climate system. A major outcome of these experiments is the substantial, yet often neglected, role of the microbial food web in the functioning and efficiency of the biological carbon pump. Moreover, our analysis provides an example for the strong potential for interactive synergistic or antagonistic effects of several environmental factors on major biogeochemical parameters. Based on this knowledge, there is an urgent need for further research on the interactive effects of environmental stressors on microbial elemental cycling under future ocean conditions and the potential for climate feedbacks.

Acknowledgements

We would like to thank A. Ludwig, N. Händel and P. Fritsche for their technical assistance in sample preparation and analysis. All members of the Kiel AQUASHIFT-team are appreciated for their help during the experiments. We are particularly grateful to E. Zöllner and the anonymous reviewers for their comments on an earlier version of this manuscript. This work was supported by Deutsche Forschungsgemeinschaft (DFG) grant no. RI 598/2-3 to U. R. and A. E. and by the Helmholtz Association (contract no. HZ-NG-102 to A. E.).

Chapter 4

The effect of cloudy and sunny weather conditions on organic matter partitioning in a marine plankton community and implications for a future warmer surface ocean

Abstract

A study was conducted to investigate the effect of sunny or cloudy weather conditions on the development of a natural overwintering plankton population from Kiel Bight. The aim was to quantify the effect of irradiance on the build-up of particulate and dissolved organic matter (POM and DOM). Two different light regimes were applied with day length and light intensities corresponding either to January or February conditions. After seven days of low light conditions (cloudy), light intensity was elevated for 6 of the 12 mesocosms to sunny conditions. While the "January cloudy" treatment showed almost no development of phytoplankton, it was possible to induce a diatom dominated phytoplankton bloom in the "January sunny" as well as in both February treatments. As expected, nutrient drawdown and net accumulation of POM increased with increasing light dose. If in the course of climate warming, sunshine hours in winter/spring were to decrease, then also the probability would decrease for those "fast" phytoplankton blooms with high POM build-up. As copepod development depends on the development of phytoplankton, cloudy weather could hence have also negative consequences for copepods, especially if their respiration and grazing activity would increase due to sea surface warming. In contrast to POM, DOM accumulation stayed relatively unaffected by the different irradiance levels. Likewise, transparent exopolymer particles (TEP) and coomassie stainable particles (CSP) showed no change in response to the light treatment in abundance or particle area. CSP were found to occur at the same magnitude of on average 8.4 x 10^6 particles L^{-1} than TEP (9.9 x 10^6 particles L^{-1}) but were larger in size with an average particle area of 49 μm^2 compared to TEP (32 μm^2). CSP are often colonized by bacteria and may therefore play an important role as hot spots for nutrient recycling and as a food source for micrograzers. However, these proteinaceous particles

have not gained as much attention as TEP in the literature so far. Our study showed that CSP are equally important for the partitioning of N as TEP for the partitioning of C during winter/spring phytoplankton blooms in this Baltic Sea region and should be considered in future studies on organic matter cycling.

Introduction

The earth's climate is warming mainly due to continuing greenhouse-gas emissions, and the further increase in global mean surface temperature caused by a doubling of the atmospheric CO_2 concentration will be likely in the range of 1.5 - 4.5 °C (IPCC 2013). Additionally, anthropogenic forcing contributed significantly to the observed increases in precipitation in the Northern-Hemisphere and other regions (Zhang et al. 2007) as warming increases the amount of water vapor in the atmosphere. Model simulations projected for the future an increase in precipitation on the global scale (Meehl et al. 2007). The projections for the Baltic Sea region especially point to an increase in winter precipitation (Helcom 2007) and hence to more cloudiness. In addition, for the Baltic Sea region, a general reduction in sunshine hours is expected for winter and spring (Meinke and Reckermann 2012).

Both, particulate and dissolved organic matter (POM and DOM) play an important role in the transport of carbon to the deep sea thereby contributing to the sequestration of carbon by the biological pump (Hansell et al. 2009). Changes in solar radiation and temperature rise may interactively affect the build-up of POM and DOM and their elemental stoichiometry during phytoplankton blooms. Sterner and Elser (2002) for instance suggested that for a nutrient *X*, the carbon (C) to *X* ratio of the autotroph (marine) biomass increases with limitation of *X* and with increasing light intensity. Although climate warming increased water temperatures in Narragansett Bay, a recent study offered for the observed decrease in winter/spring blooms an increase in cloudiness as a possible explanation (Nixon et al. 2009). The primary source of DOM in seawater is the extracellular release by phytoplankton. Dissolved organic carbon (DOC) excretion by phytoplankton was found to increase with increasing light levels (Verity 1981a; Zlotnik and Dubinsky 1989; Wolfstein et al. 2002) and longer day length in batch culture experiments (Verity 1981a). In the ocean, the largest characterized fraction of DOM are carbohydrates (CHO) (Biddanda and Benner 1997; Biersmith and Benner 1998), which are released in high amounts by phytoplankton cells during phytoplankton blooms (Ittekkot 1982; Myklestad 1995). These polysaccharides are known to be able to aggregate into transparent exopolymeric particles (TEP). TEP thereby represent a pathway for the transition from the DOM to the POM pool (Engel et al. 2004; Verdugo et al. 2004). A tight coupling between photosynthesis and TEP production was found for

three diatom species (Claquin et al. 2008). Light dependent changes in the production of DOM may therefore also affect the POM pool.

Another important component of DOM are proteins, which can coagulate to form particles, the so-called coomassie stainable particles (CSP), since they stain with the protein dye Coomassie Brilliant Blue. CSP can be as abundant as TEP or occur in seawater at higher concentrations than TEP (Long and Azam 1996) or at lower abundances than TEP with high fluctuations during the year for both particle types (Berman and Viner-Mozzini 2001). So far it does not seem predictable to what extend CSP and TEP occur in a particular area or under particular environmental conditions.

The aim of this study was to quantify the effect of sunny or cloudy weather conditions for the build-up of POM, inclusive TEP and CSP, and DOM during the phytoplankton winter/spring blooms, and investigate potential effects on elemental stoichiometry.

Material and Methods

Experimental set-up

Twelve 1400-L mesocosms were set up in four climate chambers and filled with seawater from the Kiel Fjord, Western Baltic Sea, on the 21 January, 2010. The seawater contained the natural winter/spring plankton community (phytoplankton, bacteria and protozoa). Additionally, mesozooplankton dominated by copepods of the genera Acartia and Oithona was added from net catches from Kiel Fjord, yielding a density of 15 to 20 individuals L^{-1}. For a detailed description on mesozooplankton and phytoplankton assemblage as well as on the experimental set-up see (Sommer et al. 2012b). The mean temperature for all climate chambers was $4.1 \pm 0.3°$ C over the whole experimental period and therewith two degrees above the ambient water temperature measured on the day of the mesocosm filling. (Due to technical constrains, it would not have been possible to run all climate chambers with 2.4° C.) A slow increase of temperature was programmed according to natural winter/spring conditions.

The light system simulated daily irradiance curves and a seasonal light pattern calculated from astronomic equations according to Brock (1981), controlled by a computer programme (GHL, Prometeus). The two illuminating devices on top of each mesocosm were equipped with 12 full spectrum light tubes (10 solar tropic T5 Ultra, 4,000 K, 2 solar nature T5 Ultra, 9,000 K, JBL). Two different day length regimes were applied; one simulating January (JAN) and one February (FEB) light patterns. After the filling of the mesocosms, the light was set to a low light intensity of 43 % of sea surface irradiance (cloudy) of either JAN or FEB light conditions. The virtual start point for the light programmes was set to 15 January for JAN treatments and 15 February for FEB

treatments (corresponding to the first sampling day on 22 January). The development of daily light dose is given in Sommer et al. (2012b). After 4 days the light intensities for 6 of the 12 mesocosms was elevated to a sunny week, yielding 86 % of sea surface irradiance for either JAN or FEB in triplicates each. The light treatments were applied randomly in the climate chambers. After ten days sunny week conditions, light intensity was down regulated to the previous 43 %.

As the response of phytoplankton in JAN sunny was only moderate at least for two mesocosms (M2 and M7), we initiated as second high light period with 86 % for the JAN cloudy treatment starting from day of experiment 19 until 28. We chose the former JAN cloudy for a second high light period, since it was not possible to initiate bloom conditions in this treatment. In the following we will refer to FEB always 43 % as FEB cloudy (FC), FEB with 10 d light elevation of 86 % as FEB sunny (FS), JAN 86 % light elevation day 4 to day 13 as JAN sunny I. period (JSI) and JAN 86 % light elevation to JAN sunny II. period (JSII). FS, FC, JSII, and JSI corresponded to 10.4, 5.4, 5.8, and 3.2 mol photons m^{-2} d^{-1} mean daily light dose. Since the daily light doses for the two JAN sunny periods differed considerably due to the programmed natural increase in light intensity, and nutrient concentrations in JAN sunny II period were still comparable to the initial nutrient concentrations at that point of time (Fig. 4-1), we decided to add this treatment to our analysis. As light levels at JAN (always) 43 % were obviously too low to initiate a phytoplankton bloom, data from this treatment was not included in our analysis. Initial nutrient concentrations were 0.5 µmol L^{-1} nitrite, 16.3 µmol L^{-1} nitrate, 2.8 µmol L^{-1} ammonium, 0.9 µmol L^{-1} phosphate, and 27.9 µmol L^{-1} silicate. Initial seawater salinity was 16.9. During the whole experiment the mesocosm water was gently mixed with a propeller that held cells and smaller particles in suspension, whereas larger particles and aggregates were able to sink out of the water column.

Sampling

Sampling days were Monday, Wednesday, and Friday. Additional sampling days were introduced during bloom conditions. The samples were taken with a silicone hose from the middle of the mesocosm water body between 08:30 and 09:00 in the morning (1 - 2 hours after lights turned on).

Analytical Methods

Temperature, salinity, and pH were measured with a WTW conductivity/pH probe on each sampling day at 0.2 m depth. Inorganic nutrients (nitrate, nitrite, phosphate, silicate) were determined with an autoanalyzer (AAII) according to Hansen and Koroleff (2007), and ammonium according to the method of Holmes et al. (1999) immediately after sampling or after overnight storage of the 0.2 µm (Filtropur, Sarstedt) filtrate. During

bloom conditions samples were filtered through 5.0 µm cellulose acetate filters prior to nutrient analysis. Dissolved inorganic carbon (DIC) was measured via coloumetric titration (Johnson et al. 1987). Therefore, samples were sterile filtered (0.2 µm) into borosilicate bottles, sealed with butyl/PTFE septa and stored at ~ 6 °C in a fridge until analysis. For the determination of chlorophyll *a* (Chl*a*), between 100 and 500 mL were filtered onto glass fibre filters (GF/F, Whatman) and stored overnight at -20 °C. Pigment concentration was measured fluorometrically in a 10-AU Turner fluorometer after 90% acetone (v/v) extraction (Welschmeyer 1994). For biogenic silicate (BSi) determination, 50 to 250 mL of sample were filtered onto 0.65 µm cellulose acetate filters (Sartorius) and stored at -20 °C until spectrophotometrical analysis according to Hansen and Koroleff (2007). Before analysis, biogenic silicate was converted to dissolved silicate by leaching with 0.1 M NaOH at 85 °C. For POC, PN, and POP 100-500 mL of sample were filtered onto precombusted GF/F filters (Whatman) and stored at -20 °C. For the determination of POC and PN, filters were dried at 60 °C for 6 hours prior to analysis, and C and N concentrations measured with an elemental analyzer (EuroEA-3000, Eurovector) according to (Sharp 1974). POP was determined photometrically after the treatment with one dispensing spoon of Oxisolv® (Merck) (Hansen and Koroleff, 2007). For dissolved organic carbon (DOC) and total dissolved nitrogen (TDN) determination, 15 mL of sample was filtered through pre-combusted glass fibre filters, collected in 20 mL pre-combusted glass ampoules, 200 µL 85 % phosphoric acid added, and stored at 6 °C in the dark. DOC and TDN were analysed on a Shimadzu TOC_{VSH} using the HTCO method (Sharp et al. 1995). DON was calculated by subtracting TDN with dissolved inorganic nitrogen (DIN) (DON = TDN - DIN, DIN = nitrate + nitrite + ammonium). For dissolved organic phosphorus (DOP) determination, 40 mL of sample were filtered through pre-combusted glass fibre filters, collected in Nalgene® bottles and immediately analyzed with Oxisolv® according to the method of Hansen and Koroleff (2007).

Transparent exopolymer particle (TEP) and coomassie stainable particle (CSP) concentrations were determined microscopically. For TEP, filters were prepared in duplicate by gentle filtration (~ 150 mbar) of 5 to 50 mL sample onto 0.4 µm polycarbonate filters (Whatman) and staining with Alcian Blue (Alldredge et al. 1993) and immediate transfer onto Cytoclear Slides (GE Water & Process Technologies). The filters were stored at -20 °C until processing. Additionally, filters for the colourimetrical determination of TEP were prepared and analysed (Passow and Alldredge 1995b). The dye was therefore calibrated ($f = 53.9$) with the standard polysaccharide Gum Xanthan before and after the experiment. The analysis was carried out by adding 80 % H_2SO_4 to the filters and measurement of supernatants absorption at 787 nm after 3 hours with a spectrophotometer (Hitachi U-2000). For the conversion from Gum Xanthan equivalents to carbon a factor of 0.63 was applied according to Engel (2004). For the determination of

CSP, duplicates of 5 to 30 mL sample were gently filtered (~ 150 mbar) onto 0.4 µm polycarbonate filters (Whatman) backed by two 0.45 HA filters (Millipore) and staining with Coomassie Brilliant Blue solution, following the approach of Long and Azam (1996). The coomassie (1 %) stock solution was prepared from 1 g Coomassie Brilliant Blue G250 (Serva) and 97 mL Milli-Q water. The working solution was prepared daily before use from the diluted stock solution and 0.2 µm filtered seawater in a ratio of 1:25 (vol:vol). Before use, the working solution was filtered 0.2 µm by disposable syringe filters. Coomassie stained filters were immediately transferred onto Cytoclear Slides (GE Water & Process Technologies) and -20 °C frozen until analyses. Pictures of TEP and CSP were taken with an Axiocam HRc connected to an Axioscop2plus microscope (Zeiss) at a 200x magnification. The microscopic analysis was conducted according to Engel (2009). Briefly, ~ 30 pictures per filter were taken randomly in a cross section. Size, area and abundance of particles were determined semi automatically by the help of the image analysis software ImageJ (Rasband, W., National Instituts of Healths, http://rsb.info.nih.gov/ij/index.html). Therefore, the composite RGB-pictures were split into red, green and blue channels. The pictures of the red channel, reinforcing the contrast to the blue particles, were kept for setting the threshold range. Only gel particles > 4 µm² were included in the analysis.

Calculations and statistics

Slopes for the phase of linear nutrient drawdown, were calculated with linear regressions for $NO_2^-+NO_3^-$, DIP, and DSi. For the determination of maximum POM accumulation, the concentration of day 1 was subtracted from the maximum concentration, yielding ΔChl*a*, ΔPOC, ΔPN, ΔBSi, ΔPOP. Since DOM concentrations followed no distinct pattern, mean concentrations over the whole experiment were analyzed. Although, a linear regression with ln-tansformed *y* data was proven to be a good fit for biological responses to light (Sommer et al. 2012a), linear regression models provided a better or equally good fit for our data (Tab. 4-1). Therefore, effects of daily light dose were tested for all selected parameters with linear regressions according to the model $y=ax+b$ (SigmaPlot 10.0) (Tab. 4-1). Effects of daily light dose on gel particles, analysed by microscopy, were tested with Mann-Whithey-U-tests for pooled data of all analysed days. TEP_{max} for colorimetric analysed data was analysed with t-tests. Normal distribution was checked with Shapiro-Wilks tests. Significance level was always p=0.05. Statistics were performed with Statistica 6.0 (StatSoft).

Results

Nutrient drawdown and timing of the phytoplankton blooms

A diatom *(Skeletonema costatum)* dominated phytoplankton bloom developed immediately in both February treatments, independently of cloudy or sunny weather conditions. The slopes of nutrient drawdown increased with increasing daily light dose (Tab. 4-1, Fig. 4-1), but displayed different patterns for the elements N, P, and Si. An additional ANOVA analysis revealed that while nitrate+nitrite (NO_3+NO_2) drawdown was faster in sunny treatments (p<0.01), phosphate (DIP) drawdown was faster at February conditions (p<0.05, Fig. 4-1). Dissolved silicate (DSi) drawdown showed a difference between FS and JC (ANOVA p<0.05).

From doubling light (switch to sunny) it took similar long, on average 11 days, for both February but also for JSII to the bloom peak (Chl *a* maxima) (Fig. 4-2). The exception was JSI, were Chl*a* maxima were on average after 26 days.

Tab. 4-1: Regression analysis for selected "cardinal points" according to the model $y=ax+b$.* indicates regressions with weak test power.

Cardinal point	*a*	*b*	r^2	*p*
ΔPOC_{max}	12.3	-12.2	0.86	<0.0001
ΔPN_{max}	1.44	0.605	0.85	<0.0001
Drawdown NO_3^-/NO_2^-	-0.405	0.280	0.77	<0.001
$\Delta Chla_{max}$	2.81	0.615	0.77	<0.001
Drawdown DSi	-1.09	0.139	0.68	<0.001
ΔPOP_{max}	0.047	0.114	0.61	<0.01
ΔBSi_{max}	1.42	-1.03	0.60	<0.01
Drawdown DIP	-0.001	-0.026	0.59	<0.01
mean DOC during study*	2.22	293	0.49	<0.05
POC/PN_{max}*	0.250	6.06	0.28	<0.05
mean DOP during study*	-0.004	0.198	0.35	<0.05
POC/POP_{max}*	4.97	162	0.17	n. s.
mean DON during study*	0.011	27.5	0.00	n. s.

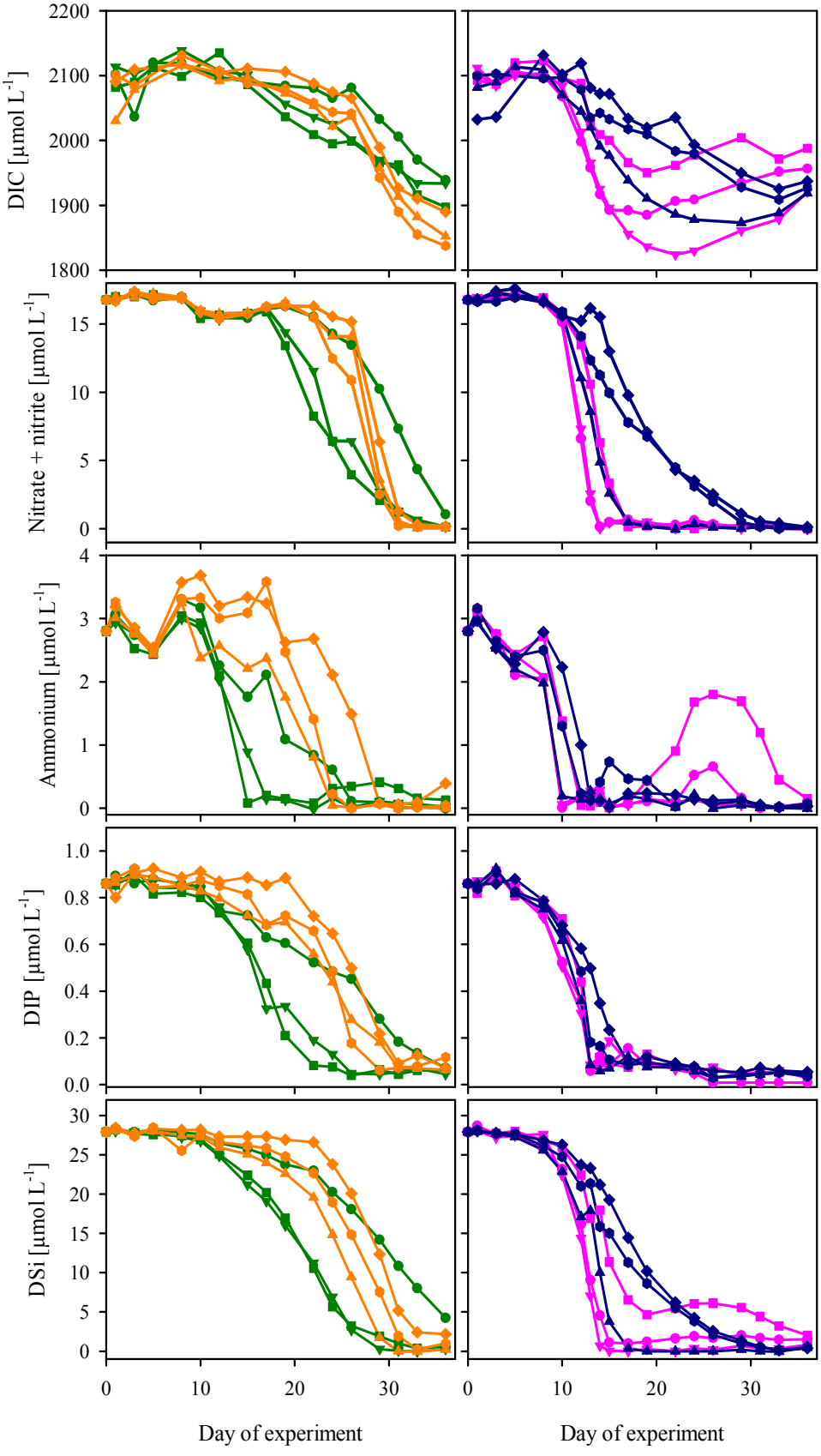

Figure 4-1: Dissolved inorganic carbon (DIC) and inorganic nutrient drawdown (Nitrite+nitrate, ammonium, dissolved inorganic phosphorus (DIP) and silicate (DSi) in January treatments (left) and February treatment (right) during the experimental period. Color code: green =JSI, yellow=JSII, blue=FC, pink=FS.

Particulate organic matter

The accumulation of chlorophyll *a* ($\Delta Chl a_{max}$) and particulate organic matter (POM) increased with increasing light dose (Tab. 4-1, Fig. 4-2). Highest Chl*a* and POM concentrations were found for FS. Chl *a* concentrations at the start of the experiment yielded 1.2 ± 0.2 µg L^{-1} and increased to Chl a_{max} of 31 ± 1 µg L^{-1} for FS, while JSII and FC achieved similar Chl *a* and POM concentrations with $Chl a_{max}$ of 18 ± 6 for FS and 17 ± 2 µg L^{-1} for JSII. In contrast, JSI showed the weakest response and the most heterogenic build-up of biomass for the three replicates with $Chl a_{max}$ of 12 ± 6 µg L^{-1}, e. g., one mesocosm of JSI showed almost no phytoplankton growth, whereas another achieved Chl *a* concentrations comparable to JSII conditions. Net particulate organic carbon build-up (ΔPOC_{max}) yielded 115 ± 19 µmol L^{-1}, 51 ± 18 µmol L^{-1}, 63 ± 7 µmol L^{-1} and 25 ± 15 µmol L^{-1} for FS, FC, JSII, and JSI, respectively (Fig. 4-2). Net particulate organic nitrogen build-up (ΔPN_{max}) showed the same pattern as ΔPOC_{max}, as it increased with increasing daily light dose, yielding 15 ± 1 µmol L^{-1}, 9 ± 3 µmol L^{-1}, 9 ± 1 µmol L^{-1}, and 4 ± 2 µmol L^{-1} for FS, FC, JSII and JSI, respectively. This pattern was also observed for net particulate silica build-up (ΔBSi_{max}) yielding 13 ± 3 µmol L^{-1}, 7 ± 4 µmol L^{-1}, 8 ± 2 µmol L^{-1}, and 3 ± 4 µmol L^{-1} for FS, FC, JSII and JSI, respectively (Fig. 4-2).

Contrary, but in line with the fastest DIP drawdown at FS and FC, these treatments achieved similar maximum net particulate organic phosphorus build-up (ΔPOP_{max}) concentrations with 0.6 ± 0.1 µmol L^{-1} for FS and 0.5 ± 0.1 µmol L^{-1} for FC, whereas JSII and JSI yielded 0.3 ± 0.0 and 0.2 ± 0.0 µmol L^{-1}, respectively (Fig. 4-2).

Stoichiometry of POM

The C/N for POM (POC/PN_{max}) showed a weak, but for the C/P (POC/POP_{max}) no clear linear trend to increase with daily light dose in this study (Tab. 4-1). POC/PN_{max} yielded 9 ± 0, 6 ± 0, 9 ± 1, and 7 ± 1 for FS, FC, JSII and JSI, respectively and 202 ± 27, 203 ± 9, 212 ± 43, and 154 ± 20 for POC/POP_{max}.

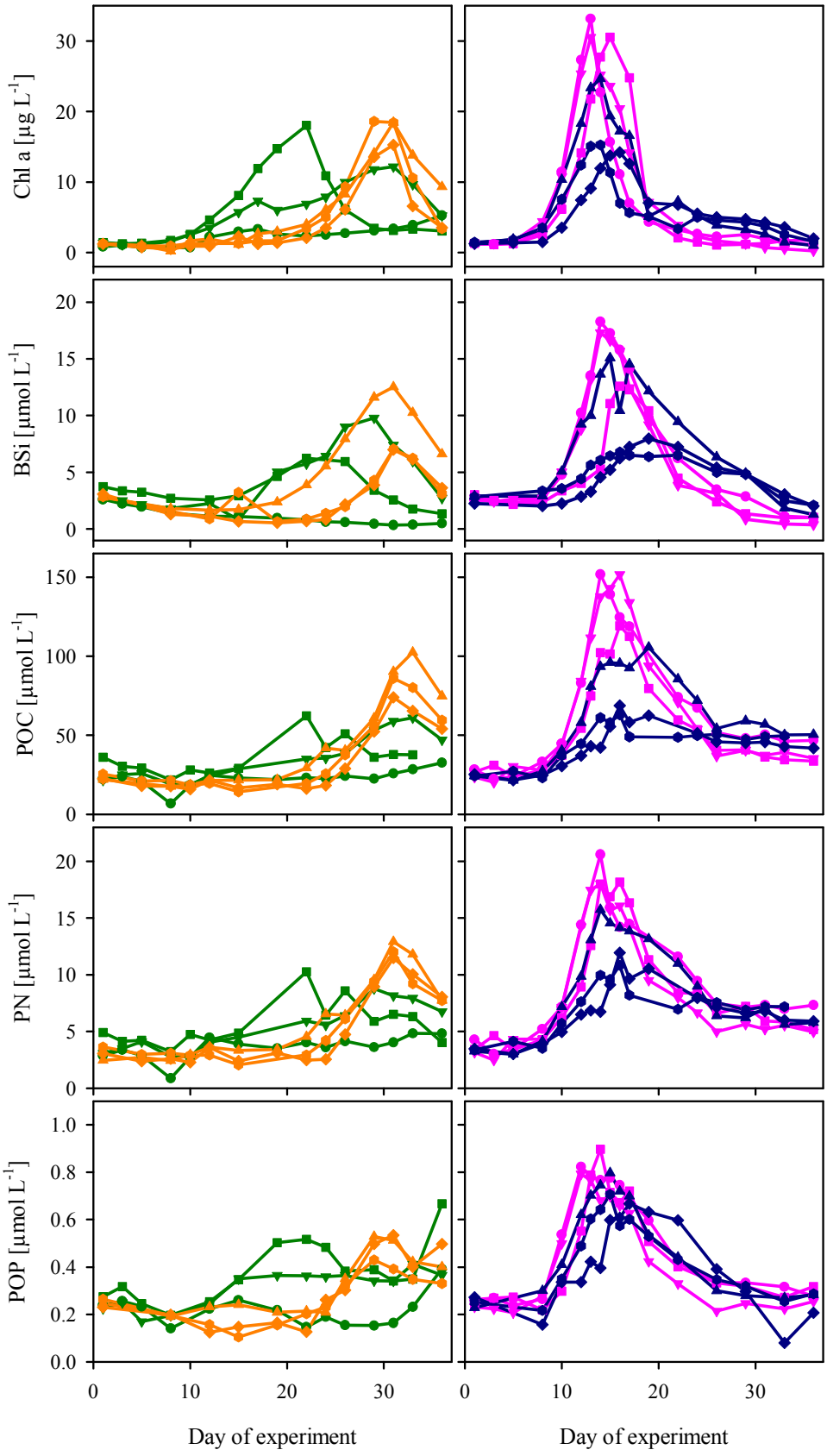

Figure 4-2: Development of chlorophyll *a* (Chl*a*) and particulate organic matter concentrations (BSi, POC, PN, POP) during the experimental period. The color code is as in figure 4-1.

Dissolved organic matter

Since dissolved organic matter (DOM) concentrations showed a high scatter and seemed not to follow a distinct pattern (Fig. 4-3), like a linear increase with daily light dose as observed for POM, we decided to compare mean concentrations over the whole experiment. The three measured DOM components, DOC, dissolved organic nitrogen (DON), and dissolved organic phosphorus (DOP) showed completely different tendencies in response to daily light dose. Mean dissolved organic carbon (DOC_{mean}) concentrations showed a tendency to increase with increasing light dose (Tab. 4-1), with 316 ± 7 µmol L^{-1}, 305 ± 6 µmol L^{-1}, 306 ± 6, and 299 ± 10 for FS, FC, JSII and JSI, respectively.

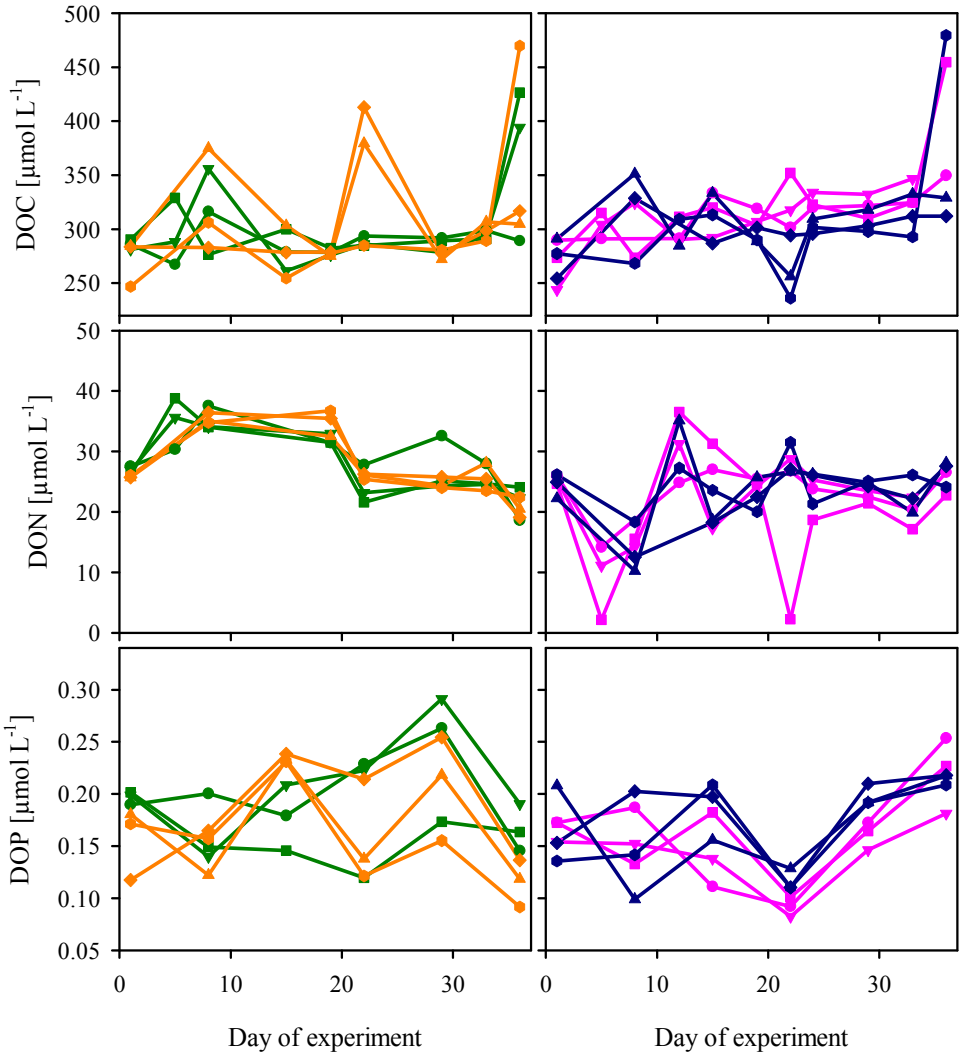

Figure 4-3: Dissolved organic matter concentrations (DOC, DON, DOP) during the experimental period. The color code is as in figure 1.

In contrast DON_{mean} did not respond to light dose with 28 ± 2 µmol L^{-1}, 26 ± 1 µmol L^{-1}, 28 ± 0 µmol L^{-1}, and 28 ± 1 µmol L^{-1} for FS, FC, JSII and JSI, respectively, while DOP_{mean} was decreasing with increasing daily light dose, yielding 0.16 ± 0.01, 0.17

± 0.01, 0.17 ± 0.02, and 0.19 ± 0.03 for FS, FC, JSII and JSI, respectively. However, the test power of the regression analysis for DOM was weak (Tab. 4-1), therefore conclusions have to be drawn with caution.

Gel particles

When comparing the mean pooled data of five analysed days in the February treatments, either in particle numbers, or as the mean total particle area, TEP in FS was not significantly different from FC (Fig. 4-4).

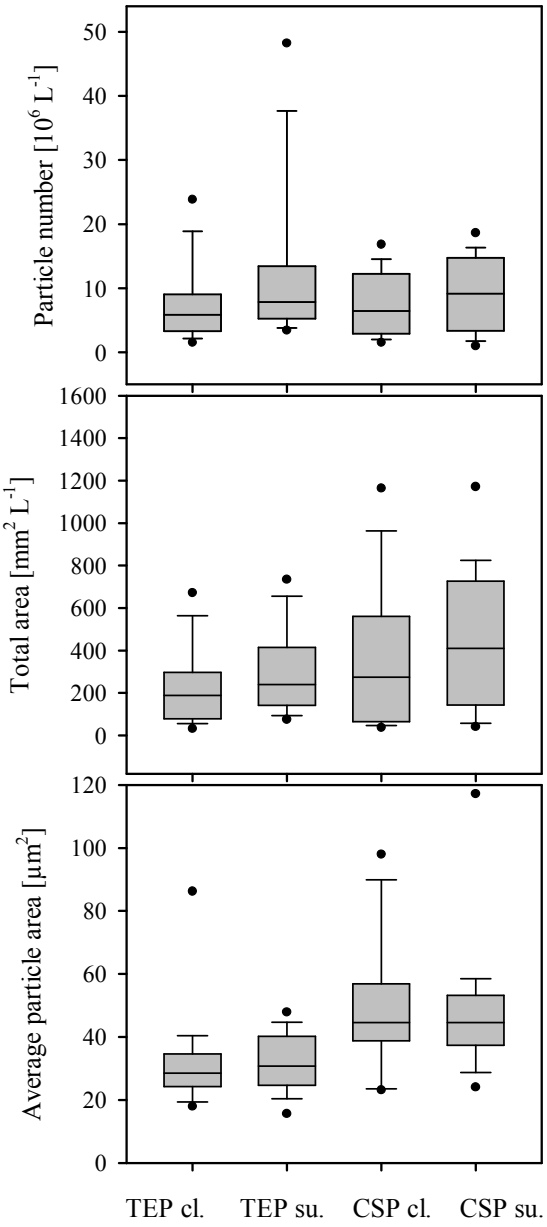

Figure 4-4: TEP and CSP abundance (particle number), total area, and average particle area in February cloudy (cl.) and sunny (su.) treatment. Pooled data of five analyzed days (TEP: days 3, 13, 17, 24, 36; CSP: days 5, 13, 17, 24, 36). The boxes indicate the 25th and 75th percentiles, the line in the middle the median. Error bars indicate the 10th and 90th percentiles, the dots indicate the 5th and 95th percentiles.

The mean TEP concentration in FS was $1.20 \times 10^7 \pm 7.37 \times 10^6$, and in FC $7.78 \times 10^6 \pm 3.84 \times 10^6$ particles L^{-1}. CSP abundance was of the same magnitude as TEP (Fig. 4-4). Mean CSP concentration yielded $9.18 \times 10^6 \pm 2.08 \times 10^6$ in FS, and

7.64 x 10^6 ± 1.33 x 10^6 particles L^{-1} in FC. The total area of all particles yielded for TEP in FS 305 ± 92 mm^2 L^{-1}, and FC 233 ± 91 mm^2 L^{-1}, and for CSP 444 ± 149 mm^2 L^{-1} in FS and 370 ± 188 mm^2 L^{-1} in FC, however, differences were insignificant.

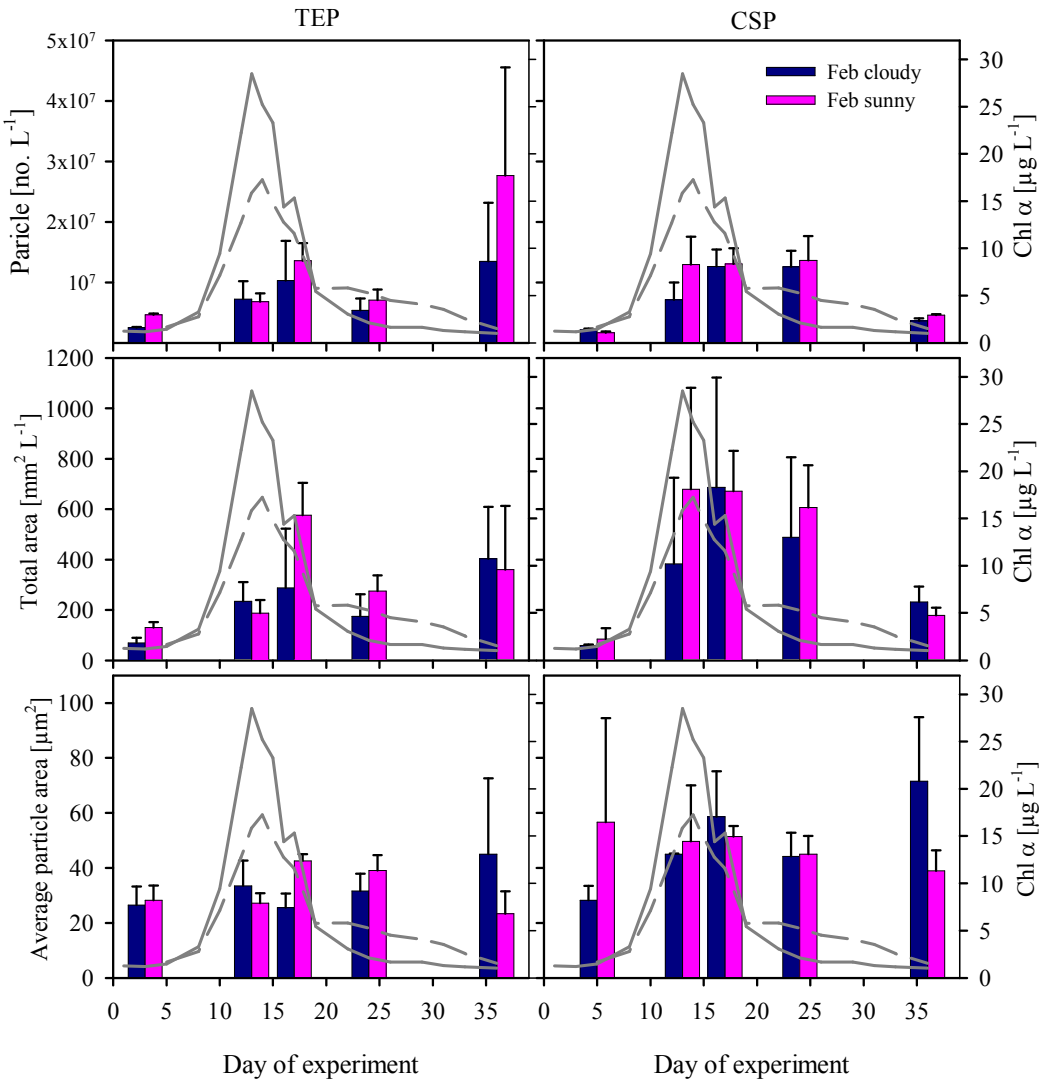

Figure 4-5: TEP (left) and CSP (right) abundance (particle number), total area and size (average particle area) in February cloudy (blue) and sunny (pink) treatment during the experimental period. The dashed line indicates the mean Chl *a* concentration for FC, the solid line that for FS.

The size (average particle area) showed the trend to be increased for CSP (49 ± 12 μm^2) in cloudy and sunny treatment, compared with TEP (32 ± 7 μm^2), (p<0.0001), although the data showed a high scatter (Fig. 4-4). When looking at the development of particle numbers and mean area over the experimental period (Fig. 4-5), TEP as well as CSP are low at pre-bloom conditions and get more abundant during the bloom period. While TEP abundance and TEP area decreased right after the bloom and rose again for FS and FC at the end of the experiment, CSP stayed on a high level right after the bloom and decreased at the end of the experiment (Fig. 4-5).

Results of the colorimetric analysis of TEP show an increased amount of TEP in February treatments and especially at sunny conditions (Fig. 4-6). A statistic comparison of maximum TEP concentrations (TEP_{max}) reveals, however, a slight insignificance between FS and FC (p=0.08).

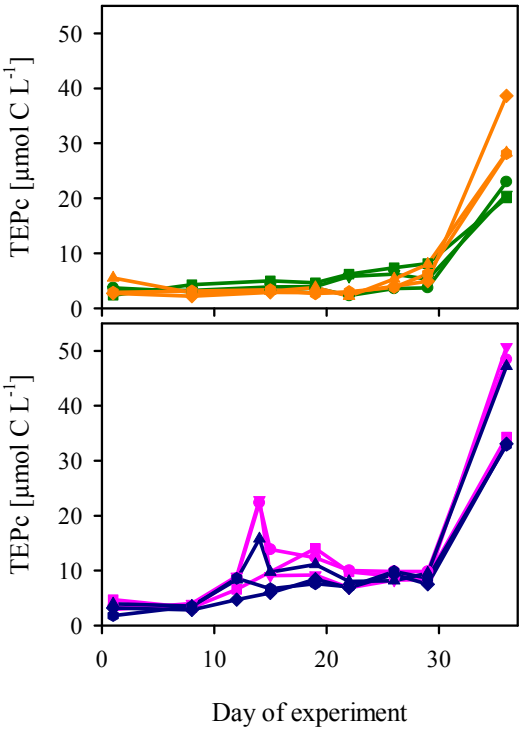

Figure 4-6: TEP analyzed by the colorimetrical method (TEPc) during the experimental period for January (top) and February (bottom). The color code is as in figure 4-1.

Discussion

Accumulation of POM

This study showed that a sunny week in the second half of January can initiate a phytoplankton bloom comparable in size and timing to a bloom in February. Slow nutrient drawdown for sunny light levels in the first half of the month January (JSI) indicate that light levels in this treatment were at a margin for the development of a phytoplankton bloom.

As expected, maximum net build-up of the individual POM components (POC, PN, POP, BSi) increased with increasing daily light dose. In one previous experiment with a factorial combination of two temperature and three light settings (Chapter 1), no significant effects on net POM accumulation were found. This study confirmed our assumption that for that former study light levels differed not far enough from each other for the detection of significant differences. In line with our results, a synthesis of six mesocosm experiments, examining the effect of warming with the co-factors light and copepod abundance, found a positive dependence of peak phytoplankton biomass on light, and a negative dependence on initial copepod abundance (Sommer et al. 2012a).

Stoichiometry of POM

The POC/PN ratio was only slightly and the POC/POP ratio not significantly affected by daily light dose during this study. The literature reports, however, of increasing POC/PN and POC/POP ratios of phytoplankton with increasing light intensity. Principally, the carbon to nutrient ratio increases with light intensity under limitation of the investigated nutrient (Sterner and Elser 2002; Dickman et al. 2006). Certain phototrophic organisms have the ability to store C in form of lipids or carbohydrates, thereby increasing their C/N and C/P ratios or a P-sparing effect can sometimes be observed for some microorganisms, thereby producing biomass with C/P and N/P ratios that exceed Redfield-ratios (Karl and Björkman 2002). "Excess carbon consumption" is named the process in which dissolved inorganic carbon is fixed by phytoplankton in excess of the Redfield C/N and C/P ratio (Sambrotto et al. 1993; Toggweiler 1993). Contrary to the results for the stoichiometry of POM, the results for the net dissolved inorganic carbon (DIC) drawdown in relation with the drawdown of inorganic nutrients (DIN, DIP) suggest excess carbon fixation for all treatments.

Comparing the build-up of POM with the initial nutrient concentrations reveals that the loss of an element (e.g. N-loss=PN-DIN) increases with decreasing mean daily light dose. The loss is probably due to grazing by copepods and lower growth rates of phytoplankton at lower irradiance prevented to compensate for the loss. Copepods were for this experiment at least 4-20 times higher than natural abundances in the Baltic Sea at this time of the year (1-5 Ind. L^{-1}, Möllmann et al. 2000). However, as copepods of the Baltic Sea are expected to react positively to the climate warming trend, with higher abundances after mild winters (Hansson et al. 2010), this study may represent a future high-copepod-abundance scenario.

The former study with three copepod densities (Chapter 2) already showed that POC/PN and POC/POP ratios decrease with increasing copepod abundance, because maximum accumulation of POC decreases with increasing copepod abundance. For that study it was concluded that copepod grazing increased nutrient recycling, therewith "refueling" the nutrient stock available for phytoplankton growth. Hence, under this "high grazing scenario" in this study, nutrient recycling may have also moderated increases in C/N and C/P of POM.

Accumulation of dissolved organic matter

Unexpected, DOC concentrations were not affected by daily light dose as it was observed in other studies (Verity 1981a; Zlotnik and Dubinsky 1989; Wolfstein et al. 2002) neither were DON or DOP affected. It is often observed that extracellular release increases after nutrient depletion during phytoplankton blooms (Nagata 2000; Engel et al. 2002). This effect was also not visible during our study. But, our former study with three densities of

copepods (Chapter 2) suggested, however, that grazing could be an important source for nutrient regeneration, thereby dampening the effect of enhanced extracellular DOC release by phytoplankton due to nutrient deficiency. One can speculate that nutrient recycling in response to the high copepod abundance in this study also dampened extracellular DOM release.

Gel particles

CSP were as abundant and comparable to TEP in area and particle area. CSP abundance and area were of the same magnitude than those of coastal Californian water, but different to our study, CSP were in that former study 3 to 13 times more abundant than TEP (Long and Azam 1996). In contrast, in Lake Kinneret, the abundance of CSP were between 12 and 50 % that of TEP (Berman and Viner-Mozzini 2001). The latter study detected seasonal ups and downs in particle concentrations and assumed that a large proportion was derived from detrital matter (Berman and Viner-Mozzini 2001). As TEP and CSP in our study increased already during bloom conditions (Fig. 4-5) a phytoplankton origin seems more likely, although for TEP an increase was also detectable at the end of the experiment. During our study, the formation of gel particles was slightly affected by light in February treatments. This is in line with findings that observed a coupling between photosynthetic activity and TEP production of diatoms (Claquin et al. 2008). As previously noted by Long and Azam (1996), TEP and CSP have to be analyzed on separate filters as both are stained with blue color. As this makes it difficult to know to which extent the particles are exclusively TEP or CSP, Berman et al. (2001) presumed that some, if not many, of the analyzed particles in their study of Lake Kinneret, had both proteinaceous as well as polysaccharide components. Long and Azam (1996) were able to distinct most CSP from TEP by the treatment of CSP with Pronase E, a non-specific protenase, that reduces CSP abundance by 78 % and CSP area by 96 %. We therefore think that the CSP in our study were as well of proteinaceous nature. In addition, CSP in this study showed a greater particle area than TEP. This makes us believe that CSP were distinguished from TEP. The importance of TEP has long been established as a bridge in the DOM-POM continuum (Engel et al. 2004; Verdugo et al. 2004), as agents in the flocculation of phytoplankton blooms (Logan et al. 1995) or living environment for attached bacteria (Mari and Kirboe 1994), thereby influencing carbon cycling in the pelagic ecosystem. CSP may be equally important for the cycling of nitrogen as TEP are for the cycling or carbon (Long & Azam 1996), although, CSP were found to play a minor role compared with TEP in aggregation dynamics (Prieto et al. 2002), they are often colonized by bacteria (Long & Azam 1996) and may therefore also play an important role as hot spots for nutrient recycling and as a food source for micrograzers (Berman & Viner-Mozzini 2001). However, these proteinaceous particles have not gained

as much attention as TEP in the literature so far. Our study showed that CSP are equally important for the partitioning of N as TEP for the partitioning of C during winter/spring phytoplankton blooms in this Baltic Sea region and should be considered in future studies on organic matter cycling.

Consequences for the future ocean

If in the course of climate warming, sunshine hours in winter/spring were to decrease, then also the probability would decrease for the in this study observed "fast" phytoplankton blooms with high POM build-up. As copepod development depends on the development of phytoplankton, cloudy weather could hence have also negative consequences for copepods, especially if their respiration and grazing activity would increase due to sea surface warming. Indeed, (Sommer et al. 2012b) report of a bottom-up transmission to mesozooplankton (mainly copepods) during the same experiment, evident by increased abundance of copepod nauplii and egg production at higher light levels. Model simulations generally project that enhanced vertical stratification due to sea surface warming favors autotroph growth in high and mid-latitude oceans (Bopp et al. 2001; Sarmiento et al. 2004). In high latitude oceans, where phytoplankton are typically light-limited, reduced mixing (caused by enhanced stratification due to warming) would keep the plankton at the surface were light levels are high (Doney 2006). This co-effect of warming may counteract reduced autotrophic production by cloudy weather conditions.

Synthesis and future perspectives

The Earth's climate depends largely on the oceans capacity to take up heat and atmospheric CO_2. In this context, one biogeochemical key process is the biological carbon pump, a mechanism transporting carbon via food-web interactions from surface water to the deep ocean. Only the portion of carbon that sinks below the sea surface mixing layer can be sequestered and contribute to a reduction of atmospheric CO_2 concentrations. On its way through the food-web a high portion of carbon is respired and released as CO_2. The efficiency of the biological pump (and carbon sequestration) depends on the balance between autotrophic production and respiration, the metabolic processes driven by temperature change (Brown 2004). Biological processes in the sea are also controlled by a variety of other abiotic factors acting synergistically or antagonistically to temperature. These include light and nutrient/substrate availability. All together these factors largely affect marine food webs due to changes in community composition, grazing activity, bacterial abundance etc. The response of the biological processes to these interacting factors will determine the future direction of the biological carbon pump.

In the following, I will present a synthesis of the observed effects of elevated temperature, changing irradiance and grazer abundance on organic matter production, stoichiometry, degradation and its partitioning between the dissolved and particulate organic matter pools followed by a section of perspectives for future research.

TEMPERATURE

Timing of phytoplankton blooms

The data presented in this thesis underlines previous findings that rising temperature accelerates autotrophic processes. The onset of nutrient depletion and phytoplankton bloom peaks were advanced by 1-2 days per degree Celsius (Chapter 1, 2, 3) (Sommer et al. 2012a; Sommer and Lengfellner 2008; Wohlers-Zöllner et al. 2011). In general, spring bloom timing in the ocean can vary by several weeks and the available marine time series data so far did not provide evidence for an advancement in diatom spring bloom timing in response to ocean warming (Edwards and Richardson 2004; Wiltshire et al. 2008).

Particulate organic matter

POM maxima declined with increasing temperature in one study (Chapter 1) and POC and POP build-up also decreased significantly in previous AQUASHIFT studies (Chapter 3). The overall effect of rising temperature, the mean effect size, however yielded a consistent negative value only for POP_{mean} (Chapter 3). These results are contradictory to

a recent mesocosm study that observed an enhanced flow of dissolved inorganic carbon with increasing temperature into the pools of POC and DOC (Taucher et al. 2012).

Lower accumulation of POM can be caused by lower photosynthetic production or by enhanced heterotrophic consumption. In line with the findings of an insignificant response of primary production (PP) to temperature in the first study (Lewandowska and Sommer 2010), a comprehensive analysis of PP revealed no significant direct response to rising temperature overall AQUASHIFT studies (Lewandowska et al. 2011). Therefore, lower POM accumulation at elevated temperature was probably due to increased heterotrophic consumption processes or enhanced sedimentation. Indeed, bacterial secondary production (BSP) and community respiration were significantly stimulated by experimental warming (Chapter 3) (von Scheibner et al. 2013). A strong stimulation of bacterial secondary production was observed at warmer temperatures already during phytoplankton bloom conditions, indicative for a closer temporal coupling of autotrophic and heterotrophic processes (Chapter 3). These findings are supported by detailed studies on the impact of warming on phyto-bacterioplankton coupling (Hoppe 2008 et al, von Scheibner 2013 et al.) and bacterial community composition (von Scheibner et al. 2013) during AQUASHIFT mesocosm experiments.

Dissolved organic matter

Concerning the dynamics in the dissolved organic matter pool, DOC and carbohydrate concentrations increased more rapidly at elevated temperature (Chapter 1, 2 and 3). This uniform pattern is in line with previous mesocosm experiments (Engel et al. 2010, Wohlers-Zöllner et al. 2011, Taucher et al. 2012) and other studies that found a more pronounced primary production and release of carbon-rich compounds at higher temperatures (Verity 1981a; Davison 1991; Morán et al. 2006; Claquin et al. 2008). Hence, one consequence of ocean warming might be a higher partitioning of organic carbon from the pool of particulate to dissolved matter. DOC increased only after the depletion of inorganic nutrients, a phenomenon that is often observed during phytoplankton blooms (Copin-Montégut and Avril 1993) and attributed to the overflow of algal photosynthates (Engel et al. 2002; Schartau et al. 2007). As carbohydrates simultaneously increased with DOC, an algal origin of this DOC is very likely and suggests that a high proportion of dissolved inorganic carbon that was fixed by photosynthesis was channelled into DOC. However, rates of dissolved algal primary production showed a negative or no response to rising temperature (Chapter 3). Possibly, bacteria were responsible for a fast recycling of these algal derived compounds and an accumulation hence not detectable.

As the heterotrophic bacterial production showed a consistent positive response to warming it was argued that also bacterial decomposition processes have contributed to

the DOC accumulation, for instance by the release of cell-surrounding material during growth or through modifications of DOM compounds (Azam 1998; Stoderegger and Herndl 1998; Ogawa et al. 2001). DOC accumulated in the water column, indicating that bacteria were temporarily not able to balance the increase in DOC. This can be due to a refractory nature of the fresh DOC (Fry et al. 1996) or nutrient limitation (Thingstad et al. 1997). Supporting the latter theory, the analysis of the carbohydrate fraction of one AQUASHIFT experiment revealed a predominant accumulation of glucose (Engel et al. 2010), a substrate usually quickly available to bacteria.

A high accumulation of DOC was observed at elevated temperature at the end of the phytoplankton bloom and bacteria were not able to balance the increase in the time frame of our studies. This may indicate that in a future warmer ocean a high proportion of DOC can potentially be exported to deeper parts of the ocean by mixing and downwelling or by abiotic aggregation into TEP.

Neither DON nor DOP showed a response to increased temperature. This can probably be attributed to the fact that N and P are limiting nutrients for algal growth, while C can normally only be rate limiting in photosynthesis. DOP is the fraction of DOM that is preferentially mineralized (Clark et al. 1998) and small molecules of DON and DOP can be utilized by phytoplankton and bacteria (Bronk 2002; Karl and Björkman 2002). Hence, DON and DOP were probably quickly recycled and, in contrast to DOC, a pronounced accumulation of DOP and DON was not detectable.

Particle dynamics

TEP dynamics differed between the studies. While TEP concentrations increased concomitant with the phytoplankton bloom in the first study (Chapter 1), they increased in the other studies (Chapter 2, 3) only at elevated temperature and only in the last days of the experiment. The latter temperature effect on TEP was also found in a previous mesocosm study (Wohlers et al. 2009) and, as polysaccharides concomitantly declined, indicate an abiotic aggregation of these compounds into TEP (Chin et al. 1998; Kerner et al. 2003).

Increasing TEP concentrations during the build-up of the bloom are indicative for the release of carbohydrate-rich cell surface material (Passow 2002). TEP production is highly species specific (Claquin et al. 2008; Engel and Passow 2001; Passow 2002a). Differences in the dominant phytoplankton species composition may be the reason for different TEP dynamics between the studies.

Earlier increase in TEP concentrations and elevated maximum TEP concentrations at higher temperature support the assumption that the release or the formation of extracellular substances is temperature sensitive. The reason might be a

temperature sensitive diversion of photosynthates from dissolved to particulate organic carbon. This principle was shown in response to an increase in CO_2 concentrations (Engel 2002). TEP can promote the flocculation of phytoplankton cells due to the high sticking efficiency of these gel particles (Engel 2000; Kiørboe and Hansen 1993) and provide enhanced particle export flux (Kahl et al. 2008). Additionally, it was shown that TEP-mediated aggregation of the diatom *Skeletonema costatum* positively correlated with temperature (Thornton and Thake 1998) and increased temperature improved the aggregation potential of phytoplankton aggregates in a mesocosm study (Piontek et al. 2009). These previous findings and the results of this study (Chapter 1) suggest that in a warmer ocean the accumulation of POM is controlled by two counteracting mechanisms. One is determined by enhanced heterotrophic remineralization processes, leading to a weakening of the biological pump. The other process provides enhanced particle aggregation and a strengthened transport of POM to deeper parts of the ocean. As TEP production is species specific the taxonomic composition of the phytoplankton community is therefore a decisive factor.

Stoichiometry of particulate and dissolved organic matter

Particulate organic matter C:N and C:P were far above the Redfield ratio during the bloom in all studies. That carbon and nitrogen dynamics can decouple after nitrate depletion during phytoplankton blooms was observed before and attributed to excess carbon fixation (Engel et al. 2002; Wetz and Wheeler 2003). Excess carbon fixation or carbon overconsumption describes the process, in which dissolved inorganic carbon relative to inorganic nitrogen (or phosphorus) is taken up by phytoplankton in excess of the Redfield-ratio (Sambrotto et al. 1993; Toggweiler 1993). Engel et al. (2002) traced increased POC:PN back to an enhanced channelling of carbon into the formation of TEP from the DOC pool. In our study, higher POC:PN ratios were observed during the bloom and were thus not directly related to TEP formation, except for one study (Chapter 1). In a recent mesocosm study, POC accumulation increased with increasing temperature, probably caused by the effect of carbon overconsumption, whereby more POC than PN accumulated leading to elevated POC:PN ratios (Taucher et al. 2012).

Many studies emphasised the preferential recycling of P or P and N compared to C (Clark et al. 1998; Shaffer et al. 1999; Loh and Bauer 2000). We expected a stimulating effect of temperature on the recycling of N and P with the consequence that C:N:P ratios of POM and DOM increase with increasing temperature. Yet, POC/PON_{max} was lower for T+6 compared to T+0 in one study (Chapter 1), and POC/POP_{mean} also only for one study (Chapter 3). It was shown that experimental warming stimulated the activity of the organic phosphorus-cleaving enzyme alkaline phosphatase (Wohlers-Zöllner et al. 2011).

Warming may have therefore stimulated the recycling of P thereby refuelling the pool of P available to phytoplankton.

In general, DOC:DON and DOC:DOP ratios were high, owing partially to relatively high DOC concentrations from the beginning of the experiments. After nitrate depletion, DOM with a C:N ≥ 16 accumulated during a phytoplankton bloom, dominated by the diatom *Chaetoceros* sp. (Wetz and Wheeler 2003). Kähler and Koeve (2001) calculated a DOC:DON of 23.5 for surface water (5 m depth) along a transect in the North Atlantic - a similar high ratio as observed for DOC:DON ratios at least for bloom conditions in our study. However, when DOC increased after nutrient depletion, DOC:DON and DOC:DOP increased as well, and the increase was more pronounced at elevated temperature (see above).

IRRADIANCE

Particulate organic matter

In the ocean, elevated sea surface temperature is accompanied by increasing water column stratification (Prentice et al. 2001). Model simulations generally assume that enhanced vertical stratification favors autotroph growth in high and mid-latitude oceans, whereby in low-latitude oceans a reduction in upwelling would lower nutrient supply thereby dampening primary productivity (Bopp et al. 2001; Sarmiento et al. 2004). The results of Chapter 4 confirmed the common expectation that inorganic nutrient drawdown and net accumulation of POM significantly increase with increasing light dose (range 5.4 to 10.4 mol photons m^{-2} d^{-1} mean daily light dose at T+2). This effect could not be observed during the first study (Chapter 1), probably because of the relatively modest differences in light levels between treatments (range 7 to 8.9 mol photons m^{-2} d^{-1}). But increasing light intensity accelerated the bloom development at T+6 evident by a significant earlier POC peak timing ($p < 0.01$) and POC concentration rise during exponential growth ($p < 0.05$) (Chapter 1, 3). Contrary, light effects at T+0 were not detected. In general, onset of light saturation increases with temperature (Kirk 1983; Mortain-Bertrand et al. 1988). Based on this, at T+0 the phytoplankton was probably light saturated at all light levels and differences between light treatments were hence not detectable. Hence, light intensity is an important yet often neglected cofactor in ocean warming experiments and should be considered in following studies on this subject.

Dissolved organic matter

DOM concentrations stayed unaffected by modifications in daily light dose (Chapter 1, 4). This is contradictory to several previous studies that found DOM excretion by phytoplankton to increase with increasing light levels (Verity 1981a; Zlotnik and Dubinsky 1989; Wolfstein et al. 2002). In the first study (Chapter 1) differences between

light levels were probably too small for the detection of distinct differences in DOM accumulation. Results from the previous studies suggested that water temperature was probably too low for a fast and pronounced DOC accumulation in the last study with water temperature of T+2 (Chapter 4). Moreover, the results of our grazing study (Chapter 2) suggest that the high abundances of copepods during this light-study enhanced the recycling of N and P and may have therefore prevented a pronounced accumulation of DOC in the water column (see below).

Particle dynamics

TEP and CSP showed no change in abundance or size in response to changes in irradiance. Although, a linear relationship was observed between photosynthesis and TEP production for three diatom species (Claquin et al. 2008). However, this study showed that CSP were as abundant and comparable to TEP in size. Hence, CSP may be equally important for the cycling of nitrogen as TEP are for the cycling of carbon (Long & Azam 1996). Although, CSP were found to play a minor role compared with TEP in aggregation dynamics (Prieto et al. 2002), they are often colonized by bacteria (Long & Azam 1996) and may therefore also play an important role as hot spots for nutrient recycling and as a food source for micrograzers (Berman & Viner-Mozzini 2001). This suggests that CSP should receive more attention in future studies on organic matter cycling, as these particles are most often neglected.

Stoichiometry of particulate and dissolved organic matter

Sterner and Elser (2002) report that for a nutrient *X*, the carbon (C) to *X* ratio of the autotroph (marine) biomass increases with limitation of *X* and with increasing light intensity. The results of this thesis, however, could not find a relationship between an increase in irradiance and the POC:PN or POC:POP ratios.

GRAZER ABUNDANCE

Particulate organic matter

Copepod abundance (in the range of 1.5 to 10 ind. L^{-1}) had no effect on the phytoplankton bloom timing, although, an enhanced top-down control on phytoplankton was detected at higher copepod abundance (Sommer and Lewandowska 2011). Grazing by copepods can be an important mechanism which causes loss of algae biomass. Lewandowska and Sommer (2010) and other mesocosm studies (Keller et al. 1999; O'Connor et al. 2009) related negative effects of elevated temperature on phytoplankton biomass to increased biomass or abundances of zooplankton. In Chapter 2 I showed that grazing significantly reduced POC accumulation. However, maximal accumulation of PN and POP were not affected by grazing (see below stoichiometry).

Not only is the abundance of grazers decisive for POM accumulation but also an increase in grazing activity with warmer temperatures. It is known from a previous similar mesocosm experiment (4 temperature regimes, one light setting) that respiration and ingestion rates of the copepod *Pseudocalanus* sp. increased by a factor of 3 in the same temperature range (Isla et al. 2008). Indeed, the difference in POC maximal accumulation between high and low copepod abundance showed the tendency to be more pronounced at elevated temperature (Chapter 2).

Dissolved organic matter

DOM did not increase due to higher grazer abundance as shown by other studies (Nagata 2000; Kragh et al. 2006). Rather, DOC decreased with increasing copepod abundance and the accumulation of carbohydrates was slower (Chapter 2, 3). First, it was speculated that the effect of grazer abundance may have masked a temperature effect on DOC dynamics by triggering a trophic cascade via ciliates and heterotrophic nanoflagellates (HNF) (Chapter 3). Low copepod abundance may have relieved bacteria from HNF grazing pressure and enhanced bacterial decomposition contributed to DOM accumulation (Zöllner et al. 2009). However, additional data could not prove a relationship between copepod and bacteria abundance (von Scheibner, pers. comm.). Furthermore, a detailed analysis of data from the "grazing study" (Chapter 2) suggested that copepod grazing and egestion enhanced the recycling of N and P, thereby increasing the availability of these nutrients for autotrophs. As inorganic nutrient limitation favours the release of DOC, nutrient deficiency was likely higher at lower copepod density and may have contributed to enhanced nutrient stress and subsequent DOC release by phytoplankton.

Stoichiometry of POM and DOM

Maximum POC accumulation decreased with increasing copepod abundance, but maximum PN and POP accumulation were unaffected (Chapter 2) hence, POC:PN and POC:POP decreased from low to high copepod density. This suggests that copepod grazing and egestion enhanced the recycling of N and P, thereby increasing the availability of these nutrients for autotrophs. It is known that consumers, via egestion and excretion, can be important drivers for nutrient regeneration and recycling. This can feed back to autotrophs by increasing the availability of nutrients (Ketchum 1962; Lehman 1980; Sterner 1986; Elser and Urabe 1999). Consumer-driven nutrient recycling probably also increased the nutrient availability for autotrophs in our study resulting in reduced C:N and C:P ratios of POM. This study, combining projected climate warming and different copepod abundances, suggests that the excess inorganic carbon consumption by phytoplankton that is favoured by nutrient stress and suspected to increase due to sea-

surface warming, could be moderated by the effect of copepod-driven nutrient recycling and counteract increases in C:N or C:P ratios of POM and DOM.

Future perspectives

Improvement of mesocosm design/methods

Mesocom experiments are often critizised for beeing artifical as this experimental setup does not account for vertical or lateral water mass movements or for a thermal water column stratification, if water depth are as low as in the mesocosms used for this thesis. Nevertheless, mesocsom experiments are recognized as a valuable tool for the investigation of climate change related effects in plankton communities and are used in diverse designs all over the world, offering researchers an experimental set-up for all kinds of investigations (e. g. Mesoaqua). Remarkably, during the three mesocosm experiments, synchrony and similar patterns were observed for the same temperature or light treatments, despite the limited numer of replicates. These findings strenghten confidence in the results observed and my opinion that mesocosms are a relieable experimental set-up. However, I am also aware of some drawbacks which are artificially introduced in these systems. Therefore, following suggestions for future studies applying mesocosms should be taken into account:

A major research focus of this thesis were potential consequences of a warmer ocean on the transport of organic matter to the deep and thus the efficiency of the biological carbon pump. A pronounced temperature-sensitivity of the bacterial community and an increase in community respiration was measurable suggesting enhanced recycling of organic matter and a weakening of the biological pump. However, in previous studies (Wohlers et al. 2009) as well as in the present thesis the sinking of cells was only a matter of speculation, as direct measurements of sedimentation rates were not possible. This was mainly caused by the fact that this mesocosm set-up was too shallow to allow sediment traps in the system. Other mesocosm designs tried to close this gap by introducing sediment trapsww (e. g. Czerny et al. 2013). Another method for investigating the formation (and degradation) of aggregates is the tranfer and incubation of organic matter into roller tanks. This approach was chosen for a previous AQUASHIFT mesocosm experiment (Piontek et al. 2009) but the sinking of aggregates or cells was not followed on a daily basis. Nevertheless, sediment traps allow sampling at high temporal resolution (e.g. daily). Alternatively, a camera that documents the sinking of aggregates would be an improvement when concipating new mesocosms. A daily removal of sedimented material would have also the advantage that processes from the bottom material are prevented from perturbing the measurements. For instance, Wohlers et al. (2009) detected a respiration signal, probably originating from degradation processes occuring at the bottom of the mesocosms.

Response of key species

In chapter 1 I suggsted that the phytoplankton species composition can be crucial for the flow of DIC into DOM and subsequent particle pool (TEP production). A change in the dominant phytoplankton specie can hence profoundly affect organic matter cycling. In line with this, Taucher et al. (2012) observed a completely different response to temperature during a summer phytoplankton bloom, as the net built-up of both POC and DOC was enhanced at higher temperature. It would hence be interesting to elucidate if there are one or more key species responsible for the bulk response. Laboratory investigations with batch cultures with single key species or mixed assemblages can therefore be a good tool.

Coomassie Stainable Particles

In chapter 4 I showed that CSP occurred at the same manitude than TEP. It would be interesting to know if CSP dynamics are like TEP temperature sensitive or sensitive to other environmental factors and thus gain a better understanding of these particles and their potential role in organic matter fluxes.

This thesis assessed only some of the factors that are about to change in the future ocean. Research on other potentially interactive factors is already done or on its way, e. g. mesocosm studies that combine projected increase in CO_2 concentrations with temperature rise. It will be, however, an enormous effort to evaluate all necessary and sometimes interactive factors. All available data of field research, mesocosms studies and laboratory culture experiments have to be merged in comprehensive models to make substantially predictions for the future directions of phytoplankton bloom dynamics and consequences for the biological carbon pump.

Danksagung

Ganz vielen Menschen möchte ich für ihre Unterstützung danken. Zuerst gilt mein Dank meinem Doktorvater Ulf Riebesell. Vielen Dank, dass du mir die Chance gegeben hast in diesem Projekt mitzuarbeiten, für dein Vertrauen und für einen guten Rat im richtigen Moment. Bedanken möchte ich mich auch bei Anja Engel für ihre Unterstützung und konstruktive Kritik und dafür dass ich ab und zu zum AWI zurückkehren durfte, um meine TEP zu mikroskopieren. An Ulrich Sommer mein Dank, der mich durch seine Ideen und sein Wissen inspiriert hat.

Bei Julia Wohlers, die mich in die Kieler Mesokosmenwelt quasi eingearbeitet hat.

Meinen Mitstreitern im Kampf mit den Mesokosmen, Aleksandra Lewandowska und Markus von Scheibner will ich danken für die vielen interessanten Diskussion zum Thema, aber auch zu allen anderen Lebenslagen und für die witzigen Momente während unserer anstrengenden Experimentphasen.

Meiner enthusiastischen Arbeitsgruppe in der biologischen Ozeanografie, allen voran meinen „room mates“ Jan Büdenbender und Scarlett Sett, für eine gute Arbeitsatmosphäre und dass Gefühl gerne zur Arbeit zu gehen. Es hat viel Spaß gemacht mit euch.

Danke an die tatkräftige Unterstützung der Techniker-crew: Peter Fritsche, Thomas Hansen, Andrea Ludwig, Kerstin Nachtigal und Nicole Händel.

Meine „Student helpers“ vielen Dank, ohne euch hätte ich die tausende von Filtern und Proben nicht bewältigen können. Eine feste Größe ist über die Jahre Scarlett Sett bei der Probennahme geworden – spezial thanks! Des Weiteren zu nennen sind Sarah Febiri, Wiebke, Marieta, Yennifer, Martin, Lena und Isabel.

Außerdem danke ich dem Leibniz-Institut für Ostseeforschung Warnemünde (IOW) für die finanzielle Unterstützung in der Endphase der Fertigstellung der Dissertation im Rahmen des "Come-back-to-research"-Programmes. Und ganz speziell Klaus Jürgens und seiner Arbeitsgruppe, die mich in ihren Kreis aufgenommen und mir eine fruchtbare und nette Arbeitsumgebung geschaffen hat, um meine Doktorarbeit nach einer längeren Elternzeit wieder in Angriff zu nehmen. Besonderer Dank gilt Ruth Anderson, Daniel Herlemann und Christian Stolle, die auch die ein oder andere Korrekturlese übernommen haben.

Meiner Familie, besonders meinen Eltern, danke ich für ihre uneingeschränkte mentale Unterstützung über all die Jahre und dass sie immer an mich geglaubt haben. Ein besonderer Dank gilt meinem Lebensgefährten Markus von Scheibner der mich mit seiner unerschütterlichen positiven Einstellung immer wieder aufgerichtet hat und der mir besonders in der Schlussphase den Rücken freigehalten hat.

References

Alldredge, A. L., U. Passow, and B. E. Logan. 1993. The abundance and significance of a class of large, transparent organic particles in the ocean. Deep-Sea Res Pt I **40**: 1131–1140.

Armstrong, R., C. Lee, J. Hedges, S. Honjo, and S. G. Wakeham. 2001. A new, mechanistic model for organic carbon fluxes in the ocean based on the quantitative association of POC with ballast minerals. Deep-Sea Res Pt II **49**: 219–236.

Azam, F. 1998. Oceanography: Microbial control of oceanic carbon flux: the plot thickens. Science **280**: 694–696.

Azam, F., T. Fenchel, J. G. Field, J. S. Gray, L. A. Meyer-Reil, and F. Thingstad. 1983. The Ecological Role of Water-Column Microbes in the Sea. Mar Ecol Prog Ser **10**: 257–263.

Bach, L. T., U. Riebesell, S. Sett, S. Febiri, P. Rzepka, and K. G. Schulz. 2012. An approach for particle sinking velocity measurements in the 3–400 μm size range and considerations on the effect of temperature on sinking rates. Mar Biol **159**: 1853–1864.

Barnett, T. P., D. W. Pierce, K. M. Achutarao, P. J. Gleckler, B. D. Santer, J. M. Gregory, and W. M. Washington. 2005. Penetration of human-induced warming into the world's oceans. Science **309**: 284–287.

Behrenfeld, M. J., R. T. O'Malley, D. A. Siegel, C. R. McClain, J. L. Sarmiento, G. C. Feldman, A. J. Milligan, P. G. Falkowski, R. M. Letelier, and E. S. Boss. 2006. Climate-driven trends in contemporary ocean productivity. Nature **444**: 752–756.

Bellerby, R. G. J., K. G. Schulz, U. Riebesell, C. Neill, G. Nondal, E. Heegaard, T. Johannessen, and K. R. Brown. 2008. Marine ecosystem community carbon and nutrient uptake stoichiometry under varying ocean acidification during the PeECE III experiment. Biogeosciences **5**: 1517–1527.

Benner, R. 2002. Chemical composition and reactivity, p. 59–90. *In* D.A. Hansell and C.A. Carlson [eds.], Biogeochemistry of marine dissolved organic matter. Academic Press, San Diego, California, USA.

Berges, J. A., D. E. Varela, and P. J. Harrison. 2002. Effects of temperature on growth rate, cell composition and nitrogen metabolism in the marine diatom *Thalassiosira pseudonana* (Bacillariophyceae). Mar Ecol Prog Ser **225**: 139–146.

Berman, T., and D. Bronk. 2003. Dissolved organic nitrogen: a dynamic participant in aquatic ecosystems. Aquat Microb Ecol **31**: 279–305.

Berman, T., and O. Holm-Hansen. 1974. Release of photoassimilated carbon as dissolved organic matter by marine phytoplankton. Mar Biol **28**: 305–310.

Berman, T., and Y. Viner-Mozzini. 2001. Abundance and characteristics of polysaccharide and proteinaceous particles in Lake Kinneret. Aquat Microb Ecol **24**: 255–264.

Bernard, C., and F. Rassoulzadegan. 1990. Bacteria or microflagellates as a major food source for marine ciliates: possible implications for the microzooplankton. Mar Ecol Prog Ser **64**: 147–155.

Biddanda, B., and R. Benner. 1997. Carbon, nitrogen, and carbohydrate fluxes during the production of particulate and dissolved organic matter by marine phytoplankton. Limnol Oceanogr **42**: 506–518.

Biermann, A., and A. Engel. 2010. Effect of CO_2 on the properties and sinking velocity of aggregates of the coccolithophore Emiliania huxleyi. Biogeosciences **7**: 1017–1029.

Biersmith, A., and R. Benner. 1998. Carbohydrates in phytoplankton and freshly produced dissolved organic matter. Mar Chem **63**: 131–144.

Bjørnsen, P. K. 1988. Phytoplankton exudation of organic matter : Why do healthy cells do it ? Limnol Oceanogr **33**: 151–154.

Bopp, L., P. Monfray, and O. Aumont. 2001. Potential impact of climate change on marine export production. Glob Biogeochem Cy **15**: 81–99.

Boyd, P., and S. Doney. 2002. Modelling regional responses by marine pelagic ecosystems to global climate change. Geophys Res Lett **29**: 1–4.

Breithaupt, P. 2009. The impact of climate change on phytoplankton – bacterioplankton interactions. Unpublished PhD thesis, Christian-Albrechts-Universität zu Kiel, Kiel, 210 pp.

Brock, T. D. 1981. Calculating solar radiation for ecological studies. Ecol Model **14**: 1–19.

Bronk, D. A. 2002. Dynamics of DON, p. 153–247. *In* D.A. Hansell and C.A. Craig [eds.], Biogeochemistry of marine dissolved organic matter. Academic Press, San Diego, California, USA.

Brown, J., J. Gillooly, A. Allen, V. Savage, and G. West. 2004. Toward a metabolic theory of ecology. Ecology **85**: 1771–1789.

Canadell, J. G., C. Le Quéré, M. R. Raupach, C. B. Field, E. T. Buitenhuis, P. Ciais, T. J. Conway, N. P. Gillett, R. A. Houghton, and G. Marland. 2007. Contributions to accelerating atmospheric CO_2 growth from economic activity, carbon intensity, and efficiency of natural sinks. Proc Natl Acad Sci USA **104**: 18866–70.

Carlson, C. A. 2002. Production and removal processes, p. 91–151. *In* D.A. Hansell and C.A. Carlson [eds.], Biogeochemistry of marine dissolved organic matter. Academic Press, San Diego, California, USA

Carlson, C. A., and H. W. Ducklow. 1995. Dissolved organic carbon in the upper ocean of the central equatorial Pacific Ocean, 1992: Daily and finescale vertical variations. Deep-Sea Res Pt II **42**: 639–656.

Carpenter, E. J., and D. G. Capone. 2008. Nitrogen fixation in the marine environment, p. 141–198. *In* Nitrogen in the marine environment. Academic Press, Elsevier Inc., Burlington, USA.

Cherrier, J., J. Bauer, and E. Druffel. 1996. Utilization and turnover of labile dissolved organic matter by bacterial heterotrophs in eastern North Pacific surface waters. Mar Ecol Prog Ser **139**: 267–279.

Chin, W., M. Orellana, and P. Verdugo. 1998. Spontaneous assembly of marine dissolved organic matter into polymer gels. Nature **391**: 568–572.

Claquin, P., I. Probert, S. Lefebvre, and B. Veron. 2008. Effects of temperature on photosynthetic parameters and TEP production in eight species of marine microalgae. Aquat Microb Ecol **51**: 1–11.

Clark, L., E. Ingall, and R. Benner. 1998. Marine phosphorus is selectively remineralized. Nature **393**: 426.

Copin-Montégut, G., and B. Avril. 1993. Vertical distribution and temporal variation of dissolved organic carbon in the North-Western Mediterranean Sea. Deep-Sea Res Pt I **40**: 1963–1972.

Cotner, J., J. Ammerman, E. R. Peele, and E. Bentzen. 1997. Phosphorus-limited bacterioplankton growth in the Sargasso Sea. Aquat Microb Ecol **13**: 141–149.

Czerny, J., K. G. Schulz, T. Boxhammer, R. G. J. Bellerby, J. Büdenbender, A. Engel, S. A. Krug, A. Ludwig, K. Nachtigall, G. Nondal, B. Niehoff, A. Silyakova, and U. Riebesell. 2013. Implications of elevated CO_2 on pelagic carbon fluxes in an Arctic mesocosm study – an elemental mass balance approach. Biogeosciences **10**: 3109–3125.

Daufresne, M., K. Lengfellner, and U. Sommer. 2009. Global warming benefits the small in aquatic ecosystems. Proc Nat Acad Sci USA **106**: 12788–12793.

Davison, I. R. 1991. Environmental effects on algal photosynthesis: Temperature. J Phycol **27**: 2–8.

Dickman, E. M., M. J. Vanni, and M. J. Horgan. 2006. Interactive effects of light and nutrients on phytoplankton stoichiometry. Oecologia **149**: 676–89.

Doney, S. C. 2006. Oceanography: Plankton in a warmer world. Nature **444**: 695–696.

Doney, S. C., V. J. Fabry, R. a. Feely, and J. a. Kleypas. 2009. Ocean Acidification: the other CO_2 problem. Ann Rev Mar Sci. **1**: 169–192.

Ducklow, H. W., D. K. Steinberg, and K. O. Buesseler. 2001. Upper ocean carbon export and the biological pump. Oceanography **14**: 50–58.

Dugdale, R. C., and J. J. Goering. 1967. Uptake of new and regenerated forms of nitrogen in primary productivity. Limnol Oceanogr **12**: 196–206.

Edwards, M., and A. J. Richardson. 2004. Impact of climate change on marine pelagic phenology and trophic mismatch. Nature **430**: 881–884.

Elser, J. J., and J. Urabe. 1999. The stoichiometry of consumer-driven nutrient recycling: theory, observations, and consequences. Ecology **80**: 735.

Engel, A. 2000. The role of transparent exopolymer particles (TEP) in the increase in apparent particle stickiness (alpha) during the decline of a diatom bloom. J Plankton Res **22**: 485–497.

Engel, A. 2002. Direct relationship between CO_2 uptake and transparent exopolymer particles production in natural phytoplankton. J Plankton Res **24**: 49–53.

Engel, A. 2004. Distribution of transparent exopolymer particles (TEP) in the northeast Atlantic Ocean and their potential significance for aggregation processes. Deep-Sea Res Pt I **51**: 83–92.

Engel, A. 2009. Determination of marine gel particles, p. 125–142. *In* O. Wurl [ed.], Practical guidelines for the analysis of seawater. CRC Press, Boca Raton, USA.

Engel, A., S. Goldthwait, U. Passow, and A. Alldredge. 2002. Temporal decoupling of carbon and nitrogen dynamics in a mesocosm diatom bloom. Limnol Oceanogr **47**: 753–761.

Engel, A., N. Händel, J. Wohlers, M. Lunau, H.-P. Grossart, U. Sommer, and U. Riebesell. 2010. Effects of sea surface warming on the production and composition of dissolved organic matter during phytoplankton blooms: results from a mesocosm study. J Plankton Res **33**: 357–372.

Engel, A., and U. Passow. 2001. Carbon and nitrogen content of transparent exopolymer particles (TEP) in relation to their Alcian Blue adsorption. Mar Ecol Prog Ser **219**: 1–10.

Engel, A., and M. Schartau. 1999. Influence of transparent exopolymer particles (TEP) on sinking velocity of *Nitzschia closterium* aggregates. Mar Ecol Prog Ser **182**: 69–76.

Engel, A., S. Thoms, U. Riebesell, E. Rochelle-Newall, and I. Zondervan. 2004. Polysaccharide aggregation as a potential sink of marine dissolved organic carbon. Nature **428**: 929–932.

Eppley, R. W. 1972. Temperature and phytoplankton growth in the sea. Fish Bull **70**: 1063–1085.

Falkowski, P. G. 1998. Biogeochemical controls and feedbacks on ocean primary production. Science **281**: 200–206.

Falkowski, P. G., and J. A. Raven. 2007. Aquatic photosynthesis, 2. ed. Princeton University Press, Princeton, New Jersey.

Field, C. B., M. J. Behrenfeld, J. T. Randerson, and P. Falkowski. 1998. Primary production of the biosphere: integrating terrestrial and oceanic components. Science **281**: 237–240.

Finkel, Z. V., J. Beardall, K. J. Flynn, A. Quigg, T. A. V. Rees, and J. A. Raven. 2009. Phytoplankton in a changing world: cell size and elemental stoichiometry. J Plankton Res **32**: 119–137.

Fogg, G. E. 1966. The extracellular products of algae. Ocean Mar Biol Ann Rev **4**: 195–212.

Fogg, G. E. 1983. The ecological significance of extracellular products of phytoplankton photosynthesis. Bot Mar **26**: 3–14.

Fry, B., C. H. Jr, and A. Nolin. 1996. Long-term decomposition of DOC from experimental diatom blooms. Limnol Oceanogr **41**: 1344–1347.

Fuhrman, J., and F. Azam. 1982. Thymidine incorporation as a measure of heterotrophic bacterioplankton production in marine surface waters: evaluation and field results. Mar Biol **66**: 109–120.

Gaedke, U., M. Ruhenstroth-Bauer, I. Wiegand, K. Tirok, N. Aberle, P. Breithaupt, K. Lengfellner, J. Wohlers, and U. Sommer. 2010. Biotic interactions may overrule direct climate effects on spring phytoplankton dynamics. Global Change Biol **16**: 1122–1136.

Gargas, E. 1975. A manual for phytoplankton primary production studies in the Baltic. Balt. Mar Biol **2**: 1–88.

Geider, R., and J. La Roche. 2002. Redfield revisited : variability of C:N:P in marine microalgae and its biochemical basis. Eur J Phycol **37**: 1–17.

Gruber, N., M. Gloor, S. E. Mikaloff Fletcher, S. C. Doney, S. Dutkiewicz, M. J. Follows, M. Gerber, A. R. Jacobson, F. Joos, K. Lindsay, D. Menemenlis, A. Mouchet, S. A. Müller, J. L. Sarmiento, and T. Takahashi. 2009. Oceanic sources, sinks, and transport of atmospheric CO_2. Global Biogeochem Cy **23**: GB1005.

Hansell, D. A., and C. A. Carlson. 1998a. Net community production of dissolved organic carbon. Global Biogeochem Cy **12**: 443–453.

Hansell, D. A., and C. A. Carlson. 2001. Biogeochemistry of total organic carbon and nitrogen in the Sargasso Sea: control by convective overturn. Deep-Sea Res II **48**: 1649–1667.

Hansell, D. A., C. A. Carlson, D. J. Repeta, and R. Schlitzer. 2009. Dissolved organic matter in the ocean. Oceanography **22**: 202–211.

Hansell, D., and C. Carlson. 1998b. Deep-ocean gradients in the concentration of dissolved organic carbon. Nature **395**: 263–266.

Hansen, H., and F. Koroleff. 1999. Determination of nutrients, p. 159–228. *In* K. Grasshoff, K. Kremling, and M. Ehrhardt [eds.], Methods of seawater analysis. Wiley VCH, Weinheim.

Hansen, H. P., and F. Koroleff. 2007. Determination of nutrients, p. 159–228. *In* K. Grasshoff, K. Kremling, and M. Ehrhardt [eds.], Methods of Seawater Analysis. Wiley-VCH, Weinheim.

Helcom. 2007. Climate Change in the Baltic Sea Area - Helcom Thematic Assessment in 2007. Balt. Sea Environ. Proc. No. 111, pp 49.

Hillebrand, H., P. Frost, and A. Liess. 2008. Ecological stoichiometry of indirect grazer effects on periphyton nutrient content. Oecologia **155**: 619–630.

Holmes, R. M., A. Aminot, R. Kérouel, B. A. Hooker, and B. J. Peterson. 1999. A simple and precise method for measuring ammonium in marine and freshwater ecosystems. Can J Fish Aquat Sci **56**: 1801–1808.

Holm-Hansen, O., J. D. H. Strickland, and P. M. Williams. 1966. A detailed analysis of biologically important substances in a profile off southern California. Limnol Oceanogr **11**: 548–561.

Hoppe, H.-G., P. Breithaupt, K. Walther, R. Koppe, S. Bleck, U. Sommer, and K. Jürgens. 2008. Climate warming in winter affects the coupling between phytoplankton and bacteria during the spring bloom: a mesocosm study. Aquat Microb Ecol **51**: 105–115.

Ikeda, T., Y. Kanno, K. Ozaki, and A. Shinada. 2001. Metabolic rates of epipelagic marine copepods as a function of body mass and temperature. Mar Biol **139**: 587–596.

IPCC 2013. Summary for policymakers. *In:* Climate change 2013: The physical science basis. Contribution of working group I to the fifth assessment report of the intergovernmental panel on climate change [T.F. Stocker, D. Quin, G.-K. Plattner, M. Tignor, S.K. Allen, J. Boschung, A. Nauels, Y. Xia, V. Bex, and P.M. Midgley (eds.)]. Cambridge University Press, Cambridge, UK and New York, USA.

Isla, J. A., K. Lengfellner, and U. Sommer. 2008. Physiological response of the copepod Pseudocalanus sp. in the Baltic Sea at different thermal scenarios. Global Change Biol **14**: 895–906.

Ittekkot, V. 1982. Variations of dissolved organic matter during a plankton bloom: qualitative aspects, based on sugar and amino acid analyses. Mar Chem **11**: 143–158.

Ittekkot, V., U. Brockmann, W. Michaelis, and E. Degens. 1981. Dissolved free and combined carbohydrates during a phytoplankton bloom in the northern North Sea. Mar Ecol Prog Ser **4**: 299–305.

Ivleva, I. V. 1980. The Dependence of Crustacean Respiration Rate on Body Mass and Habitat Temperature. Int Rev ges Hydrobiol **65**: 1–47.

Jiao, N., G. J. Herndl, D. A. Hansell, R. Benner, G. Kattner, S. W. Wilhelm, D. L. Kirchman, M. G. Weinbauer, T. Luo, F. Chen, and F. Azam. 2010. Microbial production of recalcitrant dissolved organic matter: long-term carbon storage in the global ocean. Nat Rev Microbiol **8**: 593–599.

Jickells, T. D. 1998. Nutrient biogeochemistry of the coastal zone. Science. **281**: 217–222.

Johnson, K. . M., J. M. Sieburth, P. J. le B. Williams, and L. Brändström. 1987. Coulometric total carbon dioxide analysis for marine studies: automation and calibration. Mar Chem **21**: 117–133.

Joint, I., P. Henriksen, G. A. Fonnes, D. Bourne, T. F. Thingstad, and B. Riemann. 2002. Competition for inorganic nutrients between phytoplankton and bacterioplankton in nutrient manipulated mesocosms. Aquat Microb Ecol **29**: 145–159.

Kahl, L., A. Vardi, and O. Schofield. 2008. Effects of phytoplankton physiology on export flux. Mar Ecol Prog Ser **354**: 3–19.

Kähler, P., and W. Koeve. 2001. Marine dissolved organic matter: can its C:N ratio explain carbon overconsumption? Deep-Sea Res Pt I **48**: 49–62.

Karl, D. M., and K. M. Björkman. 2002. Dynamics of DOP, p. 249–366. *In* D.A. Hansell and C.A. Carlson [eds.], Biogeochemistry of marine dissolved organic matter. Academic Press, San Diego, California, USA.

Kawasaki, N., and R. Benner. 2006. Bacterial release of dissolved organic matter during cell growth and decline: Molecular origin and composition. Limnol Oceanogr **51**: 2170–2180.

Keller, A. A., C. A. Oviatt, H. A. Walker, and J. D. Hawk. 1999. Predicted impacts of elevated temperature on the magnitude of the winter-spring phytoplankton bloom in temperate coastal waters: A mesocosm study. Limnol Oceanogr **44**: 344–356.

Kerner, M., H. Hohenberg, S. Ertl, M. Reckermann, and A. Spitzy. 2003. Self-organization of dissolved organic matter to micelle-like microparticles in river water. Nature **422**: 150–154.

Ketchum, B. H. 1962. Regeneration of nutrients by zooplankton. Rapp. procès-verbaux des réunions / Cons. Perm. Int. pour l'Exploration la Mer **152**: 142–146.

Kim, J.-M., K. Lee, K. Shin, E. J. Yang, A. Engel, D. M. Karl, and H.-C. Kim. 2011. Shifts in biogenic carbon flow from particulate to dissolved forms under high carbon dioxide and warm ocean conditions. Geophys Res Lett **38**: (L08612) 5 pp.

Kiørboe, T., and J. Hansen. 1993. Phytoplankton aggregate formation: observations of patterns and mechanisms of cell sticking and the significance of exopolymeric material. J Plankton Res **15**: 993–1018.

Kirchman, D. L., Y. Suzuki, C. Garside, and H. W. Ducklow. 1991. High turnover rates of dissolved organic carbon during a spring phytplankton bloom. Nature **352**: 612–614.

Kirk, J. T. O. 1983. Light and photosynthesis in aquatic ecosystems, Cambridge University Press, Cambridge.

Klaas, C., and D. E. Archer. 2002. Association of sinking organic matter with various types of mineral ballast in the deep sea: Implications for the rain ratio. Global Biogeochem Cy **16**: GB001765.

Kragh, T., M. Søndergaard, and N. H. Borch. 2006. The effect of zooplankton on the dynamics and molecular composition of carbohydrates during an experimental algal bloom. J Limnol **65**: 52–58.

Kroeker, K. J., R. L. Kordas, R. N. Crim, and G. G. Singh. 2010. Meta-analysis reveals negative yet variable effects of ocean acidification on marine organisms. Ecol Lett **13**: 1419–1434.

Krom, M., B. Herut, and R. Mantoura. 2004. Nutrient budget for the Eastern Mediterranean: Implications for phosphorus limitation. Limnol Oceanogr **49**: 1582–1592.

Lalli, C. K., and T. R. Parons. 1997. Biological Oceanography, 2nd edition. Elsevier Butterworth-Heinemann.

Langer, G., M. Geisen, K.-H. Baumann, J. Kläs, U. Riebesell, S. Thoms, and J. R. Young. 2006. Species-specific responses of calcifying algae to changing seawater carbonate chemistry. Geochem Geophy Geosys **7**: 1–12.

Lassen, M. K., K. D. Nielsen, K. Richardson, K. Garde, and L. Schlüter. 2010. The effects of temperature increases on a temperate phytoplankton community — A mesocosm climate change scenario. J Exp Mar Biol Ecol **383**: 79–88.

Lehman, J. T. 1980. Release and cycling of nutrients between planktonic algae and herbivores. Limnol Oceanogr **25**: 620–632.

Levitus, S., J. Antonov, and T. Boyer. 2005. Warming of the world ocean, 1955–2003. Geophys Res Lett **32**: L02604.

Levitus, S., J. I. Antonov, T. P. Boyer, O. K. Baranova, H. E. Garcia, R. A. Locarnini, A. V. Mishonov, J. R. Reagan, D. Seidov, E. S. Yarosh, and M. M. Zweng. 2012. World ocean heat content and thermosteric sea level change (0-2000 m), 1955-2010. Geophys Res Lett. **39**: L10603 pp. 5.

Lewandowska, A. M., P. Breithaupt, H. Hillebrand, H.-G. Hoppe, K. Jürgens, and U. Sommer. 2012. Responses of primary productivity to increased temperature and phytoplankton diversity. J Sea Res **72**: 87–93.

Lewandowska, A., and U. Sommer. 2010. Climate change and the spring bloom: a mesocosm study on the influence of light and temperature on phytoplankton and mesozooplankton. Mar Ecol Prog Ser **405**: 101–111.

Logan, B. E., U. Passow, A. L. Alldredge, H.-P. Grossart, and M. Simon. 1995. Rapid formation and sedimentation of large aggregates is predictable from coagulation rates (half-lives) of transparent exopolymer particles (TEP). Deep-Sea Res Pt II **42**: 203–214.

Loh, A. N., and J. E. Bauer. 2000. Distribution, partitioning and fluxes of dissolved and particulate organic C, N and P in the eastern North Pacific and Southern Oceans. Deep-Sea Res Pt I **47**: 2287–2316.

Long, R. A., and F. Azam. 1996. Abundant protein-containing particles in the sea. Aquat Microb Ecol **10**: 213–221.

López-Urrutia, A., E. San Martin, R. P. Harris, and X. Irigoien. 2006. Scaling the metabolic balance of the oceans. Proc Nat Acad Sci USA **103**: 8739–8744.

Mari, X., and T. Kiørboe. 1994. Abundance, size distribution and bacterial colonization of transparent exopolymeric particles (TEP) during spring in the Kattegat. J Plankton Res **18**: 969–986.

Meehl, G. A., T. F. Stocker, W. D. Collins, P. Friedlingstein, A. T. Gaye, J. M. Gregory, A. Kitoh, R. Knutti, J. M. Murphy, A. Noda, S. C. B. Raper, I. G. Watterson, A. J. Weaver, and Z.-C. Zhao. 2007. Global Climate Projections, *In* S. Solomon, D. Quin, M. Manning, Z. Chen, M. Marquis, K.B. Averyt, M. Tignor, and H.L. Miller [eds.], Climate Change 2007: The Physical Science Basis. Contribution of Working Group I to the Fourth Assessment Report of the Intergovernmental Panel on Climate Change. Cambridge University Press.

Van Den Meersche, K., J. J. Middelburg, K. Soetaert, P. Van Rijswijk, H. T. S. Boschker, and C. H. R. Heip. 2004. Carbon-nitrogen coupling and algal-bacterial interactions during an experimental bloom: Modeling a 13C tracer experiment. Limnol Oceanogr **49**: 862–878.

Von Scheibner, M., P. Dörge, A. Biermann, U. Sommer, H.-G. Hoppe, and K. Jürgens. 2013. Impact of warming on phyto-bacterioplankton coupling and bacterial community composition in experimental mesocosms. Env microbiol, doi:10.1111/1462-2920.12195.

Meinke, I., and M. Reckermann, [eds.] 2012. Ostseeküste im Klimawandel - Ein Handbuch zum Forschungsstand, Norddeutsches Klimabüro und Internationales BALTEX-Sekretariat, Geesthacht.

Møller, E., and T. Nielsen. 2001. Production of bacterial substrate by marine copepods: effect of phytoplankton biomass and cell size. J Plankton Res. **23**: 527–536.

Möllmann, C., G. Kornilovs, and L. Sidrevics. 2000. Long-term dynamics of main mesozooplankton species in the central Baltic Sea. J Plankton Res **22**: 2015–2038.

Mopper, K., X. Zhou, R. J. Kieber, D. J. Kieber, R. J. Sikorski, and R. D. Jones. 1991. Photochemical degradation of dissolved organic carbon and its impact on the oceanic carbon cycle. Nature **353**: 60–62.

Morán, X. A. G., Á. López-Urrutia, A. Calvo-Díaz, and W. K. W. Li. 2010. Increasing importance of small phytoplankton in a warmer ocean. Global Change Biol **16**: 1137–1144.

Morán, X., M. Sebastián, C. Pedrós-Alió, and M. Estrada. 2006. Response of Southern Ocean phytoplankton and bacterioplankton production to short-term experimental warming. Limnol Oceanogr **51**: 1791–1800.

Mortain-Bertrand, A., C. Descolas-Gros, and H. Jupin. 1988. Growth, photosynthesis and carbon metabolism in the temperate marine diatom *Skeletonema costatum* adapted to low temperature and low photon-flux density. Mar Biol **100**: 135–141.

Müren, U., J. Berglund, K. Samuelsson, and A. Andersson. 2005. Potential effects of elevated sea-water temperature on pelagic food webs. Hydrobiologia **545**: 153–166.

Myklestad, S. M. 1995. Release of extracellular products by phytoplankton with special emphasis on polysaccharides. Sci Total Environ **165**: 155–164.

Myklestad, S. M., E. Skånøy, and S. Hestmann. 1997. A sensitive and rapid method for analysis of dissolved mono- and polysaccharides in seawater. Mar Chem **56**: 279–286.

Nagata, T. 2000. Production mechanisms of dissolved organic matter, pp. 121–152. *In* D.L. Kirchman [ed.], Microbial ecology of the oceans. Wiley-Liss, Inc.

Nausch, G., R. Feistel, L. Umlauf, K. Nagel, and H. Siegel. 2010. Hydrographisch-chemische Zustandseinschätzung der Ostsee.

Nixon, S. W., R. W. Fulweiler, B. a. Buckley, S. L. Granger, B. L. Nowicki, and K. M. Henry. 2009. The impact of changing climate on phenology, productivity, and benthic–pelagic coupling in Narragansett Bay. Estuar Coast Shelf Sci **82**: 1–18.

Norrman, B., U. Zweifel, C. Hopkinson, and F. Brian. 1995. Production and utilization of dissolved organic carbon during an experimental diatom bloom. Limnol Oceanogr **40**: 898–907.

O'Connor, M. I., M. F. Piehler, D. M. Leech, A. Anton, and J. F. Bruno. 2009. Warming and resource availability shift food web structure and metabolism. PLoS Biol **7**: e1000178.

Ogawa, H., Y. Amagai, I. Koike, K. Kaiser, and R. Benner. 2001. Production of refractory dissolved organic matter by bacteria. Science **292**: 917–20.

Passow, U. 2002a. Production of transparent exopolymer particles (TEP) by phyto- and bacterioplankton. Mar Ecol Prog Ser **236**: 1–12.

Passow, U. 2002b. Transparent exopolymer particles (TEP) in aquatic environments. Progr Ocean **55**: 287–333.

Passow, U., and A. L. Alldredge. 1995a. Aggregation of a diatom bloom in a mesocosm : The role of transparent exopolymer particles (TEP). Deep-Sea Res Pt II **42**: 99–109.

Passow, U., and A. L. Alldredge. 1995b. A dye-binding assay for the spectrophotometric measurement of transparent exopolymer particles (TEP). Limnol Oceanogr **40**: 1326–1335.

Passow, U., A. L. Alldredge, and B. E. Logan. 1994. The role of particulate carbohydrate exudates in the flocculation of diatom blooms. Deep-Sea Res Pt I **41**: 335–357.

Paytan, A., and K. McLaughlin. 2007. The oceanic phosphorus cycle. Chem Rev **107**: 563–76.

Piontek, J., N. Händel, G. Langer, J. Wohlers, U. Riebesell, and A. Engel. 2009. Effects of rising temperature on the formation and microbial degradation of marine diatom aggregates. Aquat Microb Ecol **54**: 305–318.

Pomeroy, L. R., and W. J. Wiebe. 2001. Temperature and substrates as interactive limiting factors for marine heterotrophic bacteria. Aquat Microb Ecol **23**: 187–204.

Prentice, I. C., G. D. Farquhar, M. J. R. Fasham, M. L. Goulden, M. Heimann, V. J. Jaramillo, H. S. Kheshgi, C. Le Quéré, R. J. Scholes, and D. W. R. Wallace. 2001. The carbon cycle and atmospheric carbon dioxide, p. 183–237. *In* J.T. Houghton, Y. Ding, D.J. Griggs, M. Noguer, P.J. Van der Linden, X. Dai, K. Maskell, and C.A. Johnson [eds.], Climate Change 2001: The scientific basis. Contribution of working group I to the third assessment report of the Intergovernmental Panel on Climate Change. Cambridge University Press.

Prieto, L., J. Ruiz, F. Echevarría, C. M. García, A. Bartual, J. a. Gálvez, A. Corzo, and D. Macías. 2002. Scales and processes in the aggregation of diatom blooms: high time resolution and wide size range records in a mesocosm study. Deep-Sea Res Pt I **49**: 1233–1253.

Qian, J., and K. Mopper. 1996. Automated high-performance, high-temperature combustion total organic carbon analyzer. Anal Chem **68**: 3090–3097.

Redfield, A., and B. Ketchum. 1963. The influence of organism on the composition of sea-water, pp. 26–77. *In* M.N. Hill [ed.], The Sea. Wiley.

Riebesell, U., A. Körtzinger, and A. Oschlies. 2009. Sensitivities of marine carbon fluxes to ocean change. Proc Nat Acad Sci USA **106**: 20602–20609.

Riebesell, U., K. G. Schulz, R. G. J. Bellerby, M. Botros, P. Fritsche, M. Meyerhöfer, C. Neill, G. Nondal, a Oschlies, J. Wohlers, and E. Zöllner. 2007. Enhanced biological carbon consumption in a high CO_2 ocean. Nature **450**: 545–8.

Riebesell, U., and P. D. Tortell. 2011. Effects of ocean acidification on pelagic organisms and ecosystems, p. 99–116. *In* J.-P. Gattuso and L. Hansson [eds.], Ocean Acidification. Oxford University Press, Oxford, New York.

Riebesell, U., I. Zondervan, B. Rost, P. D. Tortell, R. E. Zeebe, and F. M. M. Morel. 2000. Reduced calcification of marine plankton in response to increased atmospheric CO_2. Nature **407**: 364–367.

Rivkin, R. B., and L. Legendre. 2001. Biogenic carbon cycling in the upper ocean: effects of microbial respiration. Science **291**: 2398–400.

Sabine, C. L., R. A. Feely, N. Gruber, R. M. Key, K. Lee, J. L. Bullister, R. Wanninkhof, C. S. Wong, D. W. R. Wallace, B. Tilbrook, F. J. Millero, T.-H. Peng, A. Kozyr, T. Ono, and A. F. Rios. 2004. The oceanic sink for anthropogenic CO_2. Science **305**: 367–71.

Sabine, C. L., and T. Tanhua. 2010. Estimation of anthropogenic CO_2 inventories in the Ocean. Ann Rev Mar Sci **2**: 269–292.

Sambrotto, R. N., G. Savidge, C. Robinson, P. Boyd, T. Takahashi, D. M. Karl, C. Langdon, D. Chipman, J. Marra, and L. Codispoti. 1993. Elevated consumption of carbon relative to nitrogen in the surface ocean. Nature **363**: 248–250.

Sarmiento, J. L., J. Dunne, A. Gnanadesikan, R. M. Key, K. Matsumoto, and R. Slater. 2002. A new estimate of the $CaCO_3$ to organic carbon export ratio. Global Biogeochem Cy **16**: 54–1–54–12.

Sarmiento, J. L., and N. Gruber. 2006. Ocean Biogeochemical Dynamics, Princeton University Press, Princeton, New Jersey.

Sarmiento, J. L., T. M. C. Hughes, R. J. Stouffer, and S. Manabe. 1998. Simulated response of the ocean carbon cycle to anthropogenic warming. Nature **393**: 245–249.

Sarmiento, J. L., R. Slater, R. Barber, L. Bopp, S. C. Doney, A. C. Hirst, J. Kleypas, R. Matear, U. Mikolajewicz, P. Monfray, V. Soldatov, S. A. Spall, and R. Stouffer. 2004. Response of ocean ecosystems to climate warming. Global Biogeochem Cy **18**: GB3003.

Schartau, M., A. Engel, J. Schröter, S. Thoms, C. Völker, and D. Wolf-Gladrow. 2007. Modelling carbon overconsumption and the formation of extracellular particulate organic carbon. Biogeosciences **4**: 433–454.

Shaffer, G., J. Bendtsen, and O. Ulloa. 1999. Fractionation during remineralization of organic matter in the ocean. Deep-Sea Res Pt I **46**: 185–204.

Sharp, J., R. Benner, and L. Bennett. 1995. Analyses of dissolved organic carbon in seawater: the JGOFS EqPac methods comparison. Mar Chem **48**: 91–108.

Sharp, J. H. 1974. Improved analysis for “particulate” organic carbon and nitrogen from seawater. Limnol Oceanogr **19**: 984–989.

Siegenthaler, U., and J. Sarmiento. 1993. Atmospheric carbon dioxide and the ocean. Nature **365**: 119–125.

Simon, M., and F. Azam. 1989. Protein content and protein synthesis rates of planktonic marine bacteria. Mar Ecol Prog Ser **51**: 201–213.

Sommer, U. 1994. Planktologie, Springer-Verlag, Berlin.

Sommer, U., N. Aberle, A. Engel, T. Hansen, K. Lengfellner, M. Sandow, J. Wohlers, E. Zöllner, and U. Riebesell. 2007. An indoor mesocosm system to study the effect of climate change on the late winter and spring succession of Baltic Sea phyto- and zooplankton. Oecologia **150**: 655–67.

Sommer, U., N. Aberle, K. Lengfellner, and A. Lewandowska. 2012a. The Baltic Sea spring phytoplankton bloom in a changing climate: an experimental approach. Mar Biol **159**: 2479–2490.

Sommer, U., and K. Lengfellner. 2008. Climate change and the timing, magnitude, and composition of the phytoplankton spring bloom. Global Change Biol **14**: 1199–1208.

Sommer, U., K. Lengfellner, and A. Lewandowska. 2012b. Experimental induction of a coastal spring bloom early in the year by intermittent high-light episodes. Mar Ecol Prog Ser **446**: 61–71.

Sommer, U., and A. Lewandowska. 2011. Climate change and the phytoplankton spring bloom: warming and overwintering zooplankton have similar effects on phytoplankton. Global Change Biol **17**: 154–162.

Søndergaard, M., P. J. le B. Williams, G. Cauwet, B. Riemann, C. Robinson, S. Terzic, E. M. S. Woodward, and J. Worm. 2000. Net accumulation and flux of dissolved organic carbon and dissolved organic nitrogen in marine plankton communities. Limnol Oceanogr **45**: 1097–1111.

Steemann Nielsen, E. The use of radioactive carbon (^{14}C) for measuring production in the sea. J Cons Int Explor Mer **18**: 117–140.

Sterner, R. W. 1986. Herbivores' direct and indirect effects on algal populations. Science **231**: 605–607.

Sterner, R. W., and J. J. Elser. 2002. Ecological Stoichiometry: the biology of elements from molecules to the biosphere, Princeton University Press, Princeton, New Jersey.

Stocker, R. 2012. Marine microbes see a sea of gradients. Science **338**: 628–633.

Stoderegger, K. E., and G. J. Herndl. 1999. Production of exopolymer particles by marine bacterioplankton under contrasting turbulence conditions. Mar Ecol Prog Ser **189**: 9–16.

Stoderegger, K., and G. J. Herndl. 1998. Production and release of bacterial capsular material and its subsequent utilization by marine bacterioplankton. Limnol Oceanogr **43**: 877–884.

Strom, S. L., R. Benner, S. Ziegler, and M. J. Dagg. 1997. Planktonic grazers are a potentially important source of marine dissolved organic carbon. Limnol Oceanogr **42**: 1364–1374.

Taucher, J., K. G. Schulz, T. Dittmar, U. Sommer, A. Oschlies, and U. Riebesell. 2012. Enhanced carbon overconsumption in response to increasing temperatures during a mesocosm experiment. Biogeosciences **9**: 3531–3545.

Thingstad, T. F., Å. Hagström, and F. Rassoulzadegan. 1997. Accumulation of degradable DOC in surface waters: Is it caused by a malfunctioning microbial loop? Limnol Oceanogr **42**: 398–404.

Thingstad, T. F., M. D. Krom, R. F. C. Mantoura, G. a F. Flaten, S. Groom, B. Herut, N. Kress, C. S. Law, A. Pasternak, P. Pitta, S. Psarra, F. Rassoulzadegan, T. Tanaka, A. Tselepides, P. Wassmann, E. M. S. Woodward, C. W. Riser, G. Zodiatis, and T. Zohary. 2005. Nature of phosphorus limitation in the ultraoligotrophic eastern Mediterranean. Science **309**: 1068–71.

Thornton, D. C. O., and B. Thake. 1998. Effect of temperature on the aggregation of *Skeletonema costatum* (Bacillariophyceae) and the implication for carbon flux in coastal waters. Mar Ecol Prog Ser **174**: 223–231.

Tilzer, M. M., and Z. Dubinsky. 1987. Effects of temperature and day length on the mass balance of Antarctic phytoplankton. Polar Biol **7**: 35–42.

Toggweiler, J. R. 1993. Carbon overconsumption. Nature **363**: 210–211.

Urabe, J. 1995. Direct and indirect effects of zooplankton on seston stoichiometry. Ecoscience **2**: 286–296.

Verdugo, P., A. L. Alldredge, F. Azam, D. L. Kirchman, U. Passow, and P. H. Santschi. 2004. The oceanic gel phase: a bridge in the DOM–POM continuum. Mar Chem **92**: 67–85.

Verity, P. G. 1981a. Effects of temperature, irradiance, and daylength on the marine diatom Leptocylindrus danicus Cleve. II. Excretion. J Exp Mar Biol Ecol **55**: 159–169.

Verity, P. G. 1981b. Effects of temperature, irradiance, and daylength on the marine diatom Leptocylindrus danicus Cleve I. Photosynthesis and cellular composition. J Exp Mar Biol Ecol **55**: 79–91.

Welschmeyer, N. A. 1994. Fluorometric analysis of chlorophyll a chlorophyll b and pheopigments. Limnol Oceanogr **39**: 1985–1992.

Wetz, M. S., and P. A. Wheeler. 2003. Production and partitioning of organic matter during simulated phytoplankton blooms. Limnol Oceanogr **48**: 1808–1817.

Williams, P. J. le B. 2000. Heterotrophic bacteria and the dynamics of dissolved organic material, pp. 153–200. *In* D.L. Kirchman [ed.], Microbial ecology of the oceans. Wiley-Liss, Inc., New York.

Williams, P. M., and E. R. M. Druffel. 1987. Radiocarbon in DOM in the central North Pacific Ocean. Nature **330**.

Wiltshire, K. H., A. M. Malzahn, K. Wirtz, W. Greve, S. Janisch, P. Mangelsdorf, B. F. J. Manly, and M. Boersma. 2008. Resilience of North Sea phytoplankton spring bloom dynamics: An analysis of long-term data at Helgoland Roads. Limnol Oceanogr **53**: 1294–1302.

Wiltshire, K. H., and B. F. J. Manly. 2004. The warming trend at Helgoland Roads, North Sea: phytoplankton response. Helgol Mar Res **58**: 269–273.

Winder, M., S. a. Berger, A. Lewandowska, N. Aberle, K. Lengfellner, U. Sommer, and S. Diehl. 2012. Spring phenological responses of marine and freshwater plankton to changing temperature and light conditions. Mar Biol **159**: 2491–2501.

Wohlers, J., A. Engel, E. Zöllner, P. Breithaupt, K. Jürgens, H.-G. Hoppe, U. Sommer, and U. Riebesell. 2009. Changes in biogenic carbon flow in response to sea surface warming. Proc Natl Acad Sci USA **106**: 7067–72.

Wohlers-Zöllner, J., A. Biermann, A. Engel, P. Dörge, A. M. Lewandowska, M. von Scheibner, and U. Riebesell. 2012. Effects of rising temperature on pelagic biogeochemistry in mesocosm systems: a comparative analysis of the AQUASHIFT Kiel experiments. Mar Biol **159**: 2503–2518.

Wohlers-Zöllner, J., P. Breithaupt, K. Walther, K. Jürgens, and U. Riebesell. 2011. Temperature and nutrient stoichiometry interactively modulate organic matter cycling in a pelagic algal-bacterial community. Limnol Oceanogr **56**: 599–610.

Wolfstein, K., J. De Brouwer, and L. Stal. 2002. Biochemical partitioning of photosynthetically fixed carbon by benthic diatoms during short-term incubations at different irradiances. Mar Ecol Prog Ser **245**: 21–31.

Zhang, X., F. W. Zwiers, G. C. Hegerl, F. H. Lambert, N. P. Gillett, S. Solomon, P. A Stott, and T. Nozawa. 2007. Detection of human influence on twentieth-century precipitation trends. Nature **448**: 461–5.

Zlotnik, I., and Z. Dubinsky. 1989. The effect of light and temperature on DOC excretion by phytoplankton. Limnol Oceanogr **34**: 831–839.

Zöllner, E., H.-G. Hoppe, U. Sommer, and K. Jürgens. 2009. Effect of zooplankton-mediated trophic cascades on marine microbial food web components (bacteria, nanoflagellates, ciliates). Limnol Oceanogr **54**: 262–275.

Zondervan, I., B. Rost, and U. Riebesell. 2002. Effect of CO_2 concentration on the PIC/POC ratio in the coccolithophore *Emiliania huxleyi* grown under light-limiting conditions and different daylengths. J Exp Mar Bio Ecol **272**: 55–70.

List of publications

Published Articles:

Chapter 3

Wohlers-Zöllner, Julia, **Antje Biermann**, Anja Engel, Petra Dörge, Aleksandra M. Lewandowska, Markus von Scheibner, Ulf Riebesell (2012). Effects of rising temperature on pelagic biogeochemistry in mesocosm systems: a comparative analysis of the AQUASHIFT Kiel experiments. Mar Biol 159:2503–2518.

Submitted manuscripts

Chapter 1

Biermann, Antje, Anja Engel, Ulf Riebesell (in review): Changes in organic matter cycling in a plankton community exposed to warming under different light intensities, Journal of Plankton Research.

Chapter 2

Biermann, Antje, Anja Engel, Ulf Riebesell (in review): Organic matter partitioning and stoichiometry in response to rising water temperature and copepod grazing, Marine Ecology Progress Series.

In addition, I have contributed to the following publication in the framework of the AQUASHIFT project:

Von Scheibner, Markus, Petra Dörge, **Antje Biermann,** Ulrich Sommer, Hans-Georg Hoppe, Klaus Jürgens (2013): Impact of warming on phyto-bacterioplankton coupling and bacterial community composition in experimental mesocosms, Environmental Microbiology, DOI: 10.1111/1462-2920.12195.

Declaration

The content and design of this thesis, apart from the supervisor's guidance, is my own work. The thesis has not been submitted either partially or wholly as a part of a doctoral degree to another examining body and has been prepared respecting the Rules of Good Scientific Practice of the German Research Foundation.

Antje Biermann